Biosynthesis of ZnO nanoparticles: Studying its effect on the antimicrobial activities and light absorption characteristics of biobased ointment

By Tamirat Lamaro Bate

A Thesis Submitted to

The department of chemical engineering

School of mechanical, chemical, and materials engineering

Presented in Partial Fulfillment of the Requirement for the Degree of Master's in chemical engineering (Specialization in process engineering)

Office of Graduate Studies

Adama Science and Technology University

November, 2021

Adama, Ethiopia

Biosynthesis of ZnO nanoparticles: Studying its effect on the antimicrobial activities and light absorption characteristics of biobased ointment

By Tamirat Lamaro Bate

Advisors

Dr. Melaku Tesfaye

Dr. Tatek Temesgen

A Thesis Submitted to

The department of chemical engineering

School of mechanical, chemical, and materials engineering

Presented in Partial Fulfillment of the Requirement for the Degree of Master's in chemical engineering (Specialization in process engineering)

Office of Graduate Studies

Adama Science and Technology University

November, 2021

Adama, Ethiopia

Declaration

I hereby declare that this MSc Thesis entitled " Biosynthesis of Zinc oxide nanoparticles: Studying its effect on the antimicrobial activities and light absorption characteristics of biobased ointment" is my original work. It has not been submitted for the award of any academic degree, diploma, or certificate in any other university. All sources of materials that are used for this thesis have been duly acknowledged through citation.

Tamirat Lamaro Bate		
Name of the Student	Signature	Date

Recommendation

We, the advisors of this thesis, hereby certify that we have read the revised version of the thesis entitled "Biosynthesis of Zinc oxide nanoparticles: Studying its effect on the antimicrobial activities and light absorption characteristics of biobased ointment" prepared under guidance by Tamirat Lamaro Bate submitted in partial fulfillment of the requirements for the degree of Masters of Science in chemical engineering.

Therefore, we recommend the submission of a revised version of the thesis to the department following the applicable procedures.

Dr. MelakuTesfaye	_____	_____
Major Advisor	Signature	Date
Dr. Tatek Temesgen	_____	_____
Co-Advisor	Signature	Date

Approval sheet

We, the advisors of the thesis entitled " Biosynthesis of Zinc oxide nanoparticles; Studying its effect on the antimicrobial activities and light absorption characteristics of biobased ointment" and developed by Tamirat Lamaro Bate, hereby certify that the recommendation and suggestions made by the board of examiners are appropriately incorporated into the final version of the thesis.

Dr. MelakuTesfaye	_____	_____
Major Advisor	Signature	Date
Dr. Tatek Temesgen	_____	_____
Co-Advisor	Signature	Date

We, the undersigned, members of the Board of Examiners of the thesis by Tamirat Lamaro Bate, have read and evaluated the thesis entitled "Biosynthesis of Zinc oxide nanoparticles; Studying its effect on antimicrobial activities and light absorption characteristics of biobased ointment" and examined the candidate during the open defense. This is, therefore, to certify that the thesis is accepted for partial fulfillment of the requirement of the degree of Master of Science in chemical engineering.

_____	_____	_____
Chairperson	Signature	Date
_____	_____	_____
Internal Examiner	Signature	Date
_____	_____	_____
Eternal Examiner	Signature	Date

Finally, approval and acceptance of the thesis is contingent upon submission of its final copy to the Office of Postgraduate Studies (OPGS) through the Department Graduate Council (DGC) and School Graduate Committee (SGC).

_____	_____	_____
Department Head	Signature	Date
_____	_____	_____
School Dean	Signature	Date
_____	_____	_____
Office of Postgraduate Studies, Dean	Signature	Date

ACKNOWLEDGMENT

First and foremost, I would like to thank God Almighty and holy, who has given me strength, patience, and all good things I had, have, and will have.

I would like to offer my most profound thanks and sincere gratitude to my advisors Dr. Melaku Tesfaye and Dr. Tatek Temesgen, for their valuable support, continuous follow-ups, guidance encouragement, crucial remarks, priceless suggestion, and comments throughout the thesis. Sometimes words can't express our feeling toward someone who means a lot to us. Thank you for everything you did for me. Thank you again.

I never forget to thank my families; who supported, asked, and motivated me in every Circumstances of my life. Your pray haven't been cut off still now. I love you so much. I wish long life and health for you with all good things. I would also like to express my sincere and genuine gratitude to my friend Meseret Ewunetu for her help, comments, and valuable suggestion. My thank also goes to Dr. Hiskel Tsade and Mr. Tamirat Addis for their comments and useful suggestions during documentation. I am also grateful for my friends and for those who contributed their effort directly or indirectly while conducting this thesis. I am thankful for Adama Science and Technology University who has awarded me with an ASTU full scholarship.

Finally, I would like to thank the ASTU chemical engineering department for all supports and facilities during my study.

TABLE OF CONTENTS

LIST OF TABLES

LIST OF FIGURES

LIST OF ABBREVIATIONS AND ACRONYMS

COL	Collagen
DCS	Carbon Dot Nanocomposite
DW	Distilled water
ELN	Elastin
ECM	Extracellular matrix
ET	Ethanol
ET-DW	Ethanol-distilled water
FTIR	Fourier Transmission Infrared Spectroscopy
LA	Lactic Acid
MO	Moringa oleifera
MT	Methanol
MT-DW	Methanol-distilled water
NPs	Nanoparticles
OB	Ointment base
OLLA	Oligomer L-lactic acid
SEM	Scanning Electron Microscopy
SPR	Surface plasmon resonance
TGA	Thermogravimetric analysis
XRD	X-ray Diffraction
20ZnO NPs	Zinc oxide nanoparticles
ZnO NPs - OB	ZnO NPs dispersed ointment base

LIST OF SYMBOLS AND NOTATIONS

α	Absorption coefficient
β	A line width of half maximum in radians
θ	Bragg's diffraction angle
λ	X-ray or light ray wavelength
h	Planck constant
υ	Light frequency
κ	Scherrer's constant
D	Crystal size
A	Proportional coefficient
E_g	Bandgap energy
H	Planck's constant
c	Speed of light
d	di-spacing
nm	nanometer
mm	millimeter
mL	Milli liter
g	gram
mg	milligram
µg	microgram
%	Percent
℃	Degree Celsius
Z_1	Antimicrobial activity of Calcined ZnO NPs

Z_2	Antimicrobial activity of Oven-dried ZnO NPs
Z_3	Antimicrobial activity of Moringa oleifera
F_0	Ointment base
F_1	0.5% - ZnO NPs-OB
F_2	1% - ZnO NPs- OB
F_3	3% - ZnO NPs- OB
F_4	5% - ZnO NPs- OB
F_5	5% - calcined - ZnO NPs- OB

ABSTRACT

Eco-friendly synthesis of nanoparticles provides simplicity, low cost, ambient atmosphere synthesis, non-toxicity, and environmental compatibility over conventional methods. Recently, the application of nanoparticles in the field of cosmetics has been widely used. Biosynthesized ZnO NPs incorporated into biobased ointment base provided unique properties such as an effective antimicrobial activities and UV radiation absorbing characteristics to ointment. In the biosynthesis of ZnO NPs, Moringa Oleifera leaf extract was used as reducing agents; Zn $(NO_3)_2.6H_2O$ as precursor and NaOH was used to adjust the pH. Effects of reaction parameters affecting the biosynthesis of ZnO NPs were identified. Based on the results obtained, 50:50 mL (v/v) of MT: DW was the appropriate solvent selected for the biosynthesis of ZnO NPs. Optimum points obtained for reaction parameters were nucleation time (3 hr), the temperature (80 ℃), the ratio of the volume of plant extracts to precursor solution (50:50(v/v)), precursor concentration (0.025 M), and pH (12). UV-Vis spectroscopy indicated the formation of ZnO NPs at 363 nm. TGA showed three major mass loss steps and a maximum mass loss temperature of 390 ℃. The crystalline size obtained was 12.85 and 9.1 nm for calcined and oven-dried ZnO NPs, respectively. FTIR peak appeared in the lower energy region at 497 cm^{-1}. ZnO NPs showed suitable antimicrobial activities with an inhibition zone of 16 mm and 14 mm against E. coli and S. aureus, respectively. COL/ELS was extracted from broilers skin and lactic acid were used to synthesize bioconjugate via polycondensation reaction. The synthesized bioconjugate was used as an ointment base to carry active components, i.e., ZnO NPs, to formulate ZnO NPs-DO. By mimicking important biomedical properties of ZnO NPs especially, antimicrobial and UV radiation absorbing properties, the biobased ointment was prepared at different concentrations of ZnO NPs by fusion method. The formulated ointment was characterized and analyzed by physical evaluations, UV-Vis, FTIR, and tested for its antimicrobial activity. ZnO NPs-DO absorbed UVA radiation due to the bandgap of ZnO NPs. ZnO NPs-DO showed better antimicrobial activity with an inhibition zone of 16.5 mm and 16 mm against E. coli and S. aureus, respectively. FTIR of ZnO NPs-DO show strong interaction or attachment of ZnO NPs to ointment base. Thus, this research work concludes that ZnO NPs incorporated ointment base can be used as good antimicrobial and UVA radiation-absorbing ointment for skincare applications.

***Keywords**: - Moringa oleifera, Biosynthesis, ZnO NPs, COL/ELS, ZnO NPs-DO, bioconjugate*

CHAPTER ONE

1. INTRODUCTION

1.1. Background

Recently, biomaterials have been the most rapidly developing field of study. The area has grown significantly in the past decade due to discoveries in tissue engineering, regenerative medicine, drug delivery, cosmetics, etc., and is biocompatible with the human body (Kulinets, 2015). Biomaterials are any materials in contact with human or animal biological systems to perform their intended function. It is also characterized as any material or combination of materials other than medicines of synthetic or natural origin, which can be used for any period and partially or wholly replace a tissue, an organ, or a function of the body (Zarubica, 2020).

There are three major groups of biomaterials. These are synthetic biomaterials (metals, polymers, ceramics, composites), nature-derived biomaterials (e.g., plant-derived, tissue-derived), and semi-synthetic or hybrid biomaterials. Recently, green, sustainable, and renewable natural biomaterials have gained significant attention in the scientific community. Natural materials are often similar, if not identical, to materials that the biological system can recognize and process through metabolic pathways (Kulinets, 2015). Natural biomaterials usually allow avoiding the problems of toxicity often presented by synthetic materials. Natural biomaterials are mainly composed of three types of biopolymers: Proteins, Polysaccharides, and Polynucleotides (Kulinets, 2015; Shin et al., 2003). Protein-based biomaterials gained attention due to their advanced biomedical applications.

Protein-based biomaterials have multiple and advanced applications in biomedical fields. Its application in the internal and external body surface, like the skin, has been extensively researched. The skin is the body's largest organ, and its primary role is to serve as a physical barrier to protect the body from foreign organisms and toxins (Moss, 2016). Due to its anatomic location at the external boundary of the body, skin is damaged by microbial infections, chemical or physical injuries following the burn, pathogens, and exposure to environmental factors such as chemical products, pollution, infrared, and ultraviolet(UV) radiations, etc. (Yu et al., 2017). Biobased products developed from skin materials like collagen/elastin (COL/ELS) protein are the best

options to minimize microbial infections, chemical or physical injuries, and exposure to environmental factors.

COL/ELS are the main structural proteins responsible for skin strength and elasticity. COL/ELS were used in wound cover dressings, resorbable surgical sutures, osteogenic and bone filling materials (Chattopadhyay & Raines, 2014). It has been used as an ingredient in cosmetic formulations numerously by cosmetic manufactures to promote better skin elasticity. A variety of techniques are currently available to produce cosmetic products to enhance the skin's appearance and help to preserve features such as safety, good texture, hydration, and the quality of the dermal matrix. COL/ELS, among a few essential ingredients which are often incorporated in many premium anti-aging skincare products (Yoseph et al., 2020). Different principal collagen/elastin proteins sources include calf and bull skin, bovine tendon, porcine skin, human corpses, fish, eggshells, chicken (broiler) skin, and others (Ma, 2016).

Due to modernization, broiler skin is a waste material, and a large amount of broiler skin has been disposed of to the environment. Since broiler skin consists of many COL/ELS, extracting this matrix from its skin and converting it into a useful product is economical and environmentally friendly. As mentioned earlier, COL/ELS is used as the main ingredient in premium anti-aging skincare products. In this thesis work, COL/ELS were extracted from broiler skin by following the appropriate extraction procedure. Extracted COL/ELS has a crispy yellow structure. Since it has a crisp form, it couldn't' been used directly for skin-care applications. So, it should be combined with other organic types of the carrier(fluids) like lactic acid in ointment development.

Lactic acid is water-soluble acid and stays more on the outer layers of the skin to provide additional moisture to the outer skin layers. It also stimulates the growth of new skin, improves signs of aging, stimulates COL/ELS renewal, secures the skin from UV light, and is compatible with our body. It is known to accelerate cell turnover while helping with moisturizing the skin to produce a smooth skin and balance the skin's pH level (Jarrar, 2015). This thesis work used COL/ELS and lactic acid as a carrier to synthesize ointment base by a polycondensation reaction. Finally, the biobased ointment was developed from this ointment base and nanoparticle via the fusion method for skincare applications.

An ointment is a homogeneous, viscous, semi-solid preparation intended for external use on the skin or mucous membranes. It serves as protective, therapeutic, or prophylactic and is used as

emollients or active ingredients to the skin (El-Gied et al., 2015). Most ointments contain petroleum derivatives like mineral oil, soft white, yellow paraffin, hard paraffin, and cetostearyl alcohol (Bhaskar et al., 2016; Mahendran & Abdul Rashid, 2016). Researches show that with the increase in mineral oil saturated hydrocarbon, there is an increased accumulation of mineral oil over time in human fat tissue with age. It is toxic, does not metabolize if it's a gate into the system, and tends to cloggy skin pores.

Even though petroleum derivative ointment keeps skin moisture and reduces overexposure to sunlight, it is incompatible with living systems. Therefore, it was required to find biobased and biocompatible ointment from natural biomaterials like COL/ELS and lactic acid as a carrier. To produce the most effective bio-based ointment and advance its functionality and activity, the introduction of nanoparticles (NPs) to bio-based ointment plays a crucial role. Based on their bioactivities, several cosmeceutical and pharmaceutical products use NPs (V. Gupta et al., 2020; Lisnawati et al., 2019; Mârza et al., 2019; Zarubica, 2020).

During the last few years, nanotechnology has become an emergent interdisciplinary field of research that combines material science, bio-nano science, and technology. It has considered as the technological innovation of the 21st century. NPs are particles at the atomic level (1 - 100 nm) (Król et al., 2017). Their smaller size and large surface area also enhance their ability to enter into cells and become more biologically active (V. Gupta et al., 2020). Based on their bioactivities, several cosmeceutical and pharmaceutical products use NPs in their product.

Recently, the application of NPs in the field of cosmetics has been used widely. It has entered the field of cosmetics ranging from dermal applications to nourishing creams. Several types of cosmetics, sunscreens, and personal care products containing engineered nanoparticles are commercially available in the market. Cosmetic formulations incorporated with NPs provide tactile, light scattering and matte effects. Inorganic metal and metal oxide NPs have attracted more attention over the past decade due to their ability and are generally regarded as safe materials for human beings and animals (Marathe et al., 2014). The inorganic NPs such as silver, gold, copper, copper oxide, titanium oxide, and Zinc oxide(ZnO) have profound antibacterial activities (Badnore et al., 2019).

Among the inorganic NPs, ZnO NPs were of particular interest to this study because they can be prepared quickly, are comparatively inexpensive, and are less toxic, safe material for human beings and animals than other metal oxide NPs. It has also been declared as "Generally Recognized As Safe" (GRAS) by the US Food and Drug Administration (V. Gupta et al., 2020). ZnO NPs have entered the scientific spotlight for their unique antibacterial, antifungal, wound healing, and UV filtering properties. They are compatible with the skin, have high catalytic and photochemical activity, and are used in many biomedical applications.

Generally, three available methods are physical, chemical, and biological methods for synthesizing ZnO NPs. Conventional physical and chemical synthesis methods require harsh conditions and hazardous chemicals with potentially adverse effects which cause environmental pollution (Uma & Xin, 2016). Due to this reason, the biosynthesis of ZnO NPs has emerged as an eco-friendly alternative. In this work, ZnO NPs were synthesized by biological methods using moringa oleifera leaves extract. Moringa oleifera was selected due to its availability and contained many phytochemicals (Elumalai & Velmurugan, 2015) (Ngom et al., 2021), mainly used as reducing and stabilizing agents in the biosynthesis of ZnO NPs. It is a natural antioxidant, enhances human skin facial revitalization, prevents skin dryness and aging (Ali et al., 2014). One of many biomedical applications of the ZnO NPs is antimicrobial activity and UV radiation absorbing or blocking property.

UV light is electromagnetic radiation with a wavelength range of 100 - 400 nm (Zou et al., 2018). Globally, solar UV radiation striking the surface of the Earth is highly increasing due to the depletion of the ozone layer. Exposure is associated with various skin cancers, accelerated skin aging, cataract (opacity in the eye lens), etc. As WHO report, Up to 20% or 3 million people per year were caused to skin cancer that could be ultimately due to exposure to UV radiation (Nations et al., 1994). UV radiation primarily composed of UVA (90%–95%) and UVB (5%–10%) (Amaro-ortiz et al., 2014; Moss, 2016; Orazio et al., 2013). Most recent studies have also implicated an increasing role of UVA and UVB as a carcinogen (Amaro-ortiz et al., 2014). So, to overcome this problem, other protective measures and skincare products incorporated with ZnO NPs that can absorb UV light and prevent microbial infection have to be synthesized.

Based on this inspiration, this thesis focused on the biosynthesis of ZnO NPs to overcome the drawbacks of conventional methods and development of biobased ointment to avoid petroleum-based ointment problems. The synthesized bio-based ointment was supposed to regenerate damaged skin cells and protect skin from microbial infections and harmful UV radiation. Few studies were conducted on NPs dispersed ointments, but all use synthetic ointment bases derived from petroleum derivatives, which has several drawbacks. It was observed that ZnO NPs had increased antimicrobial activities of biobased ointment and showed UVA light-absorbing characteristics.

1.2. Research Questions

This thesis work was intended to answer the following fundamental research questions:

1. Can it be possible to synthesize ZnO NPs using biological sources?
2. Would it be possible to synthesize plant oil encircled ZnO NPs to enhance antimicrobial activity?
3. How to formulate biobased ointment using natural biomaterials like ELN/COL matrix, organic body fluids (lactic acid) and biosynthesized ZnO NPs?
4. Can it be possible to synthesize biobased ointment from an entirely natural source?
5. Can it be possible to enhance antimicrobial activity and UV light absorbing property of biobased ointment by using biosynthesized ZnO NPs?

1.3. Statement of the problem

So far, various techniques of synthesizing ZnO NPs, such as physical and chemical methods, have been employed. But these methods require strict conditions such as high temperature, high pressure, long reaction times, need expensive raw material, and complicated equipment. For the growing demands of synthesizing environmentally friendly nanoparticles, researchers have used new strategies for the biosynthesis of NPs from biological materials to overcome problems caused by conventional physical and chemical methods. Thus, bio-synthesis of ZnO NPs was proposed to overcome the side effects of conventional physical and chemical methods.

Waste disposal and by-product in the food processing industry pose problems in environmental protection and sustainability (Article, 2012). The global poultry population has been estimated to be about 16.2 billion, with 71.6 % in developing countries (Milkias, 2016). As reports indicate,

the total chicken population in Ethiopia was estimated to be 49.3 million (Mulugeta et al., 2020), and national poultry meat production is beyond 76 million kilograms per year (Wilson, 2010). Poultry meat exporting industries are increasing over time in Ethiopia. Recently, commonly facing waste from the poultry meat processing industry is broiler skin waste. A large quantity of broiler skin waste is exposed to the environment that highly causes environmental pollution. If we consider local market in Adama city only, minimum of 300 to 400 broiler skin per day have been disposed to environment. So, to solve this problem, extracting COL/ELS proteins from broiler skin waste was required. COL/ELS have great biomedical applications.

Globally, solar UV radiation that strikes the surface of the Earth enormously increased due to the depletion of the ozone layer produced by global warming (Nations et al., 1994). Skin is exposed to various environmental factors like UV radiation that originates naturally from the sun due to its anatomic location at the external boundary of the body. Solar UV exposure is the leading cause of age-related changes and skin cancer. UV exposure may account for up to 80% of skin aging signs, including dry appearance, scalping, wrinkling, impaired pigmentation and photoaging associated with various skin cancers (Orazio et al., 2013)(Amaro-ortiz et al., 2014). So, to overcome these problems, other protective measures and skincare products that can absorb UV radiation must be developed. Biosynthesized ZnO NPs have such capability to absorb UV radiation and keep our skin safe from problems caused by environmental factors. It also has a significant effect on combating bacterial infections. It was supposed that biosynthesized ZnO NPs could be more effective against UV radiation if combined with natural biomaterials like COL/ELS proteins to synthesize sunscreen.

Biomaterials are engineered materials that can play an essential role in human or animal biologic systems to perform their proposed function (Zarubica, 2020). Even though engineered biomaterials have many applications, developing skin care products from biomaterials has gained attention because most skincare products were derived from petroleum derivatives like mineral oil, soft white, yellow paraffin, hard paraffin, and cetostearyl alcohol. Researches revealed that with the increase in mineral oil saturated hydrocarbon, there is an increased accumulation of mineral oil over time in human fat tissue with age. It is toxic, does not metabolize with our system, and tends to cloggy skin pores. Even though petroleum derivative ointment base tends to keep skin moisture and reduce overexposure to sunlight, it is incompatible with living systems. Therefore, it was

required to find a biobased and biocompatible ointment base from natural biomaterials like COL/ELS and organic body fluid like lactic acid as a carrier. Enhancing the activity of biobased ointment derived from natural biomaterial like COL/ELS by introducing NPs hasn't been investigated. Its effect on antimicrobial activity and UV light absorbance hasn't been explored.

In general, this thesis proposed bio-synthesis of ZnO NPs from moringa oleifera leaf extract and the development of biobased ointment using bio-synthesized ZnO NPs and bioconjugate via fusion method. Biobased ointment developed could be used for skincare application and could have enhanced antimicrobial activity and UV light absorbing/screening characteristics due to the ZnO NPs incorporated into it. It could also overcome drawbacks associated with petroleum-derived ointment and is the best candidate for a skincare application.

1.4. Objectives

1.4.1. General objective

The general objective of study was to synthesize ZnO nanoparticles using biological methods and studying its effect on the antimicrobial activities and light absorption characteristics of biobased ointment.

1.4.2. Specific Objectives

The specific objectives of the study were: -

1) To select, extract and characterize phytochemical components from Moringa oleifera leaf for the biosynthesis of ZnO NPs.
2) To biosynthesize and characterize ZnO NPs and to study the effect of different reaction parameters on the biosynthesis of ZnO NPs.
3) To extract collagen/elastin matrix from broiler skin and to synthesize bioconjugate from collagen/elastin matrix and lactic acid.
4) To study organoleptic characteristics of biobased ointment
5) To investigate the effect of biosynthesized ZnO NPs on antimicrobial and light absorption characteristics of biobased ointment.

1.5. Significance of the Study

The development of an eco-friendly approach for the synthesis of ZnO NPs appears to be the best alternative to conventional physical and chemical synthesis methods. Green synthesis of ZnO NPs can eliminate the drawbacks occurred by traditional synthesis techniques. It is simple, cost-effective, nontoxic, has good stability, and is less toxic and safe for humans and animals than other metal oxide NPs. ZnO NPs used in a lot of biomedical applications. This thesis proposed the development of a biodegradable and biocompatible green template as a carrier for biosynthesized ZnO NPs for its activity in antimicrobial and UV radiation absorbing ointment for skincare application.

Reducing environmental pollution caused by waste broiler skin was another great significance of this study. Due to the increase in poultry meat exporting industries over time in Ethiopia, commonly facing waste from the poultry meat processing industry is broiler skin waste. A large quantity of broiler skin waste is exposed to the environment that highly causes environmental pollution. So, COL/ELS proteins from broiler skin waste were extracted and used to develop biobased ointment. It is economically feasible and environmentally safe too. Several biomedical applications of COL/ELS can motivate other researchers to design their study area in this regard.

This thesis has tremendous significance in assuring the synthesis of an alternative form of ointment bases entirely from biobased, green, and compatible natural biomaterials for ointment formulation. The other primary importance of this study was replacing petroleum derivatives ointment base with the biobased ointment base. Bio-based ointment developed can substitute synthetic or petroleum-based ointment and overcome side effects associated with it.

1.6. Scope of the study

The scope of this thesis work was bounded within the given time and resources. This thesis work has covered the following sections. First, solvent selection and extraction of phytochemical components from Moringa oleifera leaves for the biosynthesis of ZnO NPs and their characterization. Secondly, biosynthesis of ZnO NPs using Moringa oleifera leaf extract and studying the effect of different reaction parameters such as reaction temperature, nucleation time, the volume of Moringa oleifera leaf extract to precursor solution, precursor concentration, and its characterization using analytical instruments. Thirdly, extraction of COL/ELS matrix from broiler

skin, synthesis of bioconjugate from extracted COL/ELS matrix, and lactic acid and its characterization. Fourth, studying organoleptic characteristics of ZnO NPs dispersed biobased ointment. Finally, an investigation of the effect of biosynthesized ZnO NPs on antimicrobial and light absorption characteristics of biobased ointment was covered.

1.7. Challenges and limitations of the study

The limitation of this thesis was determining actual particle size of biosynthesized ZnO NPs by transmission electron microscope (TEM) due to difficulties of finding instruments. Instead, XRD analysis was done to determine the crystalline size of biosynthesized ZnO NPs.

1.8. Thesis Organization

This thesis was organized into five chapters.

Chapter - 1: Presents introduction of the thesis work, motivation of study, research questions, statement of the problems, study objectives, significance, scope, challenges, and limitation of the study.

Chapter - 2: Discusses the relevant literature related to works regarding the biosynthesis of ZnO NPs, its synthesis methods, application areas, ointments in general and biobased ointment in particular; other important terminologies regarding the study was also included.

Chapter - 3: Describes the methodology followed in this thesis work. All necessary procedures and methods were stated clearly and included.

Chapter - 4: Presents the results and discussions. It involves a brief discussion of the results obtained, followed by an appropriate characterization instrument. Results of all specific objectives proposed were achieved and interpreted accordingly and compared with other related works to have the best judgment.

Chapter - 5: Presents the conclusions for results obtained and forwards further studies to be done in the future as recommendations.

CHAPTER TWO

2. LITERATURE REVIEW

2.1. Biomaterials

Recently, biomaterials have been the most researched and rapidly developing field of the study area. The word 'biomaterial' was established in the mid-twentieth century, but biomaterials have been used much earlier. The history of biomaterials shows a steady growth of interest in using foreign substances to heal and repair the human body and the development of the capability to use more sophisticated materials for these purposes. The field has grown significantly in the past decade due to discoveries in tissue engineering, regenerative medicine, drug delivery, cosmetics, etc., and is biocompatible with the human body (Kulinets, 2015).

Biomaterials are any materials coming in contact with human or animal biological systems to perform their intended function. It is characterized as any material or the combination of materials other than medicines of synthetic or natural origin, which can be used for any period and play the role of enhancing and or partially or wholly replacing a tissue, an organ, or a function of the body (Zarubica, 2020).

Biomaterials are derived from biological sources used for therapies or describe materials used for implant in the human body. It can be synthetic or natural and used in medical applications to support, enhance, or replace damaged tissue or a biological function (Patel & Gohil, 2012). A biomaterial is intended to interact at the interface of biological systems. Biomaterials are designed based on application needs.

A biomaterial must be biocompatible, i.e., it should be friendly to the biological system and not harm the system, whether at the cellular level or the system level. A biocompatible material should be able to perform its intended function in a specific application without the presence of adverse reactions. This emerging science requires and pushes unique multidisciplinary boundaries based on understanding and integrating concepts from various fields such as chemistry, biology, materials science, mechanical, chemical, electrical engineering, and medicine. Biomaterials are used to augment, repair or replace any tissue, organ, or function of the body that has been lost through trauma, disease, or injury (Bose & Bandyopadhyay, 2013).

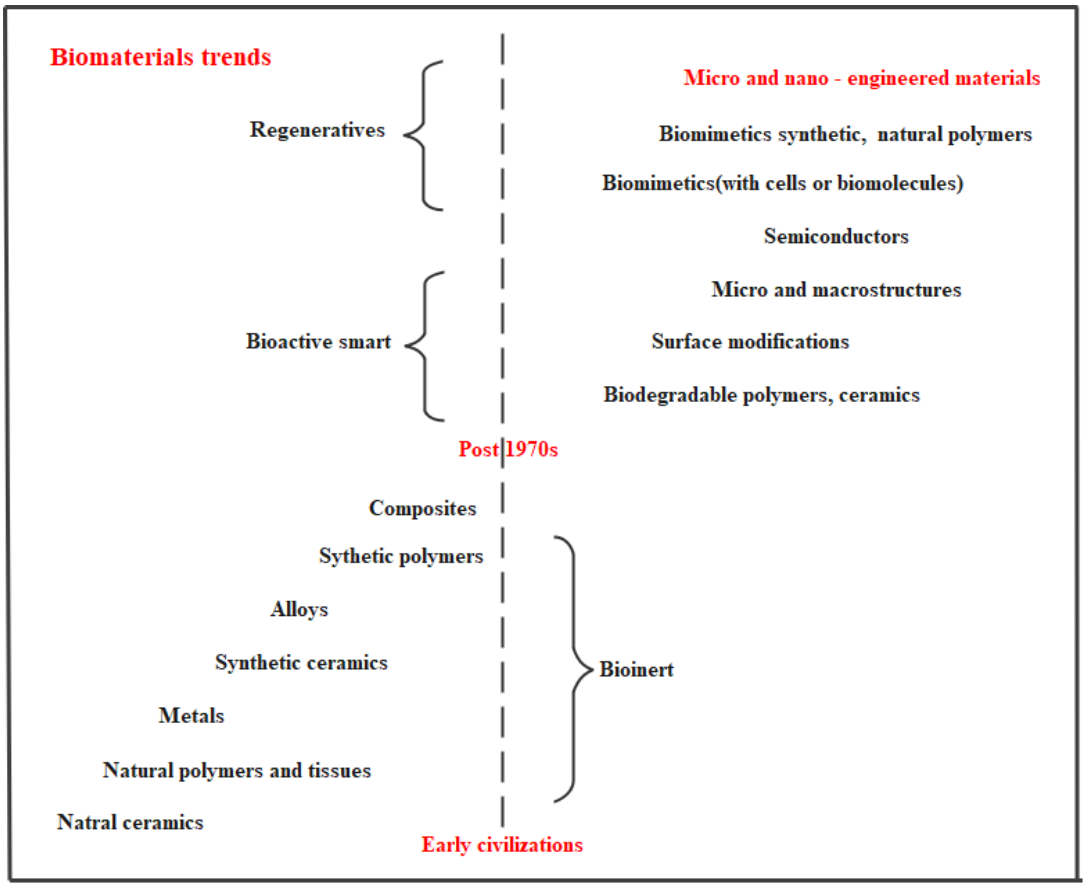

Figure 2 - 1: Illustration on the trend of biomaterial development (Bose & Bandyopadhyay, 2013)

2.2. Types of biomaterials

Biomaterials are mainly categorized into three (Kulinets, 2015): these are synthetic biomaterials (metals, polymers, ceramics, composites), nature-derived biomaterials (e.g., plant-derived, tissue-derived), and semi-synthetic or hybrid biomaterials. Recently, nature-derived biomaterials got attention from most scholars and scientists due to the problems of toxicity often presented by synthetic materials.

2.2.1. Natural biomaterials

Natural materials are often similar, if not identical, to materials that the biological system can recognize and process through metabolic pathways. Natural materials usually allow avoiding the problems of toxicity often presented by synthetic materials (Kulinets, 2015).

Natural biomaterials are principally composed of three types of biopolymers:

- ✓ Proteins - chains of amino acids (silk, collagen, elastin, fibrin)
- ✓ Polysaccharides - chains of sugar (chitin, glycosaminoglycans)
- ✓ Polynucleotides - chains of nucleotides (DNA, RNA)

Natural biomaterials might be derived from plants, animals, or humans. Natural biomaterials are mostly reparative materials with a similar structure to the native tissue they are intended to replace and have many elements helping tissue reconstruction, repair, and regeneration. Natural biomaterials have not been well researched until recent times, and they were not widely used until recent decades. Natural biomaterials have now been identified as facilitators and promoters of healing, specifically tissue repair and regeneration (Kulinets, 2015).

Protein-based biomaterials have multiple and advanced applications in biomedical fields. Its application in the internal and external body surface, like the skin, has been recently researched. Skin is one of the body's critical organs that is eventually injured, often induced by chemical or physical injuries and microbial infections following the burn, pathogens, and exposure to environmental factors (e.g., chemical products, pollution, infrared and ultraviolet radiation), etc. (Yu et al., 2017). To minimize microbial infections and replace the tissue that has been destroyed and injured skin cells, biobased products (biomaterials) developed from skin materials like collagen and elastin protein play a key role.

2.2.2.1. Elastin

Elastin is an extracellular matrix protein polymer, and it is the major abundant protein in our body next to collagen and provides resilience and elasticity to organs and tissue. It is composed of elastic fibers, which give elasticity to tissues in the body found primarily in connective tissue in combination with collagen and polysaccharides. Elastin is a biopolymer of amino acid chains with high elasticity. It is located in the body where this property is essential, particularly in arteries where it aids blood flow. Elastin is also necessary for the lungs, elastic ligaments, skin, and bladder. The loss of elastin in the skin decreases the skin's flexibility and reduces wound healing ability (Meseret Ewunetu, 2020). Elastin can be incorporated into biomaterials for a range of applications in regenerative medicine and cosmetics when combined with other materials like ZnO NPs.

Elastin forms primary and secondary β sheets or strand-like silk protein. Urry and Venkatachalam attributed the elasticity to a reduction of entropy in the segments linking the β - turns as the coils stretch by developing a model of elastin-like peptides with the repeat (VPGVG)n that formed continuous loops of β-turns (S. Zhang & Duan, 2018).

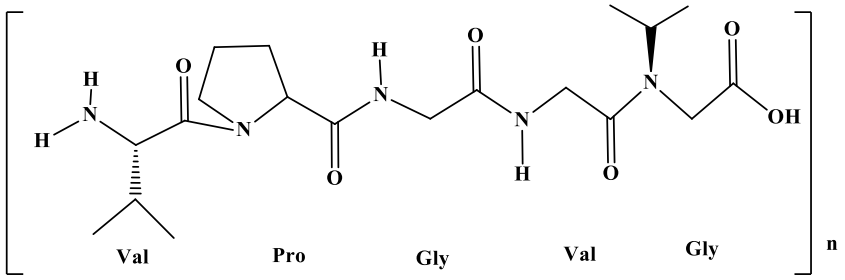

Figure 2 - 2: Amino acid repeating units (VPGVG) of Elastin.

Elastin and elastin-based materials can be obtained by various processes such as electrospinning, wet spinning, freeze-drying, and cross-linking. These can be used in solvent casting to get particles, fibers, gels, tubes, sheets, and films (Yeo et al., 2018).

Extraction of hydrolyzed elastin from an animal source

Commercially, elastin is distributed in powder form and was obtained from animal origin, such as bovine and porcine. The protein accumulates in the animal parts, making the extraction more complicated; hence the final product is expensive (Mecham, 2008). So, finding a cheaper and easier alternative with high throughput is a significant concern for elastin extraction. Hydrolyzed soluble elastin has been extracted from waste poultry skin in this work following a similar protocol used by Lansing et al. to extract elastin from broiler skin using hydrolysis of the skin by NaOH. From his work, elastin having some amount of collagen was successfully extracted (Nadalian et al., 2019). Meseret E. also successfully extracted elastin with some collagen from broiler skin using hydrolysis of the broiler skin by NaOH (Meseret Ewunetu, 2020).

It has been reported that the consumption of water-soluble elastin prepared from several animal sources positively influences human health and beauty. For example, the ingestion of water-soluble elastin improved the skin condition, such as improvement in texture and moisture of the skin. Hydrolyzed COL/ELS are major ingredients for cosmetics (moisturizing, anti-aging, and anti-wrinkle), and it is a tool for restoring, smoothing, and correcting facial deformities (Mecham, 2008) (Nadalian et al., 2019).

2.2.2.2. Collagen

Collagen accounts for about one-third of the protein of humans and two-thirds of the dry weight of skin. Collagen also plays a dominant role in maintaining the biological and structural integrity of the ECM and is a dynamic and flexible material that undergoes constant remodeling to refine cellular behavior and tissue function. Collagen is the main constituent of connective tissue and is the most abundant protein in animals, constituting 25% of total protein mass. It is found in the extracellular matrix and fibrous tissue (Chattopadhyay & Raines, 2014).

The first reported collagen biomaterial was biodegradable sutures, termed "catgut," which is a collagen biomaterial derived from the intestines of sheep. The term collagen does not refer to a single protein but a family of proteins. Collagen is the most abundant protein in animals. This fibrous, structural protein comprises a right-handed bundle of three parallel, left-handed polyproline II-type helices. Pro, Hyp, and Gly are the most common triplet (10.5%) collagen (Chattopadhyay & Raines, 2014).

Both collagen and elastin are essential structural proteins widely expressed in skin tissues. Skin relaxation during photoaging is manifested by a reduction in the content of collagen And elastin in the skin. Collagen accounts for 75% of the dermal composition and is the main component of the dermis. Although elastin only accounts for 2% of the dermal design, it has a vital function to promote the homeostasis of the skin (Abdulkhani et al., 2014).

So, collagen and elastin in the skin play an essential role in skin health. With the body's aging, collagen and elastin fibers may show signs of aging, like cross-linking and breakage. Reduction of collagen and elastin causes an increased stiffness and decreasing elasticity in the skin and more frequent formation of wrinkles that are a typical symptom of skin aging (Z. Zhang et al., 2020).

The collagen structure is organized as follows: amino acids form the primary structure; the secondary structure is the local chain configuration of the Gly-X-Y peptide; the tertiary structure is the triple-helix molecule, and the quaternary structure is the arrangement of triple-helix molecules to form microfibrils. Type I collagen occurs mainly in the skin, vessel, and tendons, and type II is the predominant collagen in cartilage, and type III collagen is found in the walls of blood vessels. Conversely, type IV collagen is a membrane constituent that separates the epithelial tissue

of mesodermal tissues. Type I collagen is the most abundant type in animals and is the most commonly used in biomedical applications (G et al., 2019).

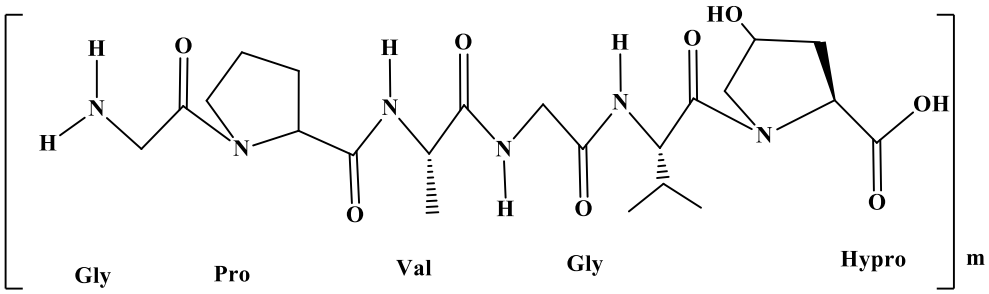

Figure 2 - 3: Repeating amino acid (GPVGVHYP) unit of collagen

The main biomedical applications of collagen are burn/wound cover dressings, resorbable surgical sutures, osteogenic and bone filling materials, hemostatic agents, and immobilization of therapeutic enzymes (Chattopadhyay & Raines, 2014).

Collagen is a crucial component in wound healing, providing a natural scaffold or substrate for new tissue growth. Thus, collagen plays an essential role in all phases of wound healing, including hemostasis, inflammation, proliferation, and remodeling. Collagen formulations for wound healing have general advantages over conventional dressings in terms of ease of application and being natural, nonimmunogenic, nonpyrogenic, hypoallergenic, and pain-free. Collagen enables wound healing by organizing and accumulating freshly formed fibers and granulation tissue in the wound bed, thus creating the optimal physiological interface between the wound surface and environment (Horch & Stark, 1998).

Hydrolyzed collagen, extracted from broiler skin, pigs, and fish, is a popular ingredient considered an antioxidant. This low molecular weight protein has been widely utilized due to its excellent biocompatibility, easy biodegradability, and weak antigenicity. It is a safe cosmetic biomaterial with good moisturizing properties on the skin. Like elastin, collagen also has antioxidant characteristics and is crucial in skincare treatment (Aguirre-Cruz et al., 2020). Collagen is used in the cosmetic industry and used in pharmaceuticals and the beverage, food, and health care areas. Biopolymers often used in cosmetics and pharmaceutical sectors are collagen, elastin, and lactic acid, a monomer of polylactic acid, a biodegradable and sustainable polymer.

2.2.2.3. Lactic acid

Lactic acid ($CH_3CHOH\ COOH$) is the most widely occurring hydroxycarboxylic acid. It was first discovered in 1780 by the Swedish chemist Scheele. Lactic acid is a naturally occurring organic acid that can be produced by fermentation or chemical synthesis. It is present in many foods both naturally or as a product of in situ microbial fermentation. Traditionally, the principal use of lactic acid is in food (e.g., as an acidifier, for preservation and flavoring) and cosmetics. With the development and commercialization of biopolymers, lactic acid use has increased considerably (Henry, 2006; Lübeck & Lübeck, 2019).

Lactic acid has long been used in pharmaceutical and cosmetic applications and formulations, particularly in topical ointments, lotions, parenteral solutions, and biodegradable polymers for medical applications such as surgical sutures, controlled-release drugs, and prostheses. A substantial part of pharmaceutical lactic acid is used as sodium salt. L (+)-lactic acid and D (–)-lactic acid is two optical isomers of lactic acid. Lactic acid can be obtained as optically pure L (+)- or D (–)-lactic acid or racemic DL-lactic acid. Di-lactide, also commonly termed lactide, is the primary feedstock for polymerization to make high molecular weight polymers of lactic acid (PLA) biodegradable thermoplastics. The L-isomer of lactic acid is the preferred feedstock for di-lactide production because it provides a high di-lactide yield and a high molecular weight polymer with a high degree of crystallinity and tensile strength (Henry, 2006; Lübeck & Lübeck, 2019).

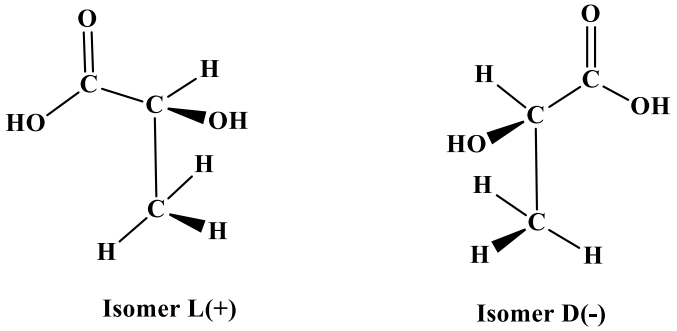

Figure 2 - 4: Structure of D (+) and L (-) isomers of the lactic acid

Lactic acid is water-soluble unglues dead cells to reveal brighter, provide additional moisture to the outer skin layers, accelerate cell turnover, balance skin's pH level. Applying lactic acid in skin regularly improves signs of aging, stimulates collagen and elastin renewal, and secures the skin from UV light (Jarrar, 2015). Lactic acid oligomer grafted biopolymers were significant areas that

have been accessed. The growth of lactic acid oligomer occurs due to free amino groups of gum and hydroxyl groups of lactic acid (Tripathi & Katiyar, 2018). In this work, Lactic acid oligomer grafted collagen and elastin were used to synthesize ointment base and, in turn, used to develop ointment in combination with nanoparticles. Notice that lactic acid is a naturally occurring organic acid mainly produced in muscle cells and red blood cells. It forms when the body breaks down carbohydrates to use for energy when oxygen levels are low. That is why lactic acid is used as a binding agent in developing an ointment base.

2.3. Ointment

An ointment is a homogeneous, viscous, semi-solid preparation intended for external use on the skin or mucous membranes; commonly, they are a greasy or thick oil with a high viscosity. They serve as protective, therapeutic, or prophylactic and are used as emollients or apply active ingredients to the skin. Ointments can be categorized as medicated and unmedicated ointments. Medicated ointments contain a medicament dissolved, emulsified, or suspended in the base, and non-medicated ointments are used for emollient or lubricating effects and the preparation of medicated ointments (El-Gied et al., 2015).

Some of the ideal properties of ointment bases are: it should not retard wound healing, pharmaceutically elegant, release the medicament efficiently at the site of application, have a low index of irritation, non-greasy and neutral in reaction, compatible with common medicaments, and also with the skin, easily washable with water, have the minimum number of ingredients, remain stable on storage, economical and easy to transport, should be inert, odorless, smooth, etc. (Bhaskar et al., 2016). All ointments contain an ointment base that acts as a drug carrier and is also used as a moisturizer for dry skin.

2.3.1. Types of Ointment Base

Ointment bases are generally classified into four groups. These are (Bhaskar et al., 2016):

1. Oleaginous bases. They are also termed hydrocarbon bases. On application to the skin to emollient effect, occlusive and dressings protect against the escape of moisture.
2. Absorption bases. Two main types of absorption bases: those which allow the incorporation of aqueous solutions resulting in the creation of water-in-oil emulsions

(e.g., hydrophilic petrolatum) and those which are water-in-oil emulsions and require additional amounts of aqueous solutions (e.g., Lanolin) to be incorporated.

3. Water removable bases. Are oil-in-water emulsions resembling creams in appearance? Due to the aqueous external phase of the emulsion, they are easily washed out of the skin and are often called 'water washable' bases. They may be diluted with water or aqueous solutions, e.g., hydrophilic ointment.
4. Water-soluble bases: Water-soluble bases do not contain oily components. These are fully water-washable and are sometimes branded 'greaseless.' Since they significantly weaken with the addition of water, these bases do not readily absorb significant volumes of aqueous solutions.

Most ointment bases contain petroleum derivatives like mineral oil, soft white paraffin, soft yellow paraffin, hard paraffin, and cetostearyl alcohol (Bhaskar et al., 2016; Mahendran & Abdul Rashid, 2016). Even though petroleum derivative ointment keeps skin moisture and reduces overexposure to sunlight, it negatively impacts compatibility with living systems. Researches show that with the increase in mineral oil saturated hydrocarbon, there is an increased accumulation of mineral oil over time in human fat tissue with age. It is toxic, does not metabolize if gated to the system, and tends to cloggy skin pores (Meseret Ewunetu, 2020). Therefore, finding a biobased and biocompatible ointment base from natural biomaterials like collagen and elastin to develop biobased ointment was required. A biobased ointment can be more effective and safer than a conventional one because of its nontoxic nature. Biobased ointment plays a crucial role in solving problems that happen due to synthetic ointments.

2.3.2. Preparation of Ointments

Ointments can be prepared in two ways (Bhaskar et al., 2016; Ghosh et al., 2019):

1. Mechanical incorporation: In this method, ointments are synthesized with the help of Mortar and pestle, ointment slab and spatula, ointment mill.
2. Fusion methods: In this method, all or some of the components of an ointment are combined by being melted together and cooled with constant stirring until thickened.

Researchers commonly use fusion methods for ointment formulation. Components not melted are added to the thick ointment base mixture as it is being cooled and stirred. Naturally, heat-labile

substances and any volatile components are added last when the mixture's temperature is low enough not to cause decomposition or volatilization of the features. Medicated ointments and ointment bases containing beeswax, paraffin, stearyl alcohol are prepared by fusion (Meseret Ewunetu, 2020).

In the preparation of ointments having an emulsion base, the method of manufacture involves both melting and an emulsification process. The water-immiscible components such as the oil and waxes are melted together in a steam bath to about 70-75 ℃. and an aqueous solution of the heat-stable. Water-soluble components are prepared and heated to the same temperature as the oily components. Then the aqueous solution is slowly added with mechanical stirring to the melted oleaginous mixture. The temperature is maintained for 20 - 30 minutes, and the mixture is gradually cooled with stirring until firm (Usha & Ashish, 2015). Fusion methods also formulated a biobased ointment in this research. Biobased ointment as a biomaterial plays an integral role by restoring function and facilitating healing for people after injury.

Recently, nanotechnology's innovative and impressive development has led to massive growth in nano-drug delivery systems for wound healing and skin regeneration. Additionally, nanoparticles of metals and their oxides have emerged in recent years with a broad range of applications in the biomedical field (V. Gupta et al., 2020). One of the biomedical applications also touches ointment science.

Concerning the technology applied in medication preparation, nanoparticles as a medication medium have been developing rapidly in recent years. One of the advantages of nanoparticles technology is increasing the compound solution and decreasing medication dosage. Moreover, nanoparticles keep the skin hydrated, permeate through the skin, and improve skin stability (Lisnawati et al., 2019). This work aimed to use nanomaterials to formulate bio-based ointment in skincare applications and to study its properties.

Nanotechnology is emerging as a new field of research dealing with the synthesis of NPs and nanomaterials for applications in various fields. (Syedmoradi et al., 2017). The particles whose size lies in the dimension area of 1–100 nm are called nanomaterials, and these materials are found to show enhanced properties based on size, distribution, and morphology (Charinpanitkul et al., 2008).

Recent advances in nanotechnology, particularly the ability to prepare highly ordered particulates of any size and shape, led to new biocidal agents. Nanomaterials are called a "wonder of modern medicine." Inorganic metal and metal oxide nanoparticles have been of great importance due to their distinctive catalytic, optical, magnetic, electronic, and antimicrobial, wound healing, and anti-inflammatory properties (Durán et al., 2005; Taylor et al., 2005).

Metal and metal oxide NPs possess a unique and broad range of physicochemical properties. Compared to their bulk materials, they possess enhanced chemical, electrical, optical, thermal, mechanical, electromagnetic, and surface properties. Au, Ag, Pt, Pd, Cu, CuO, Ni, NiO, Zn, ZnO, Iron oxide, titanium dioxide, and cerium oxide are commonly used metal and metal oxide NPs (Sajid & Płotka-Wasylka, 2020).

Over the last few decades, metal oxide nanoparticles have been studied extensively because of their potential applications in catalysis, sensors, environmental remediation, medicine, optics, electronics, solar cells, rubber, concrete, foods, cosmetics, personal care products, as well as their wound healing, anti-inflammatory, and antimicrobial properties. Among the metal oxide nanoparticles, zinc oxide has gained significant interest because of its substantial properties and its biomedical application in sunscreens to protect against UV induced skin damage, such as sunburn, cancer, premature aging, and photoallergies' (Cross et al., 2007)

2.4. zinc oxide nanoparticles

Among various nanoparticles, ZnO NPs have advantages because of their extraordinary physical, chemical, and biomedical properties. It is one of the cheap materials in the cosmetic industry, nano fertilizers, electrical devices, suitable agents for bioimaging, agent for targeted drug and gene delivery, an excellent sensor for detecting ecological pollutants and environmental remediation. It has good conductivity, optical, piezoelectric, magnetic and gas sensing, chemical stability, and, most importantly, antifungal, antibacterial and antiviral activities, which have made ZnO NPs necessary for scientific and industrial applications. Besides these properties, ZnO NPs exhibits high catalytic efficiency, strong adsorption and are used frequently in the manufacture of sunscreens, ceramics, rubber processing, and wastewater treatment. Thus, zinc oxide (ZnO) has been gaining attention in the recent past owing to its unique properties and abundant applications (Akbar et al., 2020; Jin et al., 2020; Naveed et al., 2017).

Zinc plays a vital role in maintaining the body's metabolism through hematopoiesis, enzyme regulation, maintaining cell redox balance, and DNA and protein synthesis machinery regulation (Agarwal & Shanmugam, 2020). It is an essential mineral for our body and is present in several major body parts, like the brain, muscle, bone, etc. (Jiang et al., 2018). It activates several enzymes that help synthesize proteins and nucleic acid in our body (Ruszkiewicz et al., 2017). It also acts as an antioxidant, helps in protein digestion, blood clotting, and bone metabolism. Zinc oxide, a source of the essential trace element Zinc, locally affects the skin area, releasing Zinc ions that saturate damaged tissues and promote accelerated regeneration of damaged skin (Blinova et al., 2021).

ZnO NPs have been generally recognized as safe (GRAS) material by the US Food & Drug Administration(V. Gupta et al., 2020)(Agarwal & Shanmugam, 2020). Like elemental zinc, ZnO NPs are also biocompatible towards normal mammalian cells due to their low dissolution rate but causes oxidative stress and subsequent cell damage within cancer cells. Their rapid dissolution into Zn^{2+} ions is slightly acidic pH; thereby, ZnO NPs show pH-responsive cytotoxicity. Besides, ZnO NPs exhibit various biomedical applications in tissue engineering, drug delivery systems, bioimaging and can also be used as antibacterial, antioxidant, and antidiabetic agents. ZnO NPs can easily be prepared from their several low-cost precursors (T. A. Singh et al., 2020).

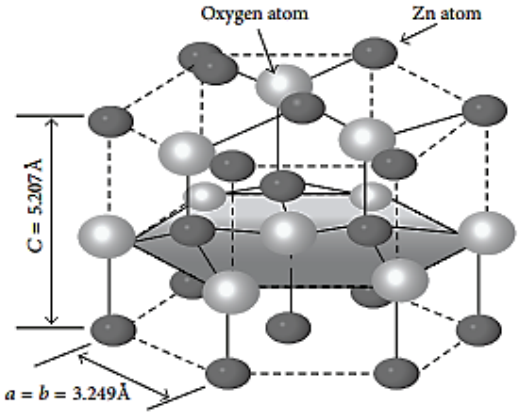

Figure 2 - 5: Hexagonal wurtzite structure of ZnO NPs

Being excellent biocompatible, bio-safe, good chemically stable under harsh process conditions, nontoxic inorganic material, ZnO NPs finds tremendous applications in different areas. ZnO NPs are also used for surgical instruments coating, screen lotion as UV light blockers, food preservatives, etc. (Mirzaei & Darroudi, 2017b). According to USFDA, ZnO NPs are nontoxic and

low-cost (Vidhya et al., 2020). Moreover, ZnO has the potential to enhance the potency of antimicrobial activity.

2.4.1. Synthesis methods of ZnO NPs

ZnO NPs are synthesized by physical, chemical, and biological methods, and these methods can be broadly classified into bottom-up and top-down approaches (Basnet et al., 2018; Rana et al., 2020).

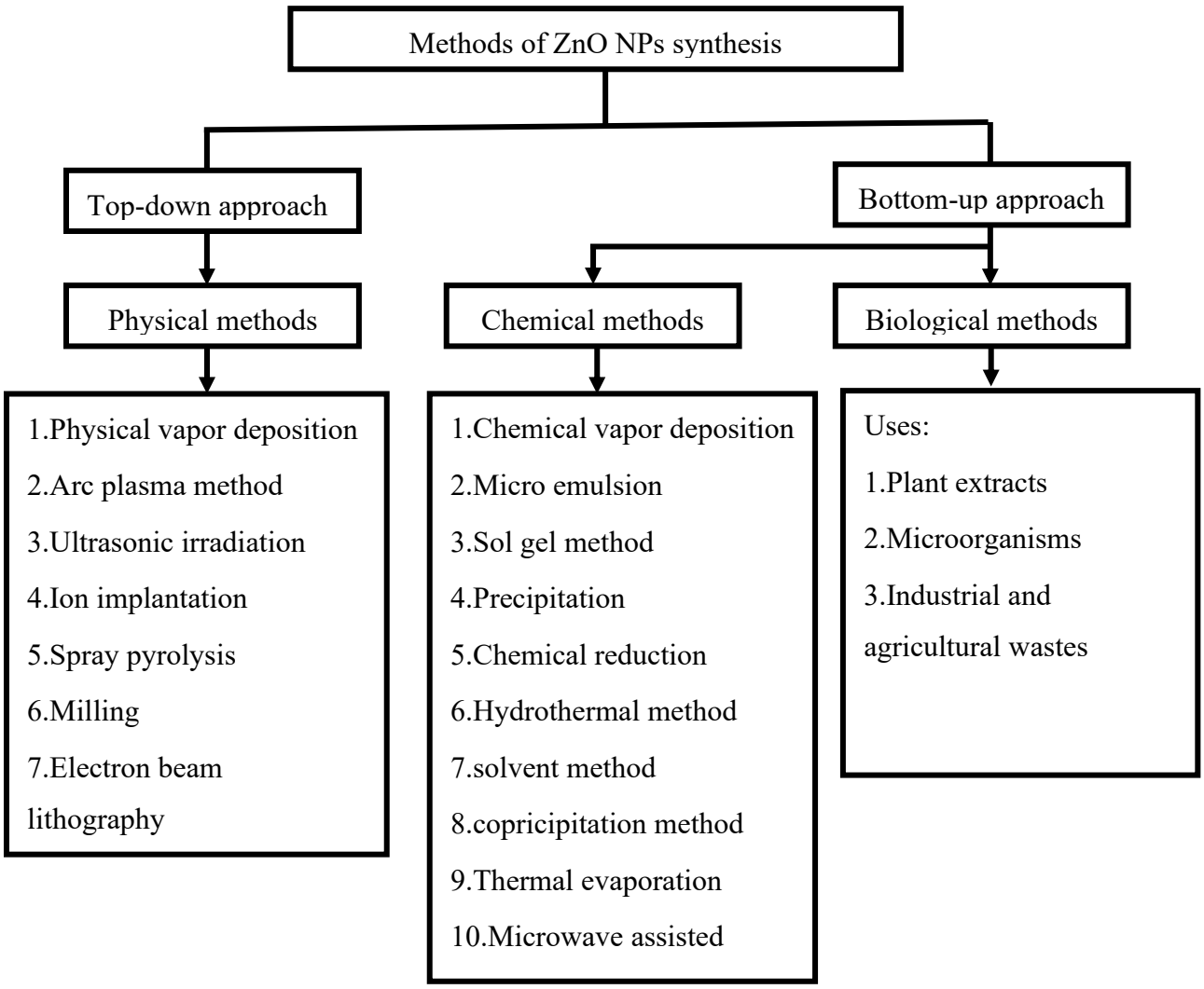

Figure 2 - 6: Block diagram for different methods of ZnO NPs synthesis

Researchers have utilized in-experienced strategies to synthesize varied metal oxide nanoparticles for pharmaceutical applications (Mirzaei & Darroudi, 2017b). Biosynthetic and environmentally

friendly technology for the synthesis of ZnO NPs is believed to be nontoxic, bio-safe, bio-compatible. Biosynthesis of zinc oxide nanoparticles was the primary goal of this study.

2.4.1.1. Biosynthesis of ZnO NPs

Conventional physical and chemical synthesis methods require harsh conditions such as high-temperature, high-pressure, long reaction times, need expensive and complicated equipment, require toxic or hazardous chemicals with potentially adverse effects which environmental pollution (Uma & Xin, 2016). Due to this reason, the biosynthesis of ZnO NPs has emerged as an eco-friendly alternative. Biological synthesis methods use either plant extract or microbes for facilitating the formation of nanoparticles (Pillai et al., 2020). Natural processes have become more known as green synthesis because they agree with the twelve principles of green chemistry (Anastas & Eghbali, 2010). Nowadays, these principles are considered the fundaments to contribute to sustainable development and comprise instructions to implement new chemical products, new synthesis, and new processes. Sustainability of the environment and minimizing waste generation is the main idea behind green or biosynthesis.

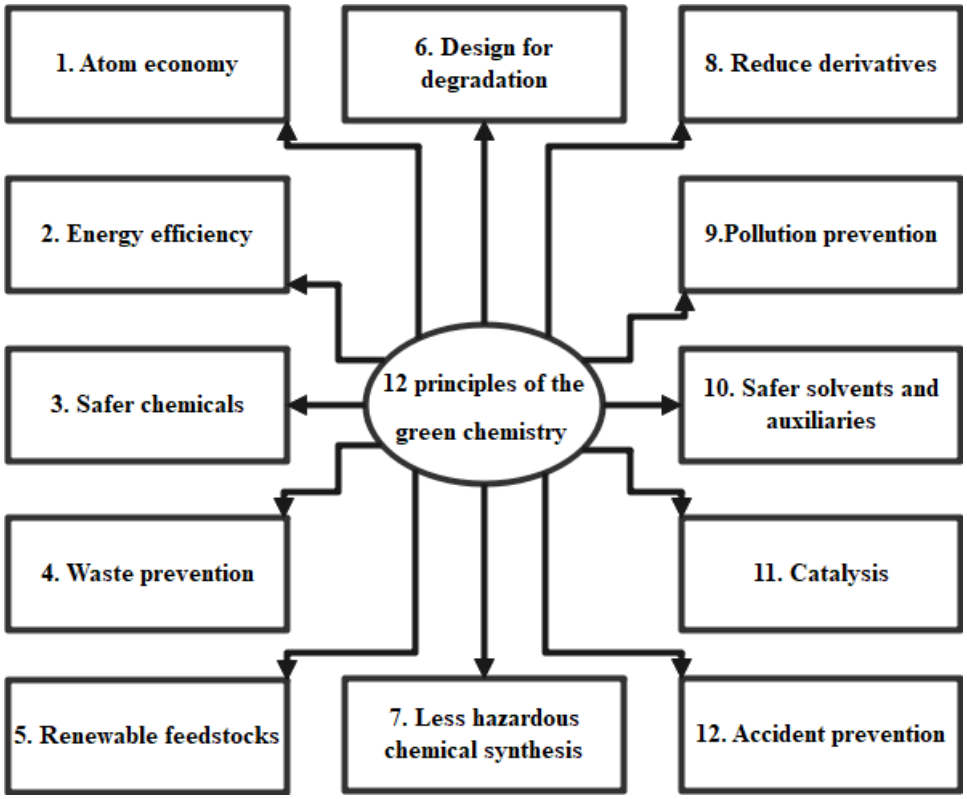

Figure 2 - 7: Twelve principles of the green chemistry (Anastas & Eghbali, 2010)

2.5. Biological substrates used to synthesize ZnO NPs

Essentially, green synthesis uses biological substrates such as plants, bacteria, fungus, and algae to replace chemical solvents and stabilizers to decrease the toxicity of both product and process (Król et al., 2017). Plants are the most common biological substrate used for the green synthesis of nanoparticles with metallic ions. This might be related to the fact that there is no exposure to health risks or concerns about safety issues related to hazardous microorganisms during the process. Vegetal substrates are believed to be more cost-effective, easy to process, and less toxic than microorganisms (Kharissova et al., 2013).

2.5.1. Plants

Plants are the most preferred source of NPs synthesis because they lead to largescale production and stable, varied shape and size NPs. Bio-reduction involves reducing metal ions or metal oxides to zero valence metal NPs with the help of phytochemicals (Heinlaan et al., 2008). In addition, plant extracts can be obtained straightforwardly by exposing the plant to a solvent, which is usually distilled water or ethanol (Chekki & Snoussi, 2016).

Plant-mediated synthesis of ZnO NPs involves a sequence of simple steps leading to the production of environment-friendly NPs. The process minimizes the risks associated with the utilization of chemical and physical methods. The initial steps (top to bottom) include washing plant material and boiling in distilled water to obtain the extract. Few subsequent yet simple and carefully observed steps, i.e., the mixing of Zinc salt with the plant extract and separation of a liquid part, leads to the accumulation of NPs at the bottom of the tube (Akbar et al., 2020).

Plant parts like leaf, stem, root, fruit, and seed have been used for ZnO NPs synthesis because of the exclusive phytochemicals that they produce. Using natural extracts of plant parts is a very ecofriendly, cheap process, and it does not involve the usage of any intermediate base groups. It takes very little time, does not involve costly equipment and precursor, and gives a highly pure and quantity enriched product free of impurities (Heinlaan et al., 2008).

The bio-reducing and stabilizing agents of the plant extract accumulate and reduce metal ions in the salt solution into nanoscale form. The bio-reducing agents are the phenolic compounds present in plant extracts, such as polysaccharides, amino acids, proteins, enzymes, vitamins, phenolics,

tannins, alkaloids, saponins, and terpenoids. These biomolecules also have medicinal values and are environmentally benign. The mechanism involves three main phases(Akbar et al., 2020).

Table 2 - 1: Main phases involved in the mechanism of plant-mediated NPs synthesis

Activation phase	Growth phase	Termination phase
✓ Reduction of metal ions by the bio-reducing agents (enzymes, proteins, flavonoids, terpenoid, cofactors)	✓ Involves growth and union of tiny particles into larger ones.	✓ Capping and stabilization of nanoparticles by plants biomolecules
✓ Bio-reducing agents present in plant extract bind to the metal ions forming metal ions + metabolites complexes	✓ This process continues until the particle assume a stable shape and size and further reduction of metal ions	✓ Determines the final shape of the nanoparticles

Despite the knowledge of the antioxidants' phytochemical properties, plant extracts constitute an enormous variety of these active compounds in different concentrations (Altemimi et al., 2017). Regarding the green synthesis of ZnO NPs, research indicates that the compounds present in the plant extract react with a zinc salt to reduce or form metal complexes. The general reaction mechanism for zinc nitrate salt is presented as follows (M. R. A. Kumar et al., 2019):

$$Zn(NO_3)_2.6H_2O(s) + \text{Plant extract(l)} + 2NaOH(aq) \longrightarrow ZnO(s) + 2NaNO_3(aq) + 7H_2O + \text{byproduct}$$

The mechanism or route of biosynthesis of ZnO NPs is based on the chemical characteristics of the flavonoids, limonoids, and carotenoids. Antioxidants were believed to chelate the zinc (II) ions and form metal coordinated complexes that are further thermally treated to degrade the complex and form zinc oxide (Fazlzadeh et al., 2017). Another plausible mechanism is that zinc ions in the solution of the natural extract from complexation with the phytochemicals with zinc in the form

of Zn^{+2}. This is then followed by the formation of zinc hydroxide ($Zn(OH)_2$) through hydrolysis, and finally, after calcination, the complex decomposes, thereby favoring the formation of ZnO nanoparticles (Basnet et al., 2018).

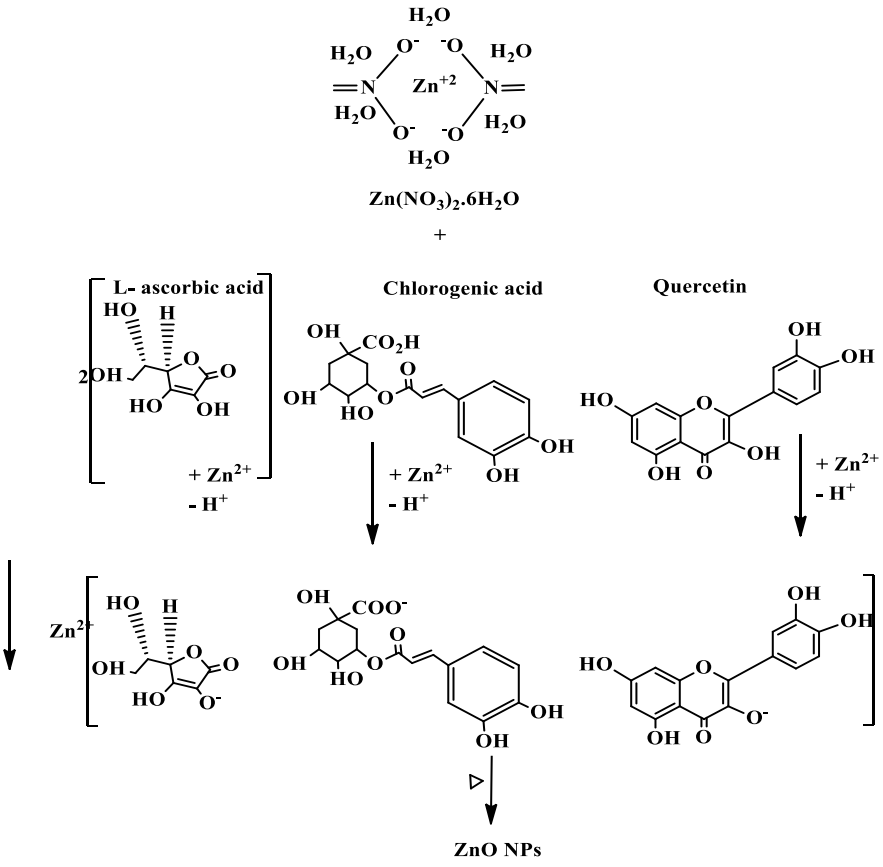

Figure 2 - 8: Synthesis of ZnO NPs via different biological compounds (Basnet et al., 2018)

Conversely, when plant leaves are utilized to produce ZnO NPs, studies have implied that zinc (II) ions are reduced by the plant active compounds to metallic zinc rather than forming a coordinated complex with them. After the bio reduction of zinc, the metallic zinc reacts with dissolved oxygen present in the solution to form the ZnO nuclei. It is also proposed that the plant compounds act as stabilizers, preventing particles and crystal growth (Madhumitha et al., 2019). In this research work, ZnO NPs synthesized using moringa oleifera leaf extract.

2.5.1.1. Moringa Oleifera

MO is a fast-growing tree belonging to the *Moringaceae* family known as a single genus family of shrubs and trees. Its different parts, such as leaves, flowers, and seeds, are used in nutritional,

medical, and environmental domains. The leaves treat diabetes, tuberculosis, fever, stomach aches, ear infections, and skin infections (Ngom et al., 2019). Moringa oleifera is one of the abundant plant materials with a relatively fast growth rate. It is a common vegetable and a good source of protein, beta-carotene, vitamin A, B, C, and E, riboflavin, nicotinic acid, folic acid, pyridoxine, amino acid, mineral, and various phenolic compound, suitable fatty acids. The phenolic compound in MO is a good source of antioxidants and antimicrobials that can be used for pharmaceutical and food industry purposes.

Figure 2 - 9: Moringa oleifera plant

The moringa plant provides a rich and rare combination of zeatin, quercetin, β-sitosterol, caffeoylquinic acid and kaempferol. Various parts of this plant, such as the leaves, roots, seed, bark, fruit, flowers, and immature pods, have medicinal values (Anwar et al., 2007).

2.5.1.2. Significance of moringa oleifera in skin treatment

Ultraviolet radiation, air pollutants, psychological stress, alcohol, smoking, and chemical exposure can make free radicals and reactive oxygen species on the skin. Free radicals are atomic, molecular, or ionic species containing an unpaired valence electron in an atomic orbital, resulting in free radicals' highly chemical reactive properties. Free radicals are highly unstable and have electrons available to react with various biological substances, including lipid molecules, proteins, and DNA, causing cell damage and homeostatic disruption. Excess free radicals generate oxidative stress and damage cell membrane and lipoproteins through lipid oxidation (Athikomkulchai et al., 2021).

The skin has endogenous antioxidants like glutathione, melanin, and enzymatic antioxidants. However, the excess formation of free radicals requires exogenous antioxidants for topical application in preventing oxidative stress. Several studies have shown that oxidation could be prevented by prior antioxidant treatment. Antioxidants protect the skin by reducing free-radical production. Scavenging free radicals with antioxidants can prevent skin aging. Free radicals can trigger the skin's melanin production, causing skin color changes. Antioxidants prevent skin pigment generation by reducing photodamage. In addition, some antioxidants were shown to increase skin hydration to revitalize the skin (Athikomkulchai et al., 2021).

Moringa oleifera is used as a natural antioxidant and moisturizer to prevent skin dryness and aging. It can protect the human skin from environmental influences and combats premature skin aging. Atif Ali et al. reported that moringa leaf extract cream could enhance human skin facial revitalization (Ali et al., 2014). Sirivan Athikomkulchai et al. conducted their work on the physical stability and chemical constituents of moringa oleifera seed oil to improve skin hydration and antioxidant activity (Athikomkulchai et al., 2021).

Chai-Yee Chin et al. used moringa oleifera leaf extract for wound healing applications. They found that aqueous leaf extracts showed the highest human dermal fibroblast and human keratinocytes cells proliferation and migration properties. They also concluded that moringa oleifera leaf extract possesses optimal physicochemical properties as wound dressing (Chin et al., 2018). Likewise, Ana Clara et al. reported MO seeds oil could accelerate chronic skin wound healing capability (Paula et al., 2021). A.B.M. Cretella et al. studied the topical effect of moringa oleifera seed oil on skin inflammation and hyperproliferation. They reported moringa oleifera seed oil significantly reduced chronic skin inflammation and epidermal hypertrophy (Beatriz et al., 2020). Some of the medicinal applications of Moringa oleifera (S. Kumar, 2017) were presented in Figures 2 -10.

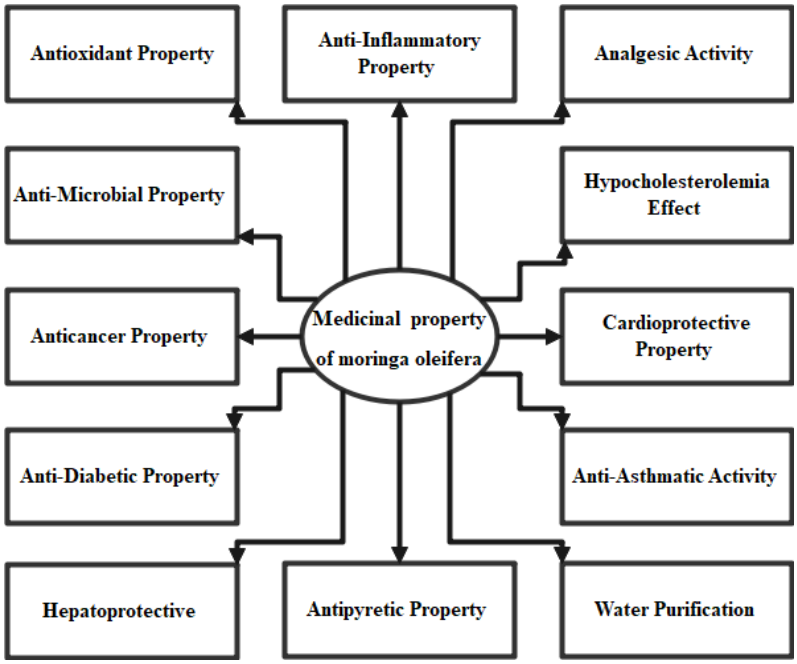

Figure 2 - 10:Medicinal applications of moringa oleifera (S. Kumar, 2017)

MO plant parts can be extracted by different solvents such as methanol, ethanol, acetone, hexane, and other solvents to extract active components with various applications. A methanol extract of seeds of MO was screened phytochemically for chemical elements (Stohs & Hartman, 2015). In this research, ZnO NPs were synthesized by adopting the biological method. Moringa oleifera leaves extract was used to reduce and stabilize reagents in the biosynthesis of ZnO NPs for biobased ointment application.

2.6. Factors affecting biosynthesis of ZnO NPs

The biosynthesis of ZnO NPs was affected by factors such as temperature, nucleation time, pH, the concentration of the substrate, and the reducing agents. These factors play an essential role in the biosynthesis of nanoparticles, such as the shape, size, and distribution (R. Prasad, 2014).

2.6.1. Temperature

Temperature is the primary physical factor that affects the formation of the NPs. The stability of the NPs depends on the temperature (R. Prasad, 2014). S. J. Stohs et al. observed that changing the thermal treatment temperature resulted in different morphologies and sizes of the ZnO NPs. The temperature has a direct influence on the shape and size of NPs. Reaction temperature directly

affects the reaction rate and affects the characteristics of the NPs formed (Bala et al., 2015). As a result, one can customize the desired properties (growth, shape, size, and particle size distribution) by altering the reaction temperature at which the NPs are synthesized. The thermodynamic properties (Gibbs free energy, ΔG; enthalpy, ΔH; entropy, ΔS; and heat capacity, Cp) and the activity of the reactants heavily rely on the surrounding (heat) energy. It was found that by altering temperature, the absorption band increases (Bala et al., 2015).

As reported by Parra et al., the thermal treatment of ZnO NPs at lower reaction temperature 30 ℃ showed irregular morphology and low crystallinity of the particles. The thermal treatment of ZnO NPs at higher reaction temperatures at 60 ℃ and 100 ℃ presented high crystallinity and agglomerates of nanoparticles. This indicates that higher temperatures increase the nucleation rate of crystal formation, which results in the aggregation of nanoparticles and larger particle sizes (Parra & Haque, 2014).

2.6.2. Nucleation time

Nucleation or reaction time is another essential factor influencing NP synthesis's size, shape, and extent using plant-based parts. An optimal reaction duration is very crucial in determining the NPs dimension. The expected results are not always proportionate to the reaction time; in some cases, a moderate reaction hour yields a good result, indicating the importance of optimizing the length of reaction duration. P. Dhandapani et al. observed that increasing the thermal treatment time at 50 ℃ from 30 to 90 min increased agglomerates and particle growth (Dhandapani et al., 2014). These findings corroborate with the results observed in the different chemical synthesis processes, where the increase of nucleation time led to larger particles of ZnO NPs (Manzoor et al., 2015).

2. 6.3. pH of medium

The pH conditions during synthesis can significantly modify the particle size and morphology of metals and metal oxides, which will consequently change the properties of the nanomaterials (Bala et al., 2015; Chitra & Annadurai, 2014; Roselina et al., 2013). Alias et al. observed that larger agglomerates were formed when ZnO was synthesized using pH 6.0 or 7.0, compared to a decrease in particle size and agglomerations when the pH was increased to 11.0. NaOH was used to control the aqueous pH (Alias et al., 2010). It also showed that the pH increase from 4.0 to 8.0 led to

decreased particle size and aggregation (Madhumitha et al., 2019; Nagarajan & Arumugam Kuppusamy, 2013).

Although the pH condition poses a notable influence on the synthesis of inorganic nanoparticles, much of the available literature on the green synthesis of ZnO NPs does not consider or report the pH of the solutions of the biological extracts. Thus, considering that each natural substrate has different compositions, the evaluation of the pH solutions would be of great interest to better understand the differences in physical-chemical properties of the nanoparticles obtained through green synthesis. When Zn^{2+} reacts with too much OH^-, particles become clustered together and agglomerate (Jacob & Suleiman, 2021).

When the pH of the reaction mixture is greater than 7, the number of OH^- ions is usually high, causing a strong attraction between the positively charged Zn^{2+} and OH^- ion; subsequently, increasing crystallization and formation of a smaller ZnO NPs. As the solution pH increases from 7, 8, 10, and 12, the purity of ZnO nanoparticles also increases, and the percentage yield rises from 42.9%, 62.2%, 64.7%, to 100%, respectively. The primary pH medium favors the formation of ZnO NPs (Jacob & Suleiman, 2021).

2. 6.4. The concentration of both plant extract and precursor

The right amount of extract (biomass dosage) enhances the shape and size of ZnO NPs and enhances ZnO NPs production. It was observed that the concentration of zinc nitrate is the factor that influences mostly the particle size among all the evaluated parameters (Chinnasamy et al., 2018). It was indicated that particle formation became more uniform and smaller with increasing zinc acetate concentration (1.0–5.0 mM) (Madhumitha et al., 2019). It was found that increasing zinc precursor concentration enhanced the homogeneity of the particles and reduced their size. It should be noted that samples obtained with zinc nitrate exhibited reduced particle size and a more regular shape than those synthesized with zinc acetate and other zinc salts. This might be because Zn (II) present in the synthesis with zinc acetate did not react with the plant compounds in total, as observed in the cyclic voltammograms (Bandeira, Possan, et al., 2020).

Furthermore, it was observed that there was a direct correlation between the concentration of plant extract and the intensity of the UV absorbance peaks observed, indicating a superior formation of

ZnO NPs. These features may be related to a higher concentration of antioxidants available during the synthesis when the plant extract increases. As it has commonly been assumed, these compounds play an essential role in the mechanism of formation of metal and metal oxides nanoparticles obtained by green synthesis (Król et al., 2017; Madhumitha et al., 2019).

Table 2 - 2: Comparison of green synthesis of ZnO NPs to physical and chemical methods (Król et al., 2017).

No	Physical and chemical methods	Green Synthesis Method
1	Costly and low production rate.	Cost-effective due to the easy availability of plant materials and active bio-components that act as reducing and capping agents. Large-scale production of nanoparticles.
2	Require a highly restricted laboratory environment.	Do not require a well-equipped laboratory for the synthesis of nanoparticles.
3	Require high or low temperature/pressure and inert environment.	Nanoparticles can be synthesized at standard temperature and pressure conditions
4	Consume high energy during the synthesis process.	Do not require a complex energy system for synthesis.
6	Produce toxic by-products to the environment.	Eco–friendly

Table 2 - 3: Summary of reported methodologies of the green synthesis of ZnO Nps

Biological substrate (Plants)	Zinc source	pH	Reaction time and temperature	Thermal treatment	Avg. size (nm)	Shape	Reference
Aloe vera leaves (NS)	Nitrate (NS)	NS	4–5 h, 150 ^{0}C	7–8 h, 80 ^{0}C	25	NS	(Salam et al., 2012)
Aloe barbadensis miller leaves (50–500 g L 1)	Nitrate (NS)	NS	5 h, 150 ^{0}C	7–8 h, 80 ^{0}C	25-55	Spheres	(Sangeetha et al., 2011)
Camelia sinensis leaves (NS)	Nitrate (50 g L $^{-1}$)	NS	NS, 60 ^{0}C	2 h, 400 ^{0}C	8	Spheres	(Naveed et al., 2017)
Citrus aurantifolia peel (20 g L 1)	Nitrate (20 g L $^{-1}$)	NS	3 h, Ta	1 h, 60 ^{0}C	11	Polyhedron	(Ul et al., 2019)
Couroupita guianensis leaves (50 g L 1)	Acetate (5 g L $^{-1}$)	NS	10 min, NS	Overnight, 60 ^{0}C	NS	Nanoflakes	(Sathishkumar et al., 2018)
Costus woodsonii leaves (30–60 g L 1)	Nitrate (100 g L $^{-1}$)	NS	60 ^{0}C, NS	2 h, 400 ^{0}C	20-25	Varied	(Khan et al., 2019)
Eclipta alba leaves (100 g L 1)	Acetate (0.2–1.1 g L $^{-1}$)	4–8	5–75 min, 20–100 ^{0}C	Not applied	3-9	Spheres	(A. K. Singh et al., 2017)
Hibiscus subdariffa leaves (20 g L 1)	Acetate (14.3 g L $^{-1}$)	NS	30 min, Ta	Four h, 30–100 ^{0}C	190-400	Dumbbell	(Bala et al., 2014)
Lycopersicon esculentum fruit (NS)	Nitrate (NS)	NS	5 min, 80 ^{0}C or microwave	4–5 h, NS	40-100	Spheres	(Saha & Bandyopadhyay, 2017)
Menta pulegium L. leaves (50 g L 1)	Nitrate (100 g L $^{-1}$)	NS	NS	2 h, 400 ^{0}C	38-49	Spheres	(Shahriyari et al., 2019)
Moringa oleifera leaves (100 g L 1)	Nitrate (6–206 g L $^{-1}$)	5	18 h, Ta	1 h, 500 ^{0}C	12-30	Spheres	(Matinise et al., 2017)
Oak fruit hull (jaft) (200 g L 1)	Acetate (33.4 g L $^{-1}$)	NS	4 h, 60–80 ^{0}C	6 h, 80 ^{0}C; 4 h, 500 ^{0}C	34 nm	Spheres	(Sorbiun et al., 2018)
Punica granatum leaves (NS)	Nitrate (18.9 g L $^{-1}$)	NS	3–4 h, 60 ^{0}C	3–4 h 400 ^{0}C	10-30	Spheres	(K. Singh et al., 2019)
Peganum harmala seed (60 g L 1)	Nitrate (NS)	NS	1 h, NS	NS, 50 ^{0}C	40	Irregular	(Fazlzadeh et al., 2017)

NS: Not specified; Ta: Ambient temperature

2.7. Biomedical application of ZnO NPs

Zinc oxide nanoparticles have played a versatile r ole in their contributions to the novel field of biomedical application (Akbar et al., 2020; Jin et al., 2020; Naveed et al., 2017). Some of the main applications are highlighted below.

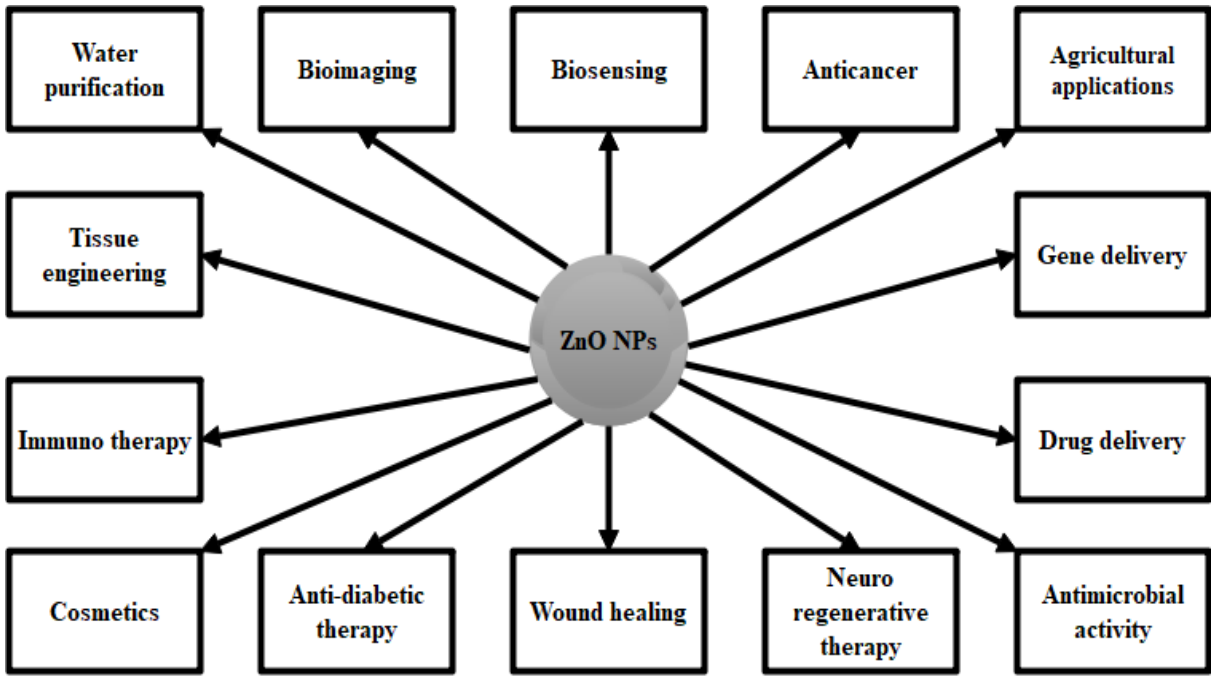

Figure 2 - 11: Biomedical application of ZnO NPs (Akbar et al., 2020; Jin et al., 2020; Naveed et al., 2017)

2.7.1. Antibacterial activities of ZnO NPs

There is a lot of mechanisms beyond the metal oxides NPs antibacterial activity. ZnO NPs of smaller size means it has superior penetrating capacity and reactivity into bacterial membranes due to their sizeable interfacial area, thus enhancing their antibacterial efficiency. Zn ion can interact with specific groups of bacterial enzymes and inhibit the functionality of the enzyme. During the bacterial cell wall destruction process, pathogenic organisms lose their ionic strength. The cell functions, such as growth, metabolic activity, replication, etc., were inhibited and led to cell death (Jayabalan et al., 2019). It was also reported in other studies that the antibacterial activities of the metal oxide nanoparticles mostly appeared on the surface and bound with the protein groups present in the cell wall. This interaction decreases the cell permeability, which leads to cell lyes. Reports also indicate that ZnO NPs rupture the outer and inner walls of the cell, resulting in

disorganization and leakage of the cell membrane, which leads to cell death (Elumalai & Velmurugan, 2015).

Some studies forward that the antibacterial activity of ZnO NPs might be due to reactive oxygen species (ROS) that affects and damages the bacterial cells. ZnO is activated, and the electron-hole pairs increase using white light. These may split H_2O molecules into hydroxyl radical (OH^-) and hydrogen ion [H^+] species. Dissolved oxygen molecules might be converted to superoxide radical anions (O_2^-), reacting with hydrogen ion [H^+] to produce HO_2^- radical. The hydroxyl radicals react with hydrogen to produce H_2O_2 molecules. These generated H_2O_2 molecules to penetrate the cells and kill the bacteria. In addition, the damage of the bacterial cell membrane may lead to the leakage of minerals, proteins, and genetic materials, causing ultimate cell death (Meenatchi et al., 2020).

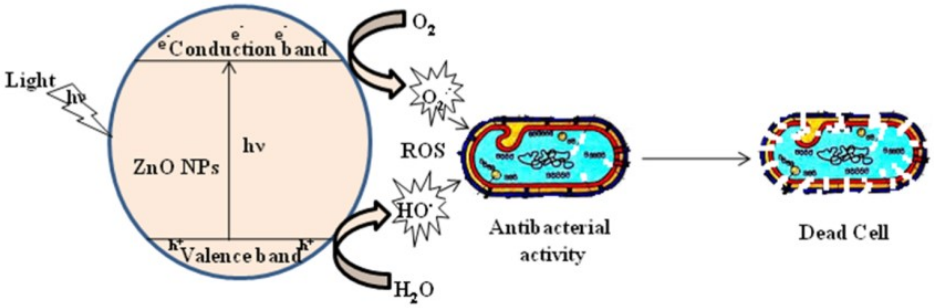

Figure 2 - 12:The action mechanism of ZnO NPs with ROS for antibacterial activity (Meenatchi et al., 2020).

2.7.2. Ultraviolet radiation, its effects on skin and prevention

Skin is exposed to various environmental factors such as UV radiation that originates naturally from the sun due to its anatomic location at the external boundary of the body. Solar UV exposure is the leading cause of age-related changes such as skin cancer development. UV exposure may account for up to 80% of skin aging signs, including dry appearance, scalping, wrinkling, impaired pigmentation, and photoaging correlates with cancer risk.

The United Nations Environment Programme has estimated that over 2 million non-melanoma skin cancers and 200,000 malignant melanomas occur globally each year. According to their report, in the event of a 10% decrease in stratospheric ozone, with current trends and behavior, an

additional 300,000 non-melanoma and 4,500 melanoma skin cancers could be expected worldwide. About 12 to 15 million people are blind from cataracts. WHO has estimated that up to 20% of cataracts or 3 million per year could be due to UV exposure. Given that, in the United States alone, it costs the US Government $US 3.4 billion for 1.2 million cataract operations per year, substantial savings in cost to health care can be made by prevention or delay in the onset of cataracts (Nations et al., 1994).

UV radiation is composed of UVA, UVB, and UVC components based on photon wavelength. UVA has the longest wavelengths (320–400 nm), UVB is with mid-range (280–320 nm), and UVC has the shortest wavelengths (100–280 nm). Ambient sunlight is composed primarily of UVA (90%–95%) and UVB (5%–10%) energy, with most solar UVC absorbed by the ozone layer (Amaro-ortiz et al., 2014) (Orazio et al., 2013).

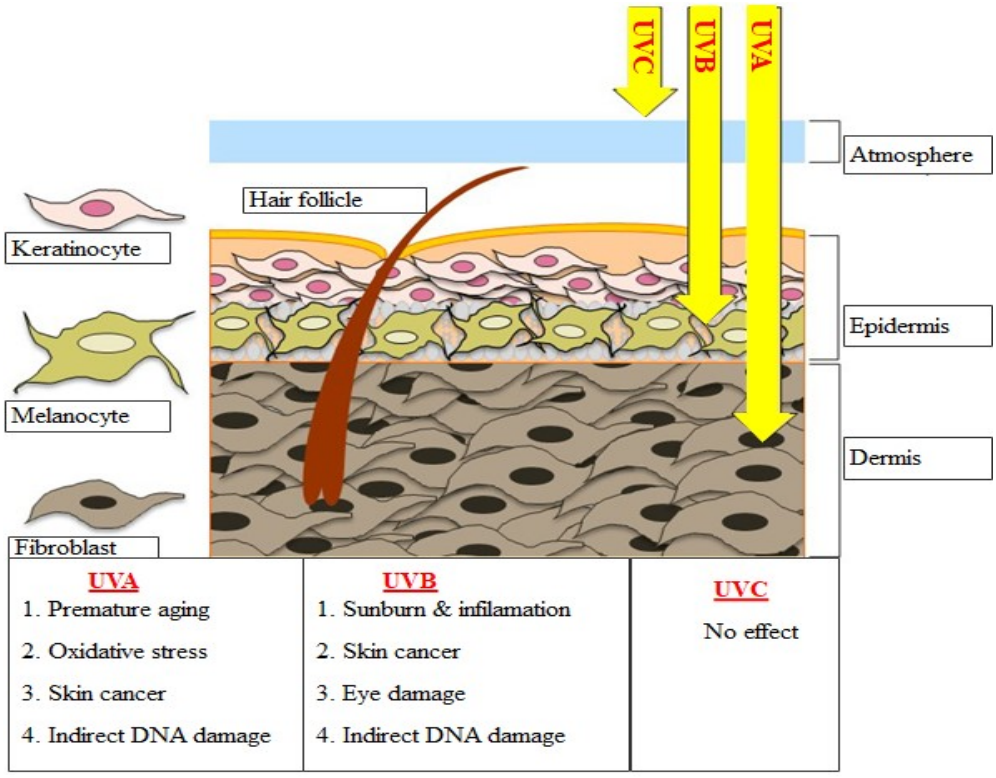

Figure 2 - 13: UV radiation and human skin (Orazio et al., 2013)

UVA is usually referred to as sunlight, is the least energetic photon but too much exposure to it can cause oxidative damage to lipids, proteins, and DNA. UVB causes direct damage to biological

systems by creating DNA lesions that block the replication and transcription of DNA. As recent reports indicate, ground UVB radiation will remain at high levels in the next several decades (Chen, 2017).

Naturally occurring UV radiation is responsible for most environmentally induced skin pathologies, including erythema and inflammation, degenerative aging changes, and cancer. Humans are exposed to UV radiation primarily as a consequence of unprotected exposure to sunlight. UV radiation has many harmful effects on cells. UV radiation produces both direct and indirect DNA damage, and each can result in mutagenesis in skin cells (Amaro-ortiz et al., 2014). UV radiation causes genetic mutations in skin cells.

Geographical variations such as altitude, latitude, and urbanization all determine ambient UV strength. Since atmospheric particles such as dust or water droplets can scatter, reflect or otherwise interfere with UV photons, the more atmosphere sunlight has to traverse, the weaker its energy will be at the surface of the Earth. At higher altitudes, with less atmosphere for sunlight to traverse before hitting land, there is higher exposure to UV and a higher risk for melanoma. There is a 2% increase in risk with every 10 m rise in altitude. Strength is strongest at the equator because sunlight hits the Earth most directly at the equator. Geographically, Ethiopia is located at the equator and high altitude above sea level. Therefore, it has an increased tendency to be affected by UV radiation. Toward the poles, sunlight hits the earth obliquely and must pass through more atmosphere (Amaro-ortiz et al., 2014).

Sunscreen formulations typically contain between 5 and 25% (wt./wt.) of the inorganic metal oxides ZnO and titanium dioxide (TiO_2), often specified as being in the nanoparticulate form and are commercially available as coated or uncoated particles. As ZnO and TiO_2 both absorb and reflect UV radiation and filters UV (Holmes et al., 2016). Zinc oxide and titanium dioxide give the cosmetic formulation a better feel and spreadability and better sun protection (Badnore et al., 2019). For this thesis, Zinc oxide was selected because of the cheap availability of precursors and is an abundant element in our body next to iron. To prevent microbial infections or pathogens causing disease in the skin, ZnO NPs are also the key active component to avoid skin infections.

2.8. Nanoparticles dispersed ointment

In the form of an ointment, herbal medications are often formulated. The ointment base is prepared, and the ointment is formulated by adding the active ingredients by trituration into the base at the most efficient ratio. The quality of the ointment is measured in terms of irritancy, spreadability, diffusion, and durability, which is done after the completion of the development (Meseret Ewunetu, 2020).

In this work, biosynthesized ZnO NPs were used as medications to enhance ointment activity and light-absorbing characteristics. It is supposed to carry active components of moringa oleifera extracts with medicinal values and further provides biobased ointment advantages. Bioconjugate developed from the extract of COL/ELS with lactic acid was used as an ointment base to synthesize ZnO NPs dispersed ointment. The fusion method is the most used method by a lot of researchers for ointment formulation. The formulation is done for different ointment types at 60 - 70 °C. Then plant extracts dispersed in petroleum derivatives-based ointment and spreadability, drug release, antimicrobial effect, pH, viscosity, irritancy, and stability were (Meseret Ewunetu, 2020)(Adeleye et al., 2021a; Badnore et al., 2019; Lisnawati et al., 2018; V. Prasad & Dorle, 2006).

Few types of research have been reported on the dispersion of NPs in the ointment. NPs were dispersed in ointment to increase their efficiency and to have unique characteristics that hit targeted goals. N.Lisnawati et al. studied the formulation and evaluation of the antibacterial activity of NPs ointment preparation using Blimbi extract using the fusion method (Lisnawati et al., 2018). They reported that the Bilimbi extract was formulated in absorbent ointment with dark brown color and unique fragrance with a pH of 6.42-6.80 and spreadability of 6.16-6.90 mm. According to the results, ointment showed better antibacterial activity against S. aureus and E. coli. Finally, they concluded that the ointment using Blimbi extract was safe and did not irritate the skin.

Adeleye et al. conducted their works on formulating and evaluating Ehretia Cymosa biosynthesized Silver Nanoparticle anti-inflammatory ointment. Their main goal was to synthesize silver nanoparticle (SNP) using an extract of the leaf of Ehretia cymosa as a reducing and stabilizing agent and to apply it as an anti-inflammatory agent in medicated ointment formulation. The ointment was formulated with the incorporation of different concentrations of the crude extract and the SNP. The required quantity of the SNP (5% w/w) was weighed into an evaporating dish (Adeleye et al., 2021a).

The ointment base was prepared by melting different ingredients at 70 ℃ with continuous stirring and allowed to cool to at room temperature and transferred into a dispensing jar. The physical characteristics of the ointment were determined by visual inspection. They reported that ointments were soft and smooth with a stable and homogenous appearance. Viscosity increased, and spreadability decreased with an increase in the concentration of bioactive ingredients. The SNP ointment exhibited significantly better anti-inflammatory activities than the crude extract and positive control (Adeleye et al., 2021a).

Amruta U. Badnore and others conducted their work on the Preparation of antibacterial peel-off facial mask formulation incorporating biosynthesized silver nanoparticles. The ointment base was synthesized by adding ingredients and was homogenized to dissolve using a magnetic stirrer to form the base formulation at 80 °C. Then it was allowed to cool until it reached room temperature. Afterward, synthesized Ag NPs were added to the prepared base formulation and agitated by a magnetic stirrer for a few min to disperse the particles uniformly in the formulation. Then antibacterial formulation tested exhibited a zone of inhibition ranging from 8 to 14 mm (Badnore et al., 2019).

Table 2 - 4:Comparative studies on various nanoparticles dispersed ointment

NPS required	Types of ointment	Formulation method	Viscosity (cp)	pH	Spread ability (sec)	Antimicrobial and other studies
Ag Nps	Antibacterial (Badnore et al., 2019)	Cold mixing 25 ℃	-	-	-	*P. aeruginosa, S. aureus, p. acnes*
Ag Nps	Anti-Inflammatory (Adeleye et al., 2021a)	Hot mixing 70 ℃	12000	-	17-25	-
PAA Nps	Antibacterial (Lisnawati et al., 2019)	Cold mixing 25 ℃	50869-129144	6.4- 6.8	6.90	E. coli & S. aureus
CDs	Antiparasitic (V. B. Kumar et al., 2018)	Cold mixing (Ice water bath,10 ℃)	-	-	-	L. major & L. donovani
ZnO Nps	Wound healing (V. Gupta et al., 2020)	Fusion method or Hot mixing 70 ℃	-	-	-	Wound healing effect on laboratory rats
Glass-Au Nps	wound regenerating (Mârza et al., 2019)	Hot mixing 45℃±2 ℃	-	-	-	Human keratinocytes cells
Ag Nps	Wound Healing (Thirumurugan et al., 2011)	Cold mixing 25 ℃	-	-	-	Animal's skin
Nano-emulsion	nanoscale-dispersed eye ointment (W. Zhang et al., 2014)	Hot mixing 75 ℃	-	7.5	-	Treatment of dry eye disease

2.9. Gaps identified from previous studies

Recently green synthesis of ZnO NPs has got great attention due to the drawbacks of conventional physical and chemical methods. In the biosynthesis of ZnO NPs, different phytochemical

compounds contained in plant extracts were used as reducing and stabilizing agents. Almost all studies on the biosynthesis of ZnO NPs were done by phytochemical compounds extracted exclusively by one solvent, i.e., mostly distilled water. One particular solvent can extract certain groups of phytochemical compounds but not others. Reports suggest that using a combination of solvents could better extract phytochemical compounds used to biosynthesize ZnO NPs (Bandeira, Giovanela, et al., 2020; Vongsak et al., 2013). So, to the best of my knowledge, there was no documentation on the biosynthesis of ZnO NPs using a combination of distilled water and methanol extract of Moringa Oleifera leaves. In addition to that, the effects of the different reaction parameters such as temperature, nucleation time, precursor concentration, pH, and volume of plant extract to precursor amount using the combination of methanol and distilled water extract of Moringa Oleifera leaves as solvent hadn't been studied so far.

All ointments contain an ointment base that acts as a drug carrier and is also used as a moisturizer for dry skin (Advance et al., 2020). Studies showed that most ointments bases were derived from petroleum-based derivatives like mineral oil, soft white paraffin, soft yellow paraffin, hard paraffin, and cetostearyl alcohol (Bhaskar et al., 2016; Mahendran & Abdul Rashid, 2016). Even though petroleum derivative ointment keeps skin moisture and reduces overexposure to sunlight, it negatively impacts compatibility with living systems. Researches show that the increase in mineral oil saturated hydrocarbon on the skin causes an increased accumulation of mineral oil over time in human fat tissue with age. It is toxic, does not metabolize if it gates the system, and tends to cloggy skin pores (Meseret Ewunetu, 2020).

The high cost of biobased and sunscreen products in the market was another constraint that people are fronting today. Few types of research have been conducted on developing biobased ointment and enhancing its activity by introducing biosynthesized nanoparticles. There is a gap in generating literature and research works in this regard. Therefore, synthesizing biobased and biocompatible products with skin cells that can enhance antimicrobial, antifungal, and UV screening activities, a product that can provide multiple advantages simultaneously, easily affordable at a low price, following green synthesis route to avoid environmental pollution was required in general. This research work was mainly focused on solving the problems mentioned above.

CHAPTER THREE

3. MATERIALS AND METHODS

Framework of Study

This thesis was conducted on the biosynthesis of ZnO NPs and studied the effect of biosynthesized ZnO NPs on antimicrobial and light-absorbing characteristics of biobased ointment. The overall framework of the thesis was presented in the Figure 3-1 below:

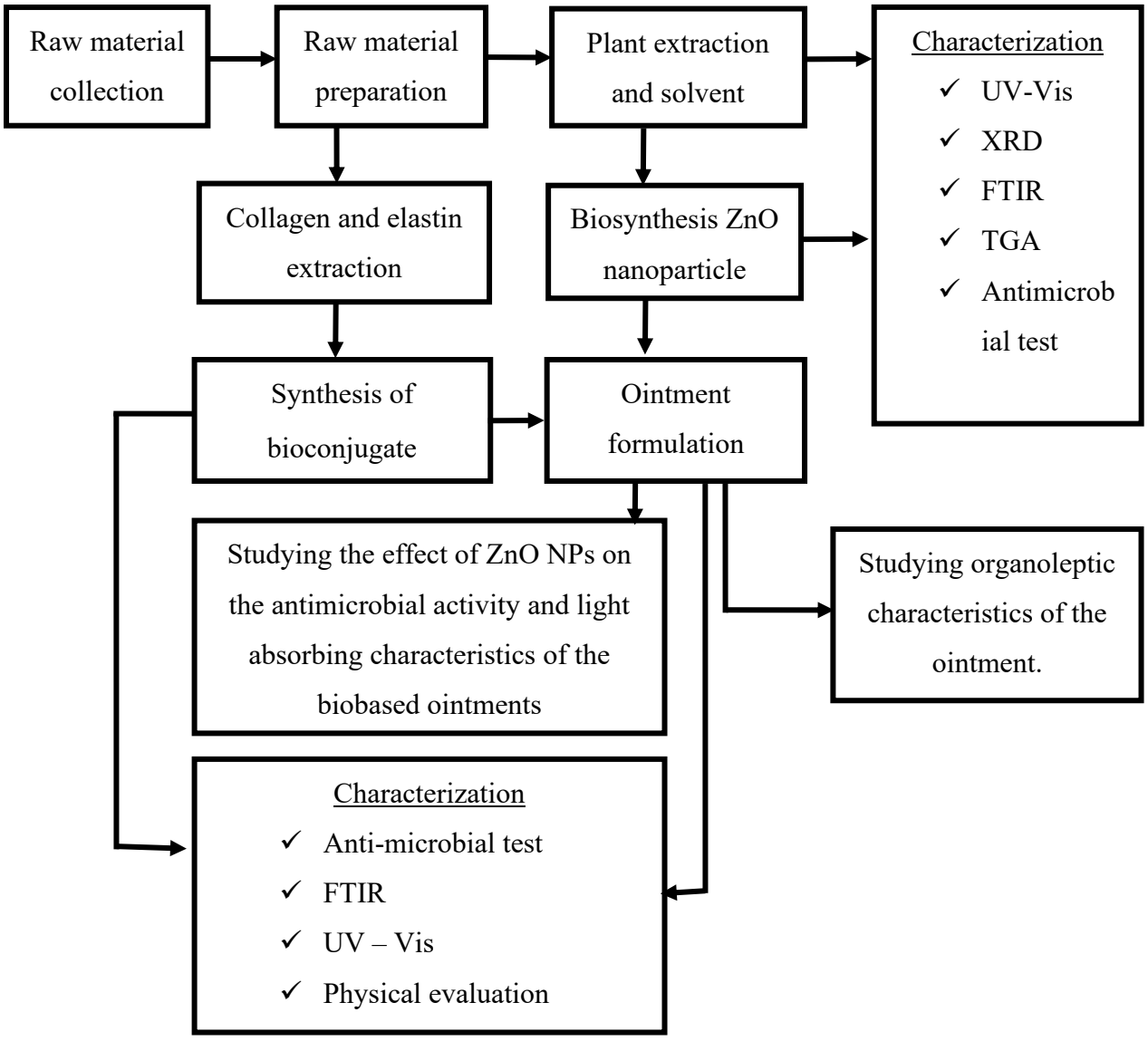

Figure 3 - 1:The overall framework of the experimental study of the thesis

3.1. Raw materials, Chemicals, and Equipment used

Raw materials, chemicals, and equipment used during this thesis works were listed in Table 3 - 1. Note that all the chemicals and reagents were analytical grade, used as received without further purification, and bought from Atomic educational materials supply plc, Addis Ababa, Ethiopia.

Table 3 - 1: Raw materials, chemicals, and equipment used

No	Processes	Raw materials	Chemicals	Equipment used
1	Extraction of moringa oleifera (MO) and solvent selection	Moringa oleifera leaves	Methanol, ethanol (99.9%), distilled water	Spatula, Sample holder, temperature magnetic stirrer, magnetic rod, digital balance, Glove, Measuring cylinder, filter paper, funnel, flat-bottom flask, and beaker
2	Biosynthesis of ZnO NPs	Moringa oleifera extract	($Zn(NO_3)_2 . 6H_2O$), ethanol (99.9%), NaOH, and distilled water	Centrifuge machine, test tube, flat-bottom flask, Measuring cylinder, Spatula, Sample holder, temperature magnetic stirrer, Petri dish, the ceramic crucible, muffle furnace, balance, glove, nose mask, eye goggle, pestle, and mortar
3	Extraction of COL/ELN matrix	Broiler Skin	NaCl, Acetone, NaOH, and distilled water	Beaker, cutter, oven, measuring cylinder, petri dish, water bath, digital balance, Separatory funnel, nose mask, Glove

No	Processes	Raw materials	Chemicals	Equipment used
4	Synthesis of bioconjugate	ELN/COL matrix	Lactic acid (88% aqueous solution) distilled water	Round bottom flask, oven, horizontal condenser, Sample holder, Chiller, Spatula, Spatula, beaker, Aluminum foil
5	Development of bio-based ointments	bioconjugate, ZnO NPs	Distilled water	Water bath, ruler, Petri dish, beaker, spatula.

3.2. Raw materials collection and preparation

Raw material "Moringa oleifera leaves" was collected from K/Didaye, Wolayta, Ethiopia. MO leaf was washed twice using tap water and then washed again with distilled water. The leaves were then dried at room temperature and crushed into a fine powder using pestle-mortar. The obtained powder was packed in a clean plastic bag, transported to ASTU Chemical engineering laboratory, and sieved with a mechanical sieve. This method was obtained with a slight modification of Elumalai et al. and others (Dejen et al., 2020; Elumalai & Velmurugan, 2015; Letsholathebe et al., 2021).

Fresh broiler skin was collected from Adama, Franko (17 Keble) from broilers merchants settled where Oromia Development Association market center. Collected broiler skin was placed in the plastic bag and transported to ASTU Chemical engineering laboratory. Then, the broiler feather was removed with the help of hot water, and another necessary procedure was also followed.

3.3. Solvent selection and extraction of active components from Moringa oleifera leaf for the biosynthesis of ZnO NPs.

Three available solvents and their combinations with distilled water were selected for extraction of Moringa oleifera. These were Methanol (MT), Ethanol (ET), Distilled water (DW), Methanol-Distilled water (50:50 MT-DW), and Ethanol-Distilled water (50:50 ET-DW). Based on UV–Vis spectroscopy absorbance, among the solvents mentioned above, the one that showed better

absorbance (higher formation of ZnO NPs) compared to each other was selected as an appropriate solvent and used throughout the biosynthesis of ZnO NPs.

10g of Moringa oleifera powder was mixed with 100 mL of each solvent and heated at 50 ℃ for 1 hr by temperature magnetic stirrer and cooled down. But for the combination of solvents, 50:50(v/v) was used. The extract was subjected to filtration using Whatman No.1 filter paper to remove the leaf debris. The clear extract filtrate obtained was stored in the refrigerator at four ℃ for further use. This method was developed from similar work of previous studies (Dejen et al., 2020; Matinise et al., 2017; Ngom et al., 2019). The process flow sheet for MO leaf extraction was presented in Figure 3 - 2.

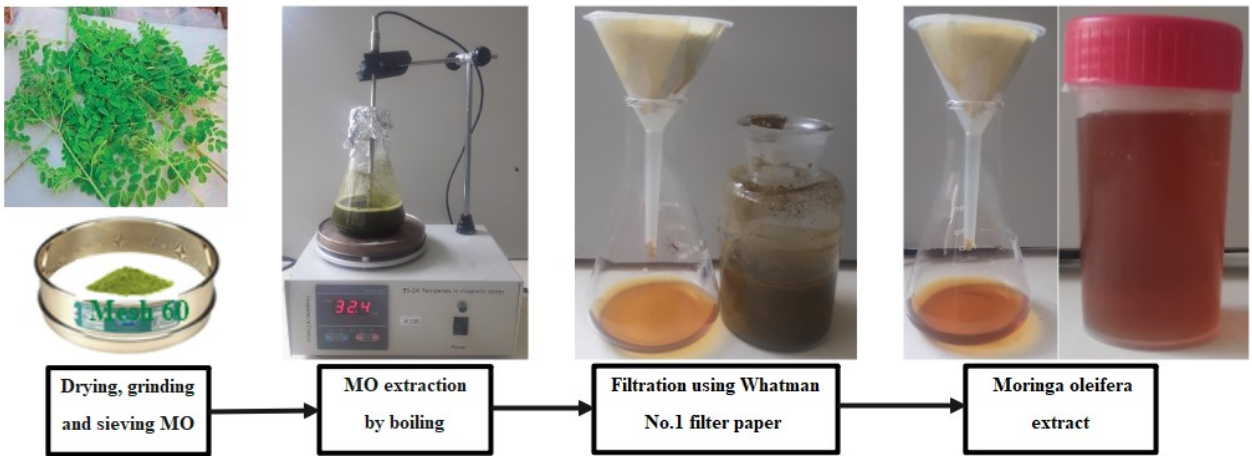

Figure 3 - 2: Process flowsheet of MO leaf extraction

3.4. Biosynthesis of ZnO NPs

The parameter effect study for the biosynthesis of ZnO NPs considered various parameters such as nucleation time, reaction temperature, the volume of leaf extract to precursor, zinc nitrate concentration, and pH. For the optimum biosynthesis of ZnO NPs, the effects of different reaction parameters were studied. Nucleation time was varied from 1 to 4 hrs at regular interval of 1 hr; the reaction temperature was changed from 50 ℃ to 90 ℃ at regular interval of 10 ℃, the volume of plant extract to specified precursor amount varied from 10:50 mL to 70:50 mL at regular interval of 20 mL, Concentration of precursor varied from 0.0025 M to 0.1 M maintained by doubling of previous values and pH of reaction medium ranged from 8 to 14 at regular interval of 2.

For the biosynthesis of ZnO NPs, zinc nitrate hexahydrate Zn $(NO_3)_2.6H_2O$ with a concentration of 0.1 M was prepared in 50 mL of distilled water. 50 mL of MO leaf extract was added to a flat-bottom flask containing precursor solution. Then the solution boiled at 60 °C by using a magnetic stirrer for 2 hr. The desired pH of the solution was adjusted by using 2 M NaOH. Then, the solution was centrifuged at 5000 rpm for 30 min. The centrifuged sample was washed three times with distilled water and then with ethanol. The sample was allowed to dry at low oven temperature, calcined in the hot air furnace, and finally ground into powder using a mortar and pestle. This method was developed from similar works by F. H. Abdullah et al., and M. Gupta et al. (Abdullah et al., 2020; M. Gupta et al., 2018). The complete process route for biosynthesis of ZnO NPs is presented in Figure 3 - 3 below.

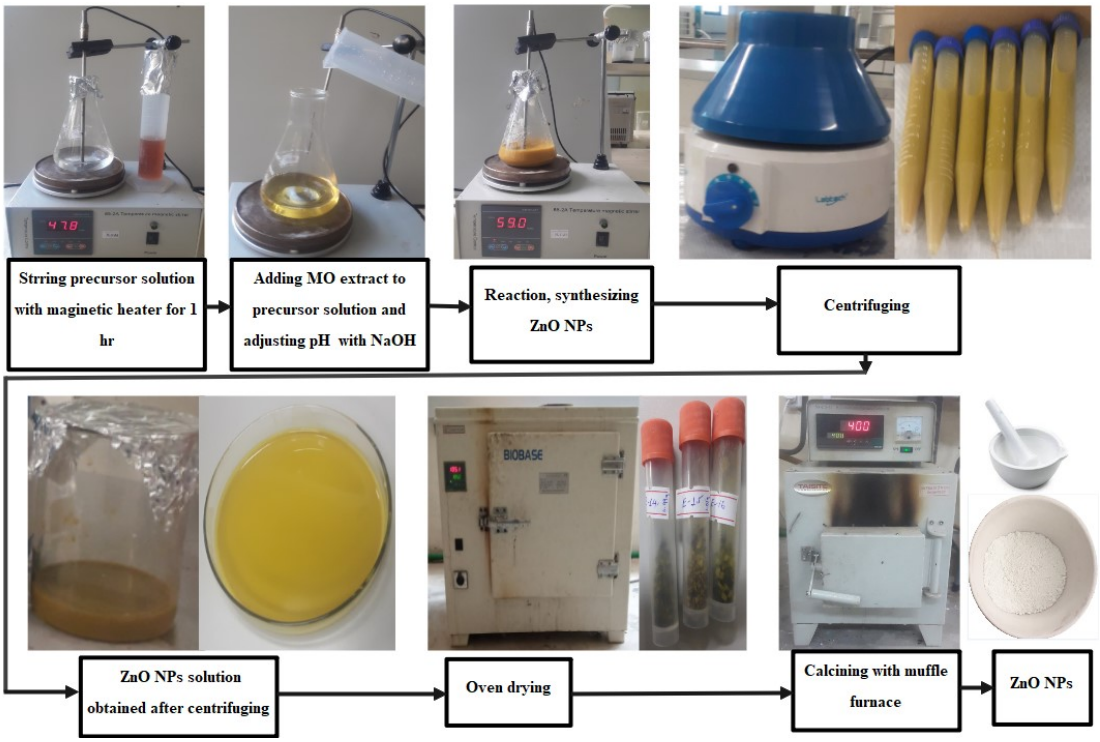

Figure 3 - 3: Schematic flow sheet for the biosynthesis of ZnO NPs.

3.5. Extraction of Collagen and Elastin

Broiler's skin had been cut into small pieces and homogenized in a 10 %vol of 1 M NaCl. After 24 hr, the extracted pellet was washed with demineralized water three times and defatted with 30 %vol acetone for 1 hour. The dry skin was suspended in 30 %vol of 0.1 N NaOH and heated for

15 min in a boiling water bath with constant shaking at 100 ^{0}C. After cooling, the residue was extracted again for 45min in 0.1 N NaOH at 100 ℃. NaOH soluble and insoluble material was washed several times in distilled water and dried in an oven at 80 ℃. This method was obtained from (Meseret Ewunetu, 2020; Nadalian et al., 2013). Process flow for extraction of COL/ELS from broiler skin was presented in Figure 3-4.

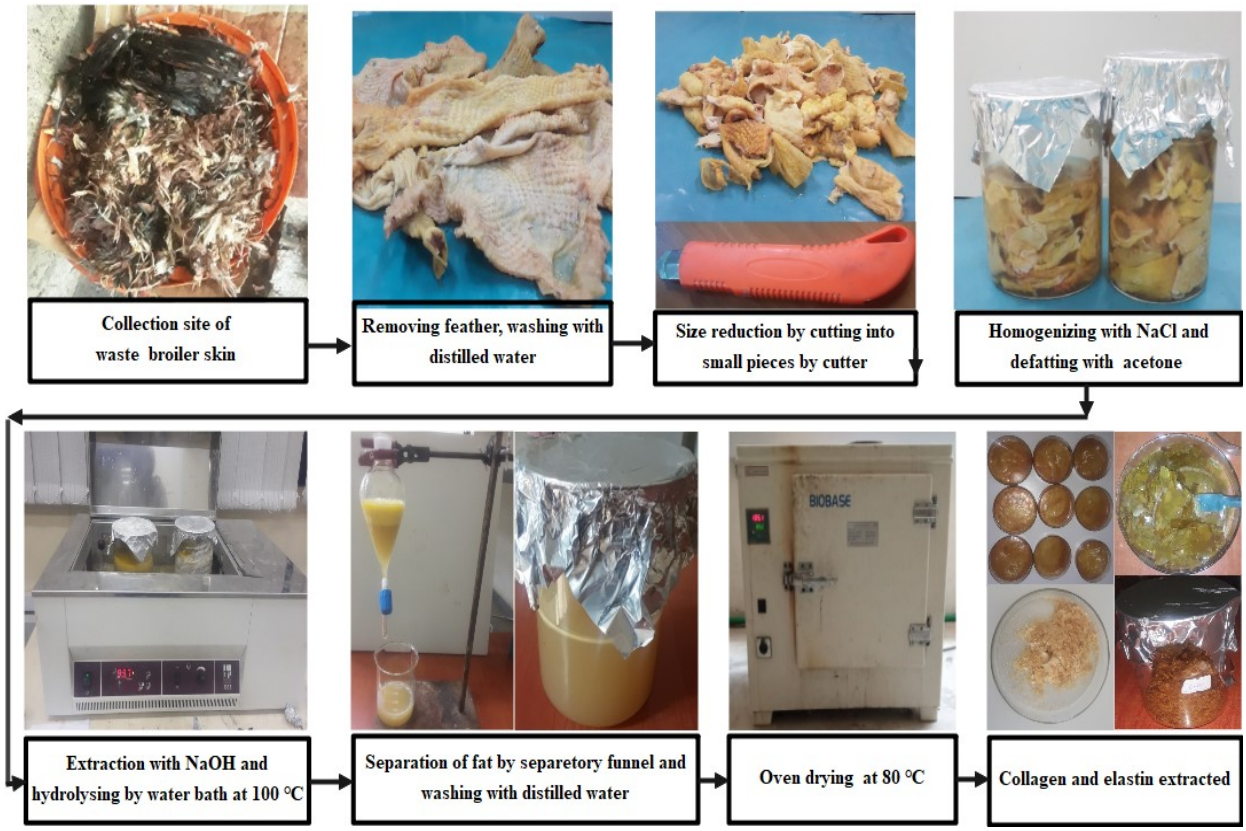

Figure 3 - 4: Process flow for extraction of COL/ELS from broiler skin.

3.5.1. Development of bioconjugate from ELN/COL-Lactic acid

The Lactic acid monomer of 100 g and COL/ ELN matrix of 20 g were initially taken in a round bottom flask and were mixed vigorously. The mixture was placed in the temperature-controlled reactor for the polycondensation reaction at a temperature of 150 ℃ for 5 hrs (Meseret Ewunetu, 2020). During the reaction, both grafting and oligomerization took place. As a result, COL/ ELN - OLLA was synthesized after the completion of the reaction. The sample was collected and kept in sealed vials for further analysis. COL/ ELN-OLLA was a bioconjugate developed and used as

an ointment base for the formulation of biobased ointment. Figure 3-5 shows the process route for synthesizing bioconjugate from ELS/COL matrix and lactic acid.

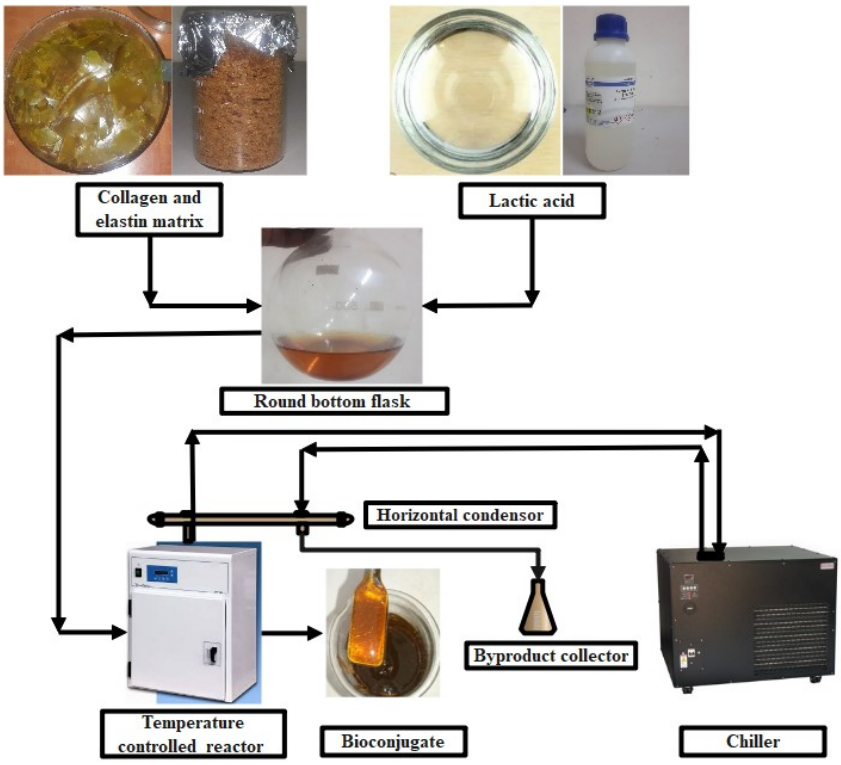

Figure 3 - 5: Process route for development of bioconjugate

3.6. Formulation of ZnO NPs dispersed ointment (ZnO NPs-OB)

The ointment was formulated by incorporating ZnO NPs to the ointment base by the fusion method. Different concentration (w/w) of the ZnO NPs to the ointment base was prepared by dispersing the biosynthesized ZnO nanoparticles into the soft mass of the ointment base from the COL/ ELN / lactic acid-based matrix, as shown in Table 3 - 2.

Table 3 - 2:Composition of ZnO NPs and ointment base in ointment formulation

No	Ingredients (g)	F_0	F_1	F_2	F_3	F_4
1	Biosynthesized ZnO NPs	0%	0.5%	1%	3%	5%
2	Ointment base	10 g	9.95 g	9.9 g	9.7 g	9.5 g

Ointment base of 10 g and 0.5%, 1%, 3%, and 5%(wt./wt.) of biosynthesized ZnO NPs were mixed inside dispensing jar (beaker) at 70 ℃ in the water bath. It was well mixed and stirred gently until

a homogenous dispersion was obtained. After particles dispersed uniformly in the formulation, it was allowed to cool at room temperature. The mixture was constantly stirred again until homogenous and fulfilling the requirement of the ointment was obtained (Adeleye et al., 2021a; Lisnawati et al., 2019; V. Prasad & Dorle, 2006).

3.7. Physicochemical Characterization of ZnO NPs

3.7.1. UV–Visible Spectroscopy

The synthesis of ZnO NPs was confirmed by recording the absorbance in multiple wavelength ranges of 200 to 800 nm using a double beam UV-Visible spectrophotometer at ASTU, department of Biology.

3.7.2. Thermogravimetric analysis (TGA)

Thermal gravimetric analysis was performed using a Nitrogen flow rate at 20.0 mL/min. The temperature was adjusted between 25℃ to 700 ℃ with a heating rate of 20 ℃ /min. The decomposition of sample weight against temperature was recorded. The sample was characterized at the Bahirdar University Institute of Technology. ZnO NPs were characterized to determine the thermal stability or degradation temperature.

3.7.3. X-ray diffraction (XRD) analysis

The crystal structure of nanoparticles was determined using XRD. The crystal structure of nanoparticles was determined was carried out using the XRD machine model of Shimadzu XRD-7000 X-ray diffractometer using Cu-Kα radiation (λ= 1.5418Å) using the operating voltage of 40 kV, a current of 30 mA, over the diffraction angle (2θ) range between 10° and 80° at ASTU, department of materials science and engineering. The crystallite size was calculated using Scherrer's formula: $D = k\lambda/\beta\cos\theta$, where D is the crystal size, k is Scherrer's constant usually taken as 0.9, λ is the X-ray wavelength of CuKa radiation (λ = 1.5406 Å), β is the line width of half maximum in radians, and θ is Bragg's diffraction angle.

3.7.4. Fourier Transform Infrared Ray (FTIR) analysis

Samples were measured on Spectrum 65 FTIR (PerkinElmer) in the wavenumber recorded at a scan range from 4000 - 400 cm^{-1} (resolution: 4 cm^{-1}, number of scans:4) using KBr pellets at Addis Ababa University, department of chemistry. In FT-IR spectroscopy, a sample is placed in the path of an IR radiation source, and its absorption of different IR frequencies is measured. FTIR spectroscopy was employed to identify the type of bonds between two or more atoms and consequently identify functional groups.

3.7.5. The antibacterial assay of ZnO NPs on selected bacterial pathogens

The disc diffusion method determined the in vitro antibacterial susceptibility test based on National Committee for Clinical Laboratory Standards (National Committee for Clinical Laboratory Standards, 2012). The medium was prepared by dissolving 38 g of Mueller Hinton agar medium in 1000 mL of distilled water and autoclaved at 121 °C for 15 min. The autoclaved medium was poured into sterile plates (20-25 mL/plate), and the plates were allowed to solidify under sterile conditions at room temperature. After solidification, the plates were seeded with overnight grown culture approximately 1.5 X 10^8 CFU/mL by swabbing evenly onto the surface of the medium with a sterile cotton swab.

The biosynthesized ZnO NPs at the specified concentrations were prepared by dissolving in DMSO. The biosynthesized ZnO NPs at the concentrations of 75 µg/mL and 100 µg/mL were prepared by dissolving in DMSO were tested for their antibacterial susceptibility test. Whatman filter paper no. 1 was used to prepare discs approximately 6 mm in diameter. The sterile discs were infused with the synthesized compounds, positioned on the medium's surface with sterile forceps, and gently pressed down to ensure contact. Ampicillin was used as standard antibiotics, and then plates were inverted and then incubated at 37 ℃ for 24 hrs. After incubation, the synthesized compounds' inhibition zone was evaluated by measuring the diameter (mm) of the clear area around the disc against the test organisms using a ruler. The biosynthesized ZnO NPs were tested for their susceptibility against Gram-positive (Staphylococcus aureus) and Gram-negative (Escherichia coli).

3.8. Physicochemical and instrumental characterization of COL/ELN matrix and bioconjugate

3.8.1. Proximate analysis of extracted COL/ELN matrix

Moisture content

The empty Petri dish dried in the oven at 105 ℃ for three hours and was weighed after being transferred to the desiccator to cool. 3 g sample (raw skin) weighed and spread uniformly to the Petri dish. The sample was then placed in the oven at 105 ℃ for three hours and then transferred to the desiccator to cool until a constant weight was gained (Feldsine et al., 2002).

$$\text{Moisture content} = \frac{w1-w2}{w1} \quad \text{.....3.1}$$

Where: w1= weight (g) of the sample before drying, w2= weight (g) of the sample after drying

Ash content

Method for ash content calculation was taken (AOAC,2000); first, the three crucibles were placed in the furnace until a constant weight was gained. Then, 5 gm of the sample (broiler skin) was put into the crucible and placed in a furnace at 550 ℃ overnight. Ash content in the sample was determined by the ratio of the weight of ash to the weight of the sample multiplied by 100% (Feldsine et al., 2002).

$$\text{Ash content} = \frac{w1-w2}{w1} \quad \text{.....3.2}$$

Where: w1= weight (g) of sample, w2= weight (g) of ash

Fat content

Method for calculating fat content was taken (AOAC,2000) with some modification**,** first the bottle was placed in the oven at 105 ℃ overnight to ensure that the weight of the bottle was stable, then five g of sample (broiler skin) to into extraction thimble and transfer into Soxhlet. Petroleum ether was used to wash the sample on the heating mantle. After 14 hr. extraction, the solvent was evaporated using Rotavapor. Finally, the bottle was placed in the oven at 85 until the solvent was completely evaporated and the bottle was completely dry. After drying, transfer the bottle was transferred to the desiccator to cool. Reweigh the bottle and its dried content (Feldsine et al., 2002).

$$\text{Fat content} = \frac{w1-w2}{w1} \quad \text{.....3.3}$$

Where: w1= weight (g) of a sample, w2= weight (g) of fat

Biuret Test for protein

A Biuret test is a chemical test used to determine the presence of a peptide bond in a substance. It is based on the biuret reaction in which a peptide structure containing at least two peptide links produces a violet color when treated with alkaline copper sulfate. The peptide bonds in Biuret reagents give a positive result for the test; hence the reagent is named so. It is considered a general test for compounds (proteins and peptides) having two or more peptide (CO-NH) bonds. The Biuret reagent is a solution composed of sodium hydroxide (10% NaOH) or potassium hydroxide (1% KOH) or copper sulfate (Feldsine et al., 2002).

3.8.2. Quality control of the bioconjugate

Quality control of the bioconjugate and its physical evaluating parameters were:

Organoleptic parameters: Organoleptic parameters include color, homogeneity, texture, phase Separation, immediate skin feel, and odor of the bioconjugate were carried out by visual observation.

pH**:** The pH of the bioconjugate was determined by using a digital pH meter. The 1 g of the weighed bioconjugate was dispersed in 100 mL of distilled water, and the pH was noted.

Homogeneity: Bioconjugate was tested for homogeneity by visual inspection.

Viscosity: The measurement of viscosity of bioconjugate was carried out with VK-2000 Viscometer. The values were done in triplicate, and average values were depicted.

Spreadability: The Spreadability of the bioconjugate was obtained by measuring the spreading diameter of 1g of gel between two horizontal plates (20 cm x 20 cm). The standard weight applied to the upper plate was 100g. Spreadability was determined by using the equation below.

$$S = \frac{M*L}{T} \quad \text{.....3.4}$$

Here S= spreadability, M= weight applied L= length of the glass slides, and T= time taken to separate the glass slides from each other (Feldsine et al., 2002).

3.8.3. Instrumental characterization of the bioconjugate

FTIR analysis: Samples were measured on Spectrum 65 FT-IR (PerkinElmer) in the wavenumber recorded at a scan range from 4000-400 cm^{-1} (resolution: 4 cm^{-1}, number of scans:4) using KBr pellets for bioconjugate.

3.9. Studying organoleptic characteristics of ZnO NPs-OB

Organoleptic examination: The prepared formulations were inspected visually for their physical appearance, color, texture, phase separation, and homogeneity. Except for homogeneity and texture, all the characteristics were inspected visually; however, the homogeneity and texture will be tested by pressing a small quantity of the bio-based ointment between the thumb and index finger.

Determination of the pH of various formulations was determined by using a digital pH meter. The 1 g of the synthesized ointment base and the formulated ZnO NPs-OB were mixed with 100 mL of distilled water, and the pH was noted.

Spreadability: The spreadability was determined by applying weight to glass slides into which formulation was placed and the time required to separate the slides in seconds. The spreadability was calculated using the formula S = M.L/T; S is spreadability, M is weight tide to upper slide, L is the length of the glass slide, and T is the time taken to separate the slide from each other.

Viscosity measurement: Viscosity was measured with a viscometer (VK 2000) instrument. The

3.10. Investigating the effect of ZnO NPs on antimicrobial and light absorption characteristics of biobased ointment

3.10.1. Light-absorbing characteristics analysis of ZnO NPs-OB

The synthesized ZnO NPs-DO were tested using a double beam UV-Visible spectrophotometer for UV light absorbance in 200 to 800 nm wavelengths. UV-visible absorption spectroscopy was used to determine ultraviolet light absorbed by biobased ointment. The ZnO NPs-OB were uniformly mixed in distilled water with a concentration of 0.1% wt., and then the solution was used to perform the UV-vis measurement (Zak, 2011). Different concentrations of biosynthesized ZnO NPs (0%,0.5%,1%,3%,5%) dispersed ointments were tasted for their UV light absorbing capability.

3.10.2. Fourier Transform Infrared Ray analysis of ZnO NPs-DO

Spectrum 65 FTIR (PerkinElmer) in the wavenumber range from 4000-400 cm-1 (resolution: 4 cm-1, number of scans:4) using KBr pellets were used to study functional groups of biobased ointment.

3.10.3. The antibacterial assay of ZnO NPs-DO on selected bacterial pathogens

The disc diffusion method determined the in vitro antibacterial susceptibility test based on National Committee for Clinical Laboratory Standards (National Committee for Clinical Laboratory Standards, 2012). The medium was prepared by dissolving 38 g of Mueller Hinton agar medium in 1000 mL of distilled water and autoclaved at 121 °C for 15 min. The autoclaved medium was poured into sterile plates (20-25 mL/plate), and the plates were allowed to solidify under sterile conditions at room temperature. After solidification, the plates were seeded with overnight grown culture approximately 1.5 X 10^8 CFU/mL by swabbing evenly onto the surface of the medium with a sterile cotton swab.

Different concentrations of biosynthesized ZnO NPs (0.5, 1, 3, 5%) dispersed ointments were tested for their antibacterial susceptibility test. The biosynthesized ZnO NPs dispersed ointment at 350 mg/mL concentrations were prepared by dissolving in DMSO. Whatman filter paper no. 1 was used to prepare discs approximately 6 mm in diameter. The sterile discs were infused with the synthesized compounds, positioned on the medium's surface with sterile forceps, and gently pressed down to ensure contact with the MHA. Ampicillin was used as standard antibiotics, and then plates were inverted and then incubated at 37 ℃ for 24 hrs. After incubation, the synthesized compounds' inhibition zone was evaluated by measuring the diameter(mm) of the clear zone around the disc against the test organisms using a ruler.

CHAPTER FOUR

4. RESULTS AND DISCUSSION

4.1. Studying the effect of factors affecting the biosynthesis of ZnO NPs

The biosynthesis of ZnO NPs was carried out by assessing the effect of types of solvents, nucleation time, reaction temperature, amount of plant extract, zinc salts(precursor), and pH. These were the main factors affecting the biosynthesis of ZnO NPs, and their effects were analyzed through UV - Vis spectroscopy by comparing their UV light absorbance to the formation of ZnO NPs. The results of each parameter were briefly discussed in the following sub-sections.

4.1.1. Solvent selection for the biosynthesis of ZnO NPs

The appropriate solvent was used to extract phenolic compounds of MO that play a significant role in the bio-reduction of zinc ions in an aqueous solution (Truong et al., 2019). Based on UV–Vis spectroscopy absorbance, the combination of 50:50(v/v) MT and DW showed better absorbance than others, i.e., higher formation of ZnO NPs. This means 50:50 (v/v) of MT and DW combination had a higher capacity to extract phytochemicals from MO leaf better than the others and formed a higher number of active sites(groups) ready for the reaction with Zn^{2+}. One particular solvent can extract certain groups of phytochemical compounds but not others. Absorbance observed by UV-Vis spectroscopy was presented in Figure 4 - 1. Since 50:50 (v/v) of MT and DW showed the higher formation of ZnO NPs, it was selected as an appropriate solvent for the biosynthesis of ZnO NPs throughout the synthesis. The characteristic peak observed at 326 nm and 324 nm, respectively, indicates ZnO NPs and MO leaf extract formation.

The 50:50 of ET and DW showed a comparable result to 50:50 MT and DT. MT, ET, and DW showed less formation of ZnO NPs than combinations of solvents; this might be due to less active sites involved in the reaction. Reaction conditions followed for solvent selection were: extraction temperature of MO (50 ℃), amount of biomass (MO) load used (10g/100 mL DW), reaction temperature (60 ℃), reaction time (2 hrs.), precursor concentration (0.1 M), the volume of MO extract to the precursor solution (50:50). The full biosynthesis method of the ZnO NPs was stated in section 3.4.

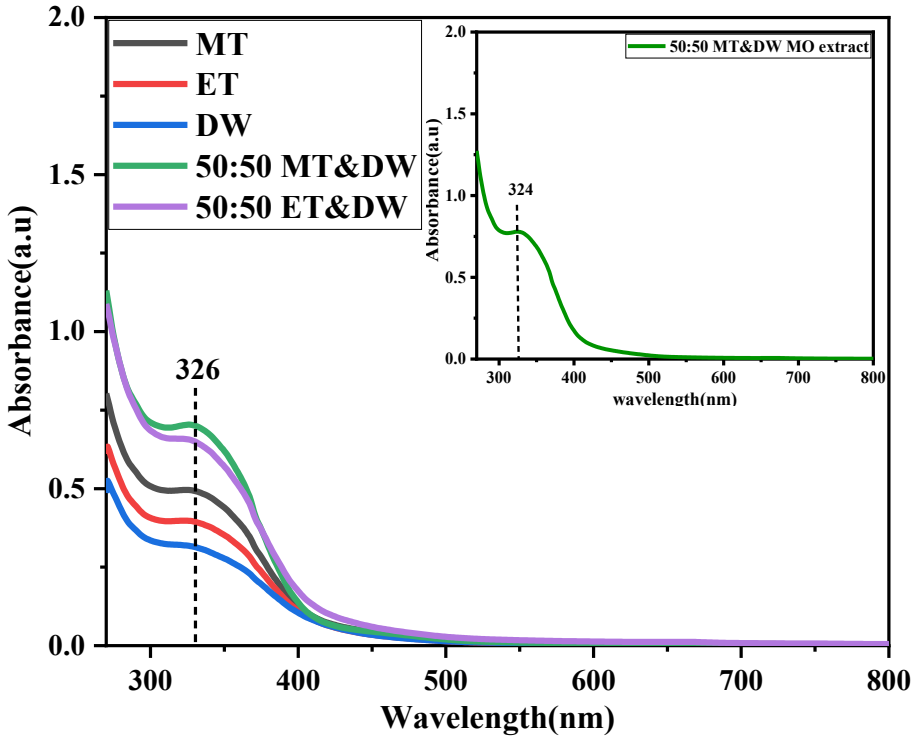

Figure 4 - 1: UV - Vis spectra showing biosynthesis of ZnO NPs at different solvents

Similar works reported by D. H. Truong et al., on "evaluation of the use of different solvents for phytochemical constituents, antioxidants activities" indicated that MT is the most effective solvent for the extraction, resulting in the highest extraction yield and the highest content of phenolic, flavonoid, alkaloid, and terpenoids and used in the biosynthesis of ZnO NPs (Truong et al., 2019). Another report also indicated that a combination of ethanol and distilled water results in higher ZnO NPs than synthesis exclusively by distilled water. It was revealed that extraction of phenolic substances exclusively by a single solvent is not efficient compared to using a combination of solvents (Bandeira, Giovanela, et al., 2020; Vongsak et al., 2013).

4.1.1.1. FTIR analysis of MO leaf extract

The phytochemicals were confirmed by functional group analysis, which has a vital role in forming nanoparticles that stabilize and capping agents (Venkatachalam & Jesuraj, 2021). FTIR spectra were recorded in the range of 400-4000 cm^{-1}. FTIR analysis was done for 50:50 MT and DW for MO leaf extract presented in Figure 4-2. FTIR spectroscopy analysis on the MO extract was carried out to identify the possible biomolecules or groups involved in 50:50 MT: DW(v/v) leaf extract.

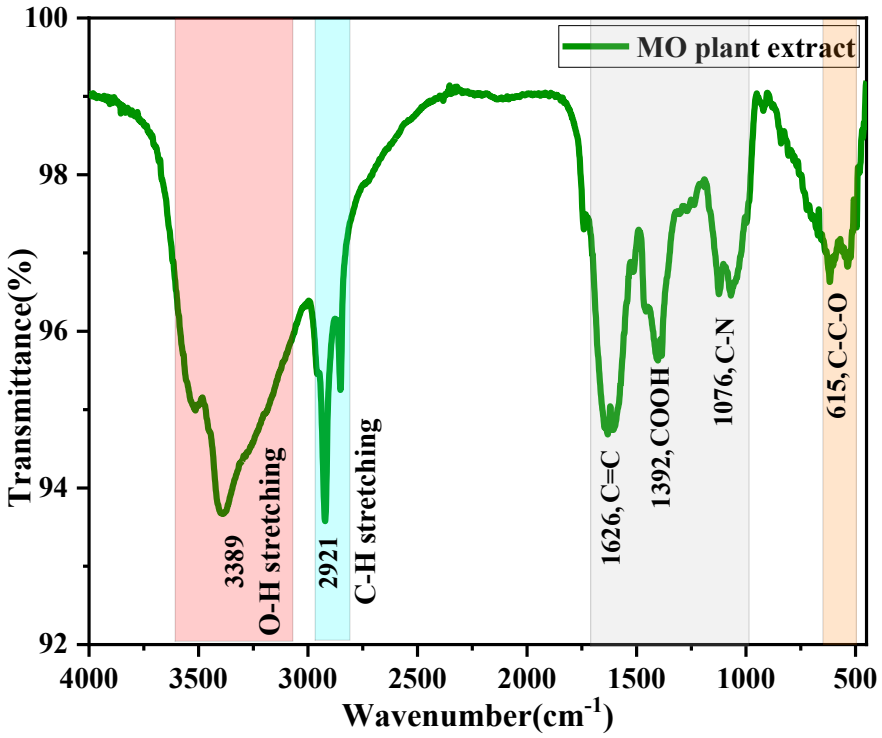

Figure 4 - 2: FTIR spectra of leaf extract of MO

The peak observed at approximately 3389 cm^{-1} was assigned to the stretching of hydroxyl(O-H) groups. This was due to hydroxyl functional groups in phenolic compounds present in leaf extract of MO. The absorption band of about 2921 cm^{-1} was attributed to the C-H absorption, indicating the presence of polysaccharides molecules in MO leaf extract. The medium peak observed approximately at 1626 cm^{-1} was attributed to the characteristic stretching of C=C. The absorption band of about 1392 cm^{-1} might confirm the presence of carboxylic groups (COOH). Peaks around 1076 cm^{-1} might indicate the characteristic absorption of amine (C-N stretching). The presence of amine groups indicates that MO extract contains proteins or amino acids. The absorption bands at 615 cm^{-1} could be characteristic of the C-C-O stretching band. Result obtained was in line with similar studies on methanolic extract of MO leaves (Mabrouki et al., 2020)(Jeyakumar et al., 2020).

4.1.2. Effect of nucleation time on the biosynthesis of ZnO NPs

Nucleation time is the period required for the complete reduction of the metal ions to synthesize metal NPs. The study was conducted at the 1, 2, 3, and 4 hr to study the effect of reaction time on the biosynthesis of ZnO NPs. The characteristic peak at 330 nm was recorded in all reaction times,

even though they have different absorption peaks. As indicated in Figures 4-3, increasing the reaction time from 1 hr to 4 hr resulted in increasing the formation of ZnO NPs. A small absorption peak was observed at 1 hr, whereas a maximum absorption peak was obtained at 4 hrs.

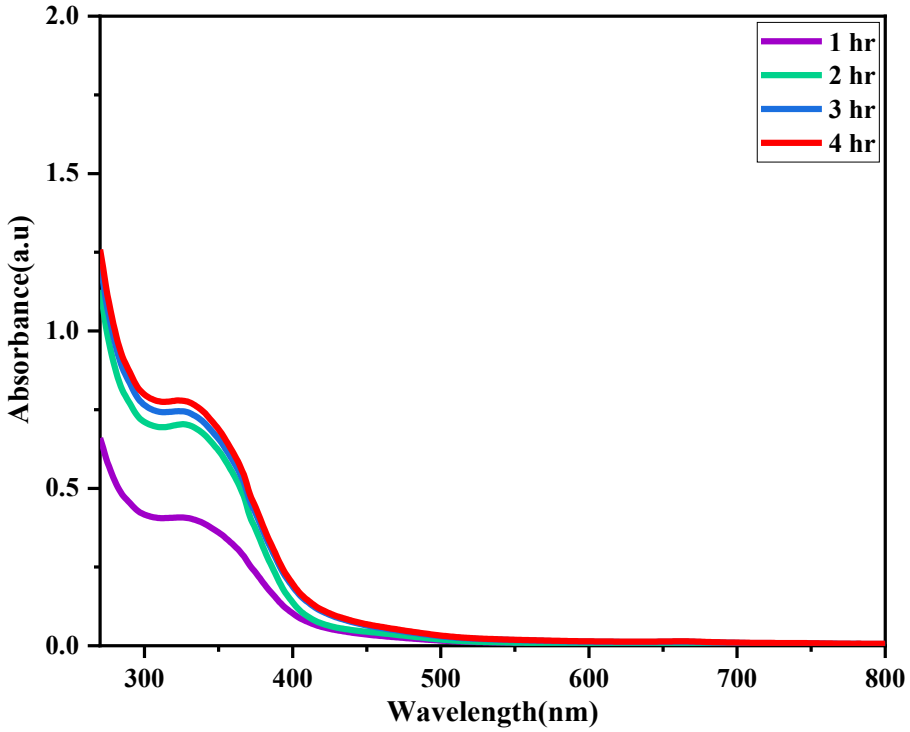

Figure 4 - 3: UV-Vis spectra of the ZnO NPs synthesized at different nucleation times

Even though the maximum absorption peak was obtained at 4 hr, no significant (big) change in the formation of ZnO NPs was observed at a nucleation time of 2 hr to 4 hr, i.e., a very slight change in absorption peak was observed at nucleation time of 2 hr and 4 hr. The change in the formation of ZnO NPs was insignificant. Therefore, 3 hrs reaction time was selected for the biosynthesis of ZnO NPs.

Reaction conditions followed to study the effects of nucleation time were: solvent used was (50:50(v/v) MT and DW), precursor concentration (0.1 M), the volume of MO extract to the precursor solution (50:50), and reaction temperature (60 ℃). The obtained was supported by similar studies on the biosynthesis of ZnO NPs carried out at nucleation time of 3 hrs (Darvishi et al., 2019; K. Gupta & Chundawat, 2020; Król et al., 2019; Yoon & Oh, 2021).

4.1.3. Effect of reaction temperature on the biosynthesis of ZnO NPs

Temperature plays a crucial role in green nanoparticle synthesis as it controls the nucleation process during the formation of nanoparticles. Other parameters were kept constant to see the effect of temperature on the biosynthesis of NPs. Effects of temperature on the biosynthesis of ZnO NPs observed as shown in Figures 4 - 4. The maximum peak was observed at 90 ℃ (high formation of ZnO NPs), whereas a small absorption peak was observed at 50 ℃, implying less formation of ZnO NPs. As the temperature increased from 50 ℃ to 90 ℃, ZnO NPs formation was also increased.

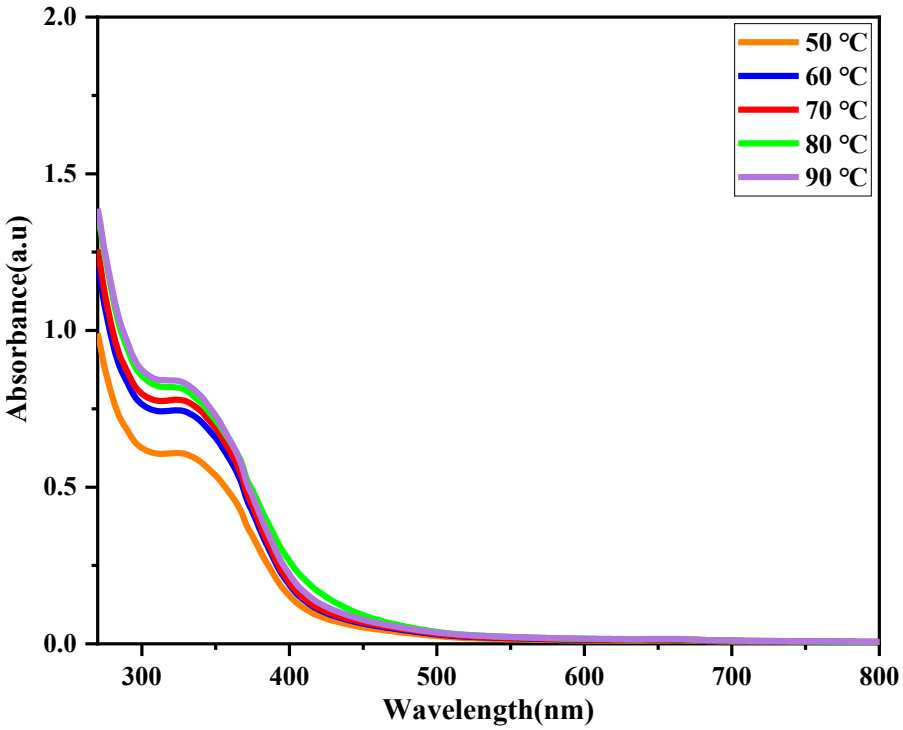

Figure 4 - 4: UV-Vis spectra of the ZnO NPs synthesized at different reaction temperatures

Increasing temperature favors the formation of ZnO NPs, as observed from Figure 4-4. No significant change was observed in the formation of ZnO NPs in further increasing temperature from 80 ℃ to 90 ℃. Since the formation of ZnO NPs is not significantly affected, fixing temperature at 80 ℃ as local optimum was a reasonable choice for the biosynthesis of ZnO NPs throughout the rest of the experiment. Temperatures were varied, whereas other parameters such solvent used (50:50(v/v) MT and DW), precursor concentration (0.1 M), the volume of MO extract to the precursor solution (50:50), and reaction time (3 hrs.) were kept constant. Similar works were

done on the biosynthesis of ZnO NPs at a temperature of 80 ℃. This result was in line with results reported by Tean Zaheer et al., V.A. Soares et al., Khushbu Gupta et al., and M. Golmohammadi et al. (Golmohammadi et al., 2020; K. Gupta & Chundawat, 2020; Soares et al., 2020; Zaheer et al., 2021).

4.1.4. Effect of volume of MO extracts to the volume of precursor solution

The volume of plant extract is another significant parameter that affects the formation of ZnO NPs. It was observed that there was a direct correlation between the volume of MO extract and UV absorbance, as observed in Figures 4-5. The volume of MO extract to precursor solution on the biosynthesis of ZnO NPs ranged from 10:50 mL to 70:50 mL at a fixed precursor amount (0.1 M in 50 mL DW). As observed from Figures 4 - 5, increasing the volume of plant extract to a fixed precursor ratio resulted in increased ZnO NPs. This might be due to the Zn^{2+} ion that completely reacted with enough MO leaf extract or an excess amount of MO leaf extract.

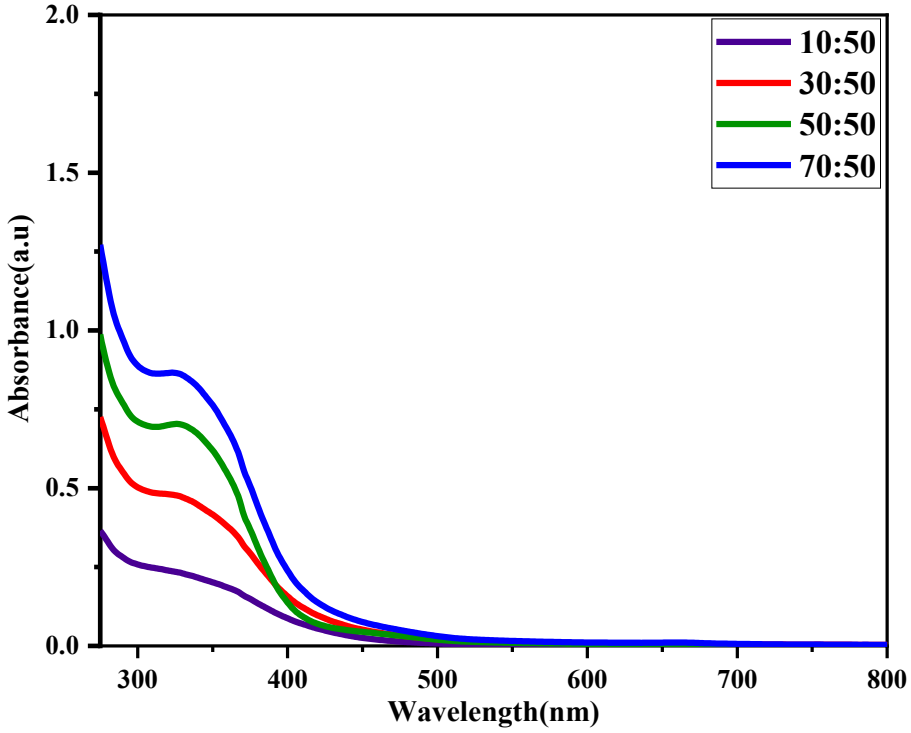

Figure 4 - 5: UV – Vis spectra of the ZnO NPs synthesized at the different volumes of MO extract

When 10:50 mL, 30:50 mL, and 50:50 mL volume of MO leaf extract was used for the biosynthesis of ZnO NPs, the formation of yellowish color was observed. On the other hand, at the increased

amount of MO leaf extract of 70:50 mL, formation of green color was observed (i.e., color of MO leaf extract). Studies indicated that qualitatively, yellowish color indicates the formation and synthesis of ZnO NPs (A. K. Singh et al., 2017). So, the green color observed was due to an excess amount of plant extract in the solution.

It was observed that the increased absorbance at 70:50 mL indicated an excess amount of plant extract. Thus, a 50:50 mL volume of MO leaf extract to specified precursor solution was selected for the biosynthesis of ZnO NPs throughout the rest work. Reaction conditions were: Solvent used (50:50(v/v) MT and DW), precursor concentration of (0.1 M), reaction temperature of (80 ℃), and nucleation time of (3 hrs.) were kept constant.

4.1.5. Effect of precursor concentration on the biosynthesis of ZnO NPs

Biosynthesis of ZnO NPs was also affected by the precursor concentration. The impact of zinc nitrate hexahydrates concentration as a precursor for the biosynthesis of ZnO NPs was studied in this work. As observed from Figure 4-6, ZnO NPs formation was increased while increasing precursor concentration from 0.0025 M to 0.025 M whereas, its formation decreased when further increasing precursor concentration from 0.025 M to 0.1 M. This decrement might be due to settling down or agglomeration of NPs when the precursor concentration increases beyond 0.025M. Less absorption peak (i.e., less formation of ZnO NPs) was observed at 0.0025M due to a lower precursor concentration.

Based on the result obtained, the best synthesis concentration of ZnO NPs was 0.025 M. The increased absorbance was observed as the concentration increased from 0.0025M to 0.025M could be related to the increased density of ZnO NPs. Similar trends were also observed (A. K. Singh et al., 2017).

Jamdagni et al. also observed a similar trend indicated increasing concentrations of different precursor concentrations from 0.0025 to 0.01 M were used to optimize the synthesis of ZnO NPs. Rising concentrations of precursor increased the number density of ZnO NPs up to a certain point. But the further increase in concentration decreased the number density of ZnO NPs (Jamdagni et al., 2018). Reaction conditions; Solvent used (50:50(v/v) MT and DW), the volume of MO leaf extract to the precursor (50:50), reaction temperature (80 ℃), and reaction time (3 hrs.) were kept constant.

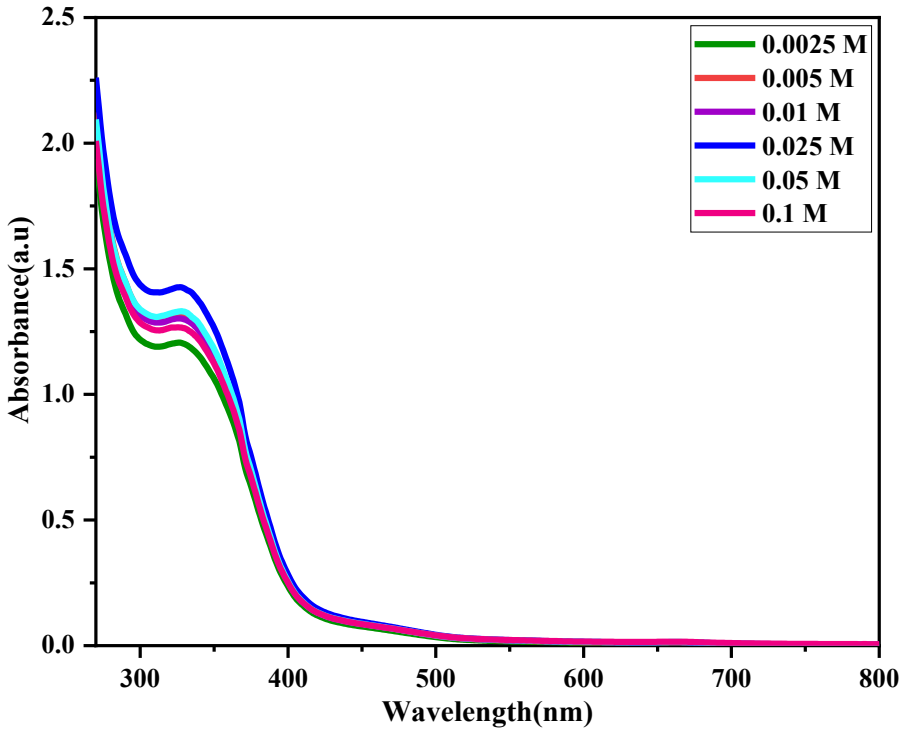

Figure 4 - 6: UV – Vis spectra of the ZnO NPs synthesized at different precursor concentrations

4.1.6. Effect of pH on the biosynthesis of ZnO NPs

The pH of the reaction mixture plays a crucial role in NPs synthesis. UV-Vis spectroscopy technique was used to study the impact of pH on the biosynthesis of ZnO NPs. The pH was maintained at 8, 10, 12, and 14 using 2 M NaOH. Figure 4- 7 presents the absorption spectra of biosynthesized ZnO NPs at different pH. It was seen that at all pH, except pH of 8, the characteristic absorption peak of biosynthesized ZnO NPs was observed at 345 nm. The spectra reveal that the absorbance increases with increasing pH values but further increases beyond pH of 12 resulted in decreased absorbance (i.e., reduced formation of ZnO NPs). This decrement was due to the settling down of particles. Based on the results obtained, a pH of 12 was chosen as the optimal pH for the biosynthesis of ZnO NPs.

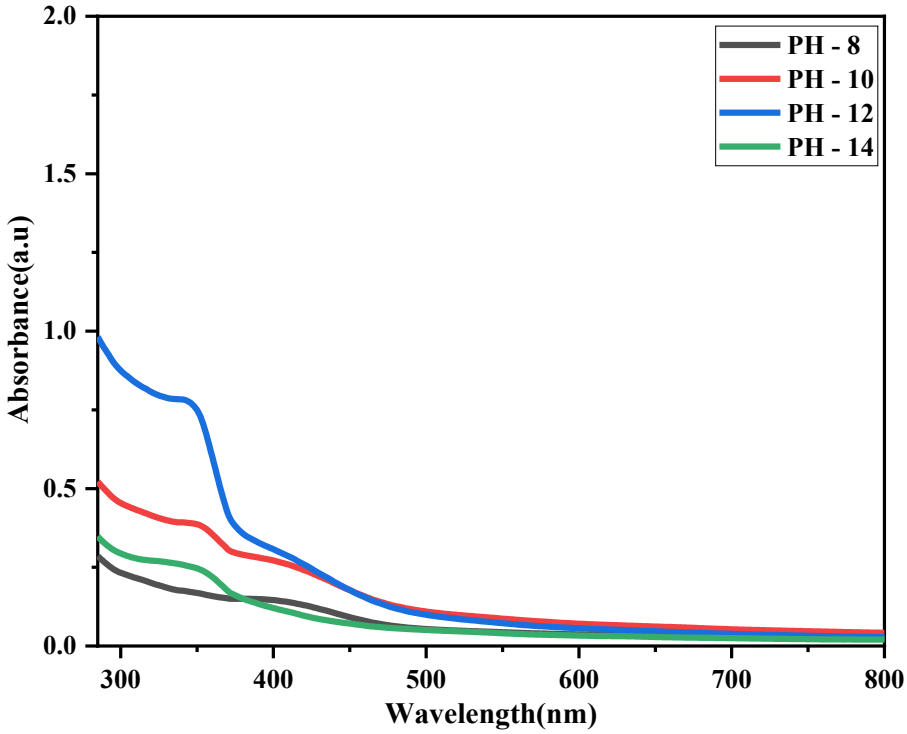

Figure 4 - 7: UV - Vis spectra of ZnO NPs at different pH

Similarly, Abdullah et al., and Gupta et al., also found that NPs were spherical at a pH of 12 and reported that pH of 12 was optimum pH for the biosynthesis of ZnO NPs (Abdullah et al., 2020; M. Gupta et al., 2018). Suleiman et al. also noted that increasing the solution pH in a primary medium increased the purity of biosynthesized ZnO NPs and the percentage yield of ZnO NPs (Jacob & Suleiman, 2021). Scholars also suggest that a more alkaline medium enhances the synthesis of ZnO NPs. This may be due to a higher rate of reduction of zinc ions.

4.1.7. Summary on studying effects of reaction parameters

Six parameters were studied to determine optimum points using a UV-Vis spectrophotometer. Based on that, 50:50 MT and DW were selected as an appropriate solvent, nucleation time (3 hr), reaction temperature (80 ℃), the volume of plant extracts to the volume of precursor solution (50:50), precursor concentration (0.025 M), and pH (12) were optimum points obtained for the biosynthesis of ZnO NPs. For optimum reaction parameters, biosynthesized ZnO NPs were annealed at high temperature by a muffle furnace at 500 ℃. UV-Vis spectrophotometer result was observed in Figure 4-8 with its bandgap energy. A characteristic absorption peak was observed at 363 nm.

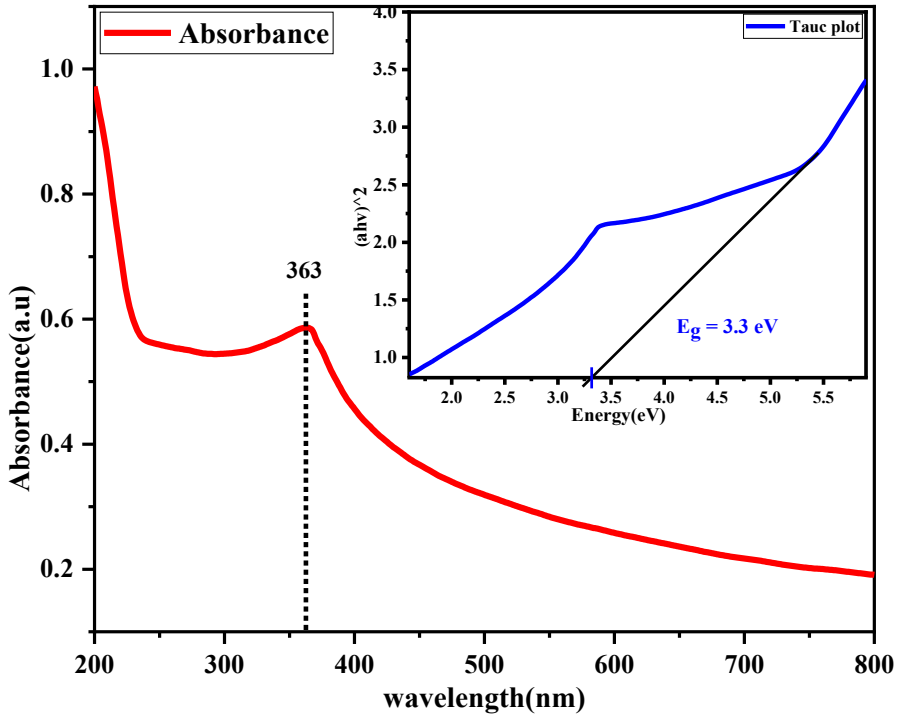

Figure 4 - 8: UV - Vis spectra of the ZnO NPs synthesized using optimum parameters and its bandgap energy

Bandgap energy (Eg) is the minimum amount of energy required to excite an electron up to a state in the conduction band where it can participate in conduction. The bandgap energy of ZnO NPs synthesized from MO leaf extract was shown in Figures 4-8. The value of E_g for the samples was calculated by using Tauc relation (Meenatchi et al., 2020; Series, 2021).

$$\alpha = \frac{A(h\upsilon - Eg)^{1/2}}{h\upsilon} \quad \text{.....4.1}$$

Where **A** is the proportional coefficient, α is the absorption coefficient, **h** is the Planck constant, **v** is the light frequency, **hυ** is the photon's energy, and $\mathbf{E_g}$ is the bandgap energy.

The bandgap of the biosynthesized ZnO NPs was found to be 3.30 eV as calculated from the Tauc relation. This value was obtained using the Tauc plot by extrapolation of the linear portion of the curve $(\alpha h\upsilon)^2$ versus $(h\upsilon)$ to the x-axis, which gives the energy of the bandgap directly. This result was well consistent with previously reported works whose bandgap energy was 3.26 eV (Ngom et al., 2019). This value was also in line with the other reported results of the bandgap of ZnO NPs, which is 3.37 eV (Matinise et al., 2017). Similar bandgap energy of 3.3 eV was obtained by other

research works too (Lu et al., 2019; Meenatchi et al., 2020; Yoon & Oh, 2021). ZnO NPs are used as sunscreen and are effective against UV radiation due to their bandgap energy.

4.2. Thermogravimetric analysis of ZnO NPs

TGA/ DTG of ZnO NPs was presented in Figures 4-9 with decomposition peaks as a function of temperature. Based on the TGA result, ZnO NPs showed major degradation peaks in three major mass loss steps. These decomposition peaks were seen in the DTG curve. The first decomposition peak showed a 26.7% weight loss in the temperature of about 148 ℃. This degradation might be occurred due to the decomposition of organic materials. The second and third had a weight loss of 72% and 95%, which were at the temperature of 390 ℃ and 548 ℃, respectively. No considerable loss is observed after 550 ℃, indicating that ZnO NPs are thermally stable above 550 ℃.

Moreover, decomposition temperatures at weight loss of $Wt\%_{10}$, $Wt\%_{50}$, $Wt\%_{max,}$ and $Wt\%_{90}$ were 69 ℃, 308 ℃, 390 ℃, and 470 ℃ respectively. TGA results show that the maximum weight loss of ZnO NPs occurred at the temperature of 390 ℃ whereas maximum degradation rate occurred at temperature of 548 ℃. This might be due to nitrate decomposition of ($Zn(NO_3)_2.6H_2O$), which was used as a precursor for the biosynthesis of ZnO NPs. Similarly, studies also showed that the decomposition of precursor ($Zn(NO_3)_2.6H_2O$) at around 400 ℃ for the biosynthesis of ZnO NPs.

This result was also in line with previous studies by R.A. Chimal et al., who revealed that three major mass loss steps were observed in the biosynthesis of ZnO NPs. They reported that organic material was combusted at decomposition temperature around 140 ℃ and precursor decomposition at around 400 ℃ (Álvarez-chimal et al., 2021). Similarly, N. Matinise et al. also reported another TGA result, indicating that TGA of ZnO NPs had three major mass loss steps. They stated that the peak around 139 ºC might be attributed to the loss of volatile surfactant molecules adsorbed on the surface of Zinc based complexes and decomposition of organic materials during synthesis conditions, whereas 400 ℃ was the temperature where ZnO NPs occurred (Matinise et al., 2017).

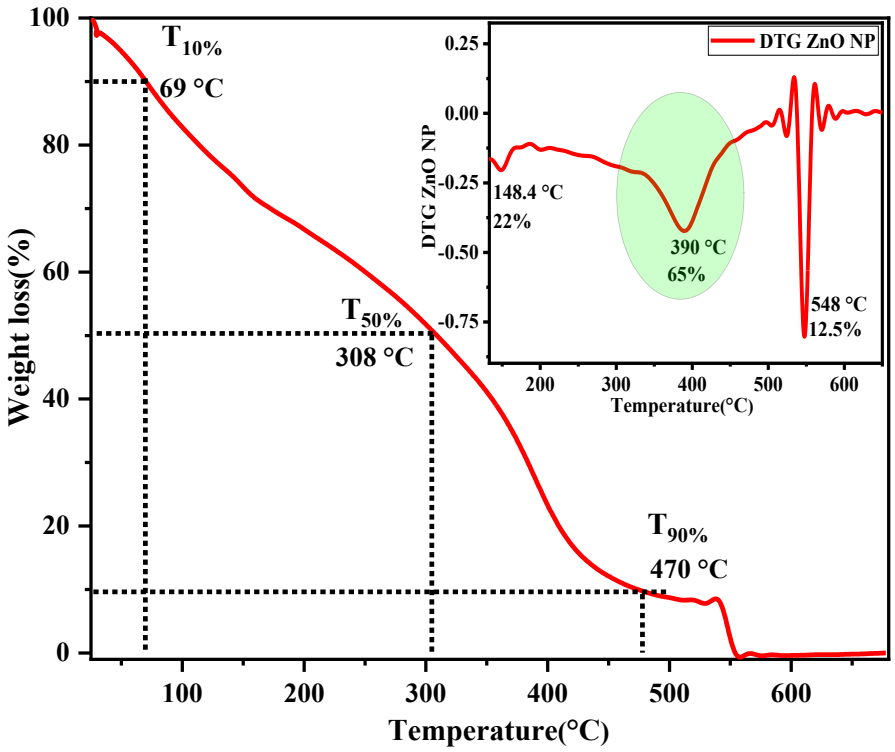

Figure 4 - 9: TGA/ DTG of ZnO NPs

4.3. Fourier transforms infrared spectroscopy analysis of ZnO NPs

FTIR is widely used to characterize the attachment of organic ligands to organic/inorganic NPs and surfaces in his case (Meenatchi et al., 2020). As observed from Figures 4-10, ZnO NPs in the spectral range of 400-4000 cm^{-1} have appeared at lower wavenumbers of about 497 cm^{-1}. Thus, the presence of a characteristic peak at 497 cm^{-1} indicated the presence of the ZnO NPs. This result was in line with the findings of Elumalai et al. and Pal et al., who reported that the region between 400 and 600 cm^{-1} is assigned for zinc-oxygen bond (Elumalai & Velmurugan, 2015; Pal et al., 2018).

It was also reported that wavenumbers at 487 cm^{-1} peaks indicate stretching vibration mode of pure ZnO (Ngom et al., 2019). Likewise, the FTIR spectrum of the biosynthesized ZnO NPs showed an absorption peak exhibited in lower wavenumbers of 481 $cm^{-1,}$ as reported by N. Matinise et al., (Matinise et al., 2017). Result obtained in this work was also matches the results of previously reported outcomes.

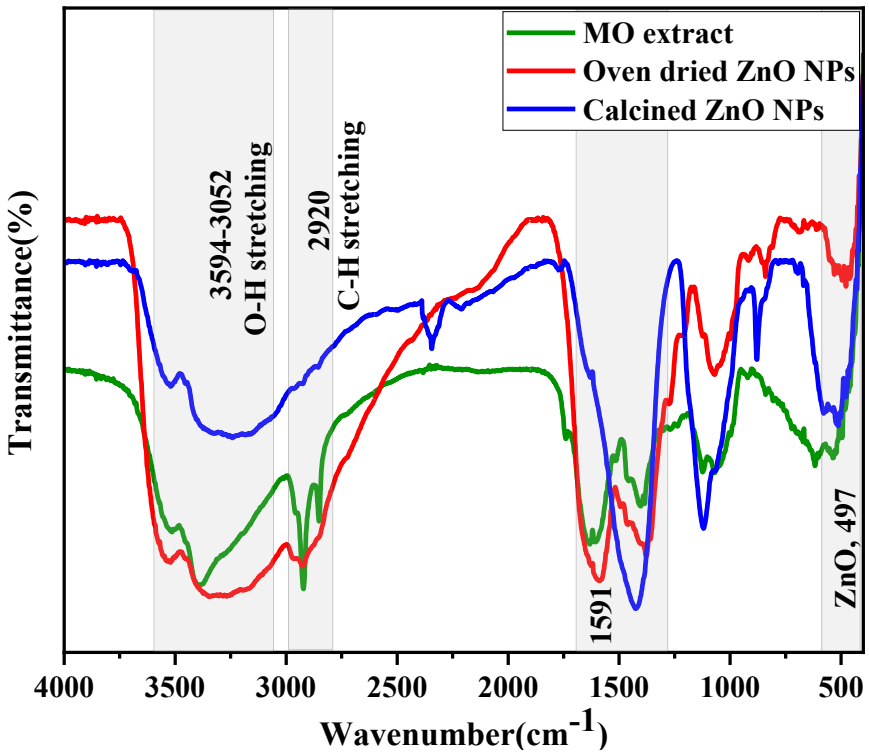

Figure 4 - 10: FTIR spectra of leaf extract of MO, calcined and oven-dried ZnO NPs

The intense broadband region at 3594-3052 cm^{-1} could be assigned to OH stretching bands. Calcined ZnO NPs have a less intense OH spectrum than MO extract and oven-dried ZnO NPs. This was due to organic matter contained in oven-dried ZnO NPs being subjected to high annealing temperatures. The C-H stretching band observed at 2920 cm-1 depicts the presence of the phenolic compound in both MO extract and slow oven dried ZnO NPs. The C-H stretching disappeared in calcined ZnO NPs because organic compounds were removed or destroyed when treated at high temperatures.

The absorption peak that appeared at 1591 cm^{-1} indicates the presence of the C=C functional group in ZnO NPs. The C=C functional group was observed for slow oven dried ZnO NPs. The C=C attachment appeared in oven-dried ZnO NPs but was not observed for calcined ZnO NPs because of thermal treatment at high temperatures. Other peaks that appeared in the fingerprint regions were not presented due to the overcrowding of functional groups.

The existence of some phytochemicals was observed in calcined ZnO NPs. Studies by different scholars also indicated the participation of phenolic compounds in biosynthesized ZnO NPs.

Matinee et al. also stated overall observation that proves the existence of some phenolic compounds, terpenoids, or proteins that bounded to the surface of ZnO NPs (Matinise et al., 2017).

4.4. X-ray diffraction analysis of ZnO NPs

The crystal structure of nanoparticles was determined using XRD. XRD verifies the formation of NPs, their structural properties, purity, and determination of the crystallinity of NPs (Shabaani et al., 2020). The XRD pattern of NPs demonstrated a hexagonal wurtzite structure with the presence of strong differentiation peaks in 31.78, 34.47, 36.26, 47.57, 56.58, 61.98, 62.89, 66.40, 68.02º that are respectively reflected in the reference lattice planes of (100), (002), (101), (102), (110), (103), (112), (200) and (201). It was important to observe that the (101) diffraction peak seems to be the most intense. All peaks were indexed as hexagonal wurtzite phase of ZnO nanocrystals, as other similar works reports indicated (Letsholathebe et al., 2021). The XRD peaks with a distinct line broadening and sharp peaks showed the crystalline nature of NPs and the prepared particles in the nano-scale range.

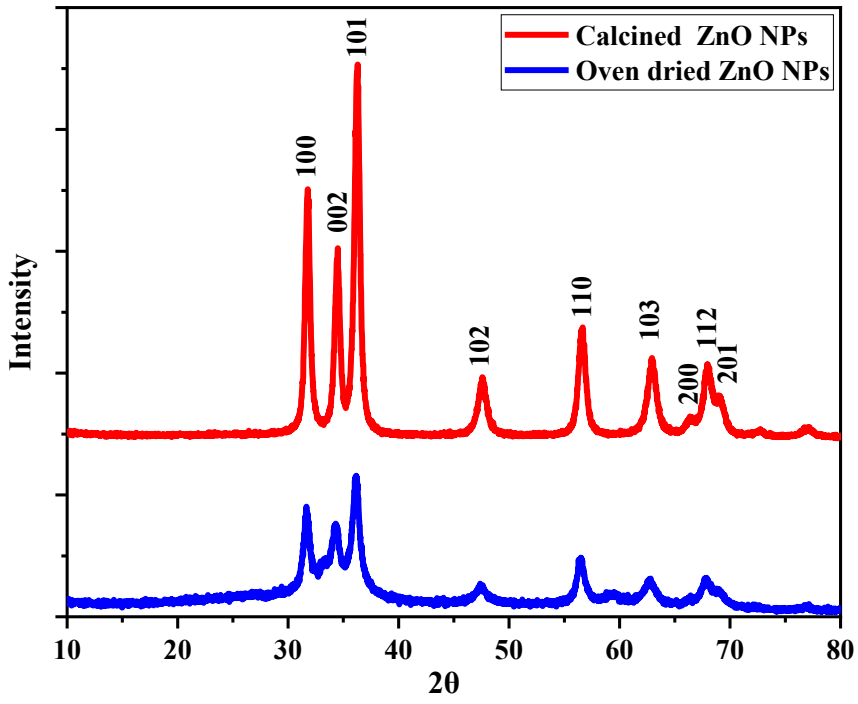

Figure 4 - 11: XRD pattern of ZnO NPs synthesized via MO leaf extract

The crystallite size of ZnO NPs was calculated using Scherrer's formula: $D = k\lambda/\beta\cos\theta$, where D is the crystal size, k is Scherrer's constant usually taken as 0.9, λ is the X-ray wavelength of CuKa

radiation (k = 1.5406 Å), β is the line width of half maximum in radians, and θ is Bragg's diffraction angle. X-ray diffraction (XRD) patterns of ZnO NPs were presented in Fig 4 - 11. Average crystallite size calculated from Scherrer's formula was 12.85 nm for calcined ZnO NPs and 9.1 nm for oven-dried ZnO NPs. The d-spacing, i.e., the distance between planes of atoms that give rise to diffraction peaks, was calculated using Bragg's equation: $d= n\lambda/2\sin\theta$ where, n=1, λ is the wavelength of incidence X-ray, θ is peak position (in radians) and d is interplanar distance. Based on that, the average d-spacing between atoms of oven-dried and calcined ZnO NPS was 0.201 and 0.1854 nm, respectively. For the oven-dried sample, it was observed that a series of small particles approximately with a certain degree of short-range atomic ordering was formed. This might be due to MO leaf oil that encircles ZnO NPs that avoids clustering of particles together.

The XRD results obtained were consistent with the results of biosynthesized ZnO NPs using the MO extract and reported that the crystalline particle size of NPs synthesized was between 14 and 27 nm (Elumalai & Velmurugan, 2015; Matinise et al., 2017; Ngom et al., 2019). It was also revealed that a significant increase in crystalline size was observed as the sample was subjected to increased temperature (Rajarajeswari et al., 2020). The crystalline size of NPs synthesized in this work was lower and better than the reported results. This indicates better crystallinity compared to similar works previously done.

The sharp and intense peaks observed indicate that the samples were highly crystalline. No other diffraction peaks appeared shown no impurity was found, confirming the high purity of the biosynthesized ZnO NPs. Similar results were also reported on "Green synthesis of ZnO NPs using MO and investigating its photocatalytic and antibacterial activity (Elumalai et al., 2015; Fadhlan et al., 2020; Matinise et al., 2017; Ngom et al., 2020).

4.5. Antimicrobial activity of biosynthesized ZnO NPs

The disc diffusion method determined the in vitro antibacterial susceptibility test based on National Committee for Clinical Laboratory Standards (National Committee for Clinical Laboratory Standards, 2012). Among the various metal oxide NPs investigated for their antibacterial activity, ZnO NPs depict selective toxicity to bacterial species but reveal a negligible impact on human cells (A. K. Singh et al., 2017). Antibacterial activity of ZnO NPs and MO leaf extract was presented in Figures 4-12. Biosynthesized ZnO NPs were tested by the disc diffusion method using selected organisms such as gram-negative bacteria (E. coli) and gram-positive bacteria (S. aureus).

In this method, the antibacterial activity of prepared ZnO NPs was analyzed against E. coli and S. aureus, while Ampicillin (Amp) was used as a positive control. As the concentration of ZnO NPs increases, the zone of inhibition also increased against bacteria strain. Zone of inhibition values was determined at the concentration of 75µg/ml and 100 µg/ml. ZnO NPs have a significant growth inhibition effect against S. aureus and E. coli bacteria. This effect was due to the high surface area to volume ratio of ZnO NPs and their small size. As observed from the results, biosynthesized ZnO NPs were more effective against gram-negative bacteria.

Table 4 - 1: List of bacteria species and zone of inhibition

Sample name	Concentration	Bacteria Species and Zone of Inhibition in mm	
		Gram-Negative Escherichia coli (E. coli)	Gram-Positive Staphylococcus aureus (S. aureus)
Z_1(A)	75 µg/mL	10	9
Z_1(B)	100 µg/mL	12	11
Z_2(A)	75 µg/mL	13	12
Z_2(B)	100 µg/mL	16	14
Z_3(A)	75 µg/mL	9	9
Z_3(B)	100 µg/mL	11	10
Ampicillin (Amp)	75 µg/mL	14	13

Where MO leaf extract (Z_3), oven-dried ZnO NPs (Z_2), and calcined ZnO NPs (Z_1)

It was observed that as the concentration of ZnO NPs increases, the zone of inhibition also increases against bacteria strain. A low zone of inhibition (lower activity) was obtained for MO. In contrast, a maximum area of inhibition (higher activity) was obtained for oven-dried ZnO-NPs at a 100 µg/ml concentration against E. coli. Oven-dried ZnO-NPs showed better antimicrobial activity than calcined ZnO-NPs. This implies active constituents (phytochemicals) derived from MO leaf extract gave additional action for ZnO NPs and thus had better antimicrobial activity. However, for calcined ZnO NPs, these active MO constituents didn't appear because of the thermal treatment of ZnO NPs at high temperatures. Its antimicrobial activity was only due to the presence of ZnO NPs.

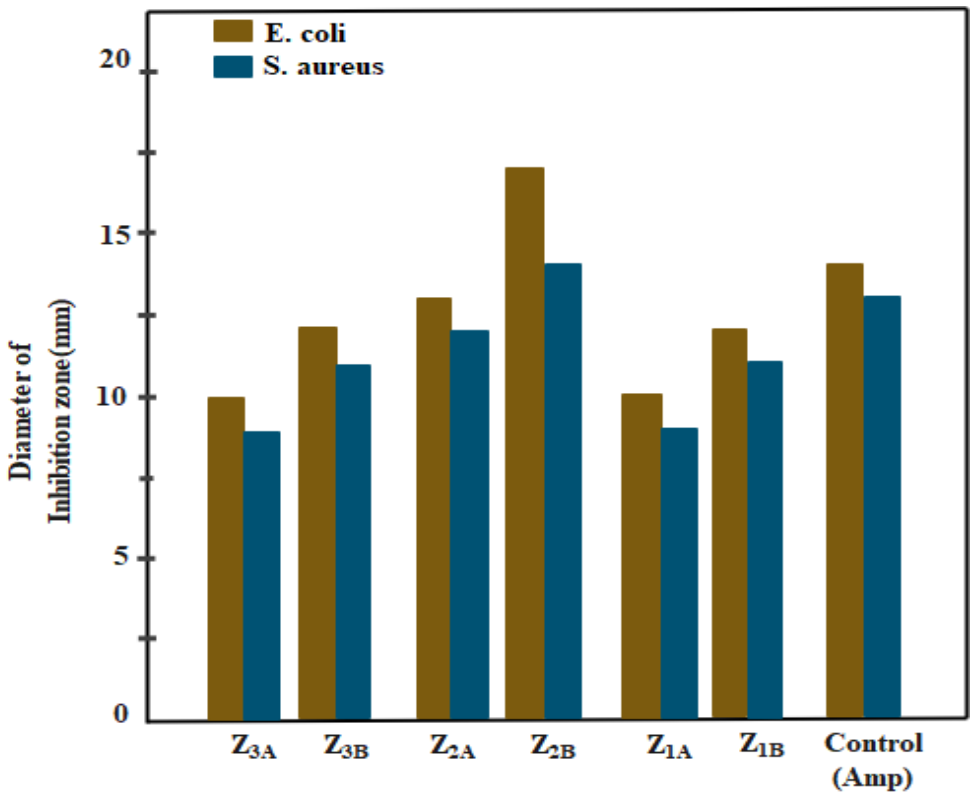

Figure 4 - 12: Antibacterial activity of ZnO NPs and MO leaf extract

Overall, the reduction in bacterial growth was observed to increase the concentration of biosynthesized MO and ZnO NPs. The antibacterial activity result of ZnO NPs obtained agreed with similar works previously done (Król et al., 2017) (Elumalai et al., 2015) (Meenatchi et al., 2020)(Pal et al., 2018) (Jayabalan et al., 2019).

4.6. Extraction of Collagen/Elastin matrix

Collagen and elastin matrix was successfully extracted from the broiler skin was presented in Figure 4-13. Collagen contributes to the strength and structural integrity of the skin, while elastin provides elasticity and tensile strength to the skin. Studies indicated that COL/ELS could be used in burn/wound cover or dressings, resorbable surgical suture, osteogenic and bone filling materials, hemostatic agents, and immobilization of therapeutic enzymes and have been used as an ingredient in cosmetic formulations numerously by cosmetic manufactures to promote better skin elasticity (Chattopadhyay & Raines, 2014).

Figure 4 - 13: COL/ELS matrix extracted from waste broiler skin

4.6.1. Proximate analysis of broiler skin

The proximate analysis such as fat, moisture, and ash content of broiler skin was presented in Table 4 - 2. Ash content represents incombustible components that remain after the sample is completely burned. As illustrated in table 4-2, ash content of about 1.12% indicates that broiler skin contains small inorganic residues; this indicates broiler skin was derived from entirely organic residues. A similar report on the determination of ash content of COL/ELS matrix from broiler skin was less than or equal to 1% (Meseret Ewunetu, 2020). A Biuret test analysis was another proximate analysis test used to determine the presence of a peptide bond in a broiler skin.

Table 4 - 2: Proximate analysis of broiler skin and extracted COL/ELS.

Proximate Analysis	**Broiler skin**
Moisture Content (%)	20%
Ash Content (%)	1.12
Fat Content (%)	3.20
Biuret Test for protein	Positive Violet color

4.6.2. The solubility and reaction mechanism of COL/ELS matrix within lactic acid

It was observed that COL/ELS extracted from broiler skin had been completely dissolved in lactic acid. Solubility of COL/ELS matrix in lactic acid was presented in Figure 4-14**(a)**. Lactic acid facilitates the delamination of α helix and β sheet stacks of COL/ELS respectively by weakening

the secondary structure formed by the NH and C=O bond of the consecutive chains of the peptide bonds. This phenomenon helps to initiate the oligomerization of lactic acid within the protein-peptide chains. It might be the reason for forming a new secondary structure between COL/ELS and lactic acid oligomer.

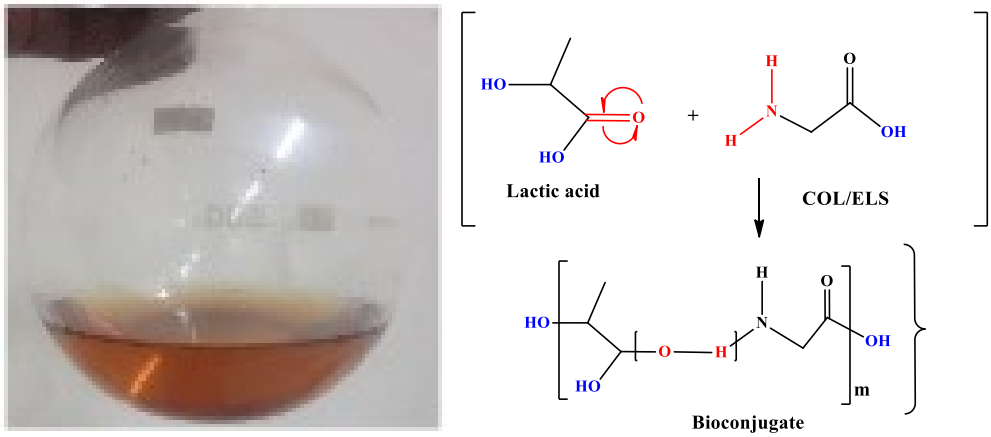

a) b)

Figure 4 - 14: Solubility and reaction mechanism of COL/ELS matrix in lactic acid

After complete solubilization of COL/ELS matrix in lactic acid monomer, polycondensation reaction was taking place at 150 ℃ for 5 hrs in the temperature-controlled reactor. Oligomerization of lactic acid occurs in the temperature-controlled reactor after the delamination of the secondary structure of the extracted COL/ELS. It opens its chain by giving water as a byproduct. There was an interaction between lactic acid oligomer (OLLA) and secondary structure of COL/ELS matrix. Because of this interaction, there was a weak secondary bond between the carboxyl group (C=O) and the NH group of delaminated sheets of COL/ELS. The possible reaction mechanism of COL/ELS with lactic acid was presented in Figures 4-14**(b)**. Similarly, the previous report indicated a strong interaction between the lactic acid oligomer and the COL/ELS matrix (Meseret Ewunetu, 2020). The synthesized bioconjugate was used as an ointment base in the formulation of ZnO NPs dispersed ointment.

4.6.3 Synthesis and characterization of bioconjugate

4.6.3.1. Organoleptic characteristics of bioconjugate

The organoleptic properties of the ointment base include physical appearances like appearance or color, phase separation, and homogeneity. Results indicated that the ointment base had a cosmetically appealing appearance and was homogenous with no signs of phase separation. The synthesized ointment base had a brown color.

Table 4 - 3:Sensory analysis for the synthesized ointment base

Sample	Color	Physical appearance	Homogeneity	Phase Separation
Bioconjugate (F_0)	Brown	Thick	Homogeneous	No

4.6.3.2. FTIR analysis of the bioconjugate

FTIR spectra of synthesized bioconjugate were presented in Figures 4-15. The broad FTIR spectra observed around 3624 - 3060 cm^{-1} commonly indicate the presence of hydroxyl (OH) and NH groups in synthesized bioconjugate. The presence of the OH group might be due to the presence of OH in the secondary structure of COL/ELS and lactic acid.

FTIR spectral region at 2977 cm^{-1} reveals the presence of the CH group in bioconjugate. It was expected that formation of weak secondary interaction between lactic acid oligomer C=O group and the delaminated NH group of the secondary structure of COL/ELS. The formation of a broad shoulder-like peak at 1745 cm^{-1} confirms the existence of COL/ELS within the lactic acid oligomer. The peak was observed for lactic acid oligomer (OLLA) at 1649 cm^{-1}. This result was well consistent with findings of previous work on grafting of lactic acid on COL/ELS matrix (Meseret Ewunetu, 2020)(Yoseph et al., 2020).

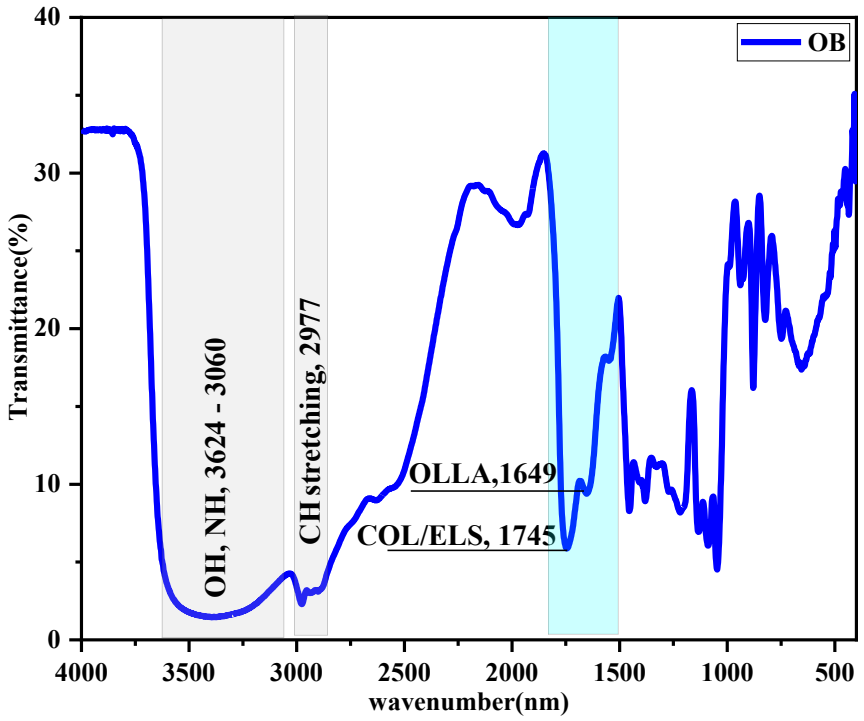

Figure 4 - 15: FTIR spectra for synthesized ointment base.

4.7. Organoleptic characteristics of the ointment

Ointment's organoleptic properties include physical appearance, color, phase separation, homogeneity, etc., for the biobased ointment presented in Tables 4 - 4. Results obtained were indicated that the ointment was semi-solid(thick), had emollient characteristics, brown color, and homogenous with no signs of phase separation. The pH values for the synthesized base matrix and ointment were also determined. The base matrix and biobased ointment had acidic pH because of lactic acid. Since lactic acid is an organic acid and body fluid, it does not irritate the skin. The increase in pH might be due to the presence of phenolic groups in ZnO NPs. The color of synthesized ointment had shown in Figure 4-16 below.

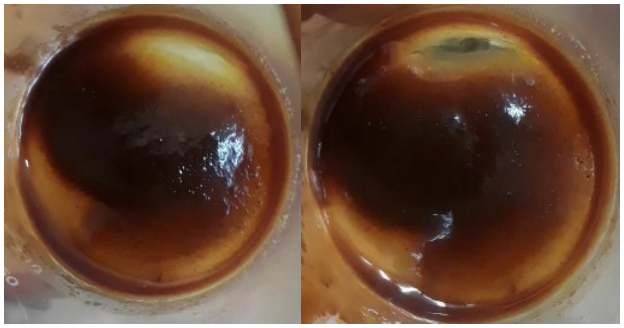

Figure 4 - 16: Color of ZnO NPs dispersed ointment

Table 4 - 4: Organoleptic evaluation of the ointment

Formulation	Color	Homogeneity	Phase Separation	physical appearance	pH
F_0	Brown	Homogenous	No	Thick	4.2
F_1	Brown	Homogenous	No	Thick	4.37
F_2	Brown	Homogenous	No	Thick	4.52
F_3	Brown	Homogenous	No	Thick	4.68
F_4	Brown	Homogenous	No	Thick	4.94

Spreadability and viscosity of the ZnO NPs dispersed ointment

Spreadability is the ability of topical preparations such as ointments, creams, gels, pastes, etc., to spread when applied to the skin evenly. It was observed that the spreadability of the ointment decreases with the increasing concentration of ZnO NPs. The synthesized base matrix was spreadable with lubricant characteristics. It was observed that the synthesized ointment base was also applied easily without being runoff. On the other hand, increasing the concentration of ZnO NPs from 0.5% to 5% in the base matrix resulted in increased viscosity of ointment. As a result, the spreadability of the ointment decreased. Spreadability and viscosity results were tabulated in Tables 4 - 5.

Table 4 - 5: Spreadability and viscosity of the ointment

Parameter	F_0	F_1	F_2	F_3	F_4
Time (sec)	19	22	26	31	38
Spreading diameter	18.18	15.7	13.3	11.14	9.09
Viscosity(cp)	>5000	>5000	>5000	>5000	>5000

Viscosity is the most important parameter as it governs the formulation's many properties, such as spreadability, and pourability of the product (Lisnawati et al., 2019). Increased concentration of

ZnO NPs dispersed on ointment base had increased viscosity. The viscosity of the ointment base and ZnO NPs dispersed ointment base had a viscosity of more than 5000cp. Similar works by N. Lisnawati et al. on the viscosity of nanoparticles ointment preparation using Blimbi extract were greater than 5000 cp (Lisnawati et al., 2018). Likewise, O. Adeleye et al. reported works on formulating and evaluating Ehretia Cymosa biosynthesized silver nanoparticle anti-inflammatory ointment. Their work said that the viscosity of developed ointment was greater than 10,000 (Adeleye et al., 2021b). Another report on similar work also revealed the viscosity of ointment greater than 5000 cp (Meseret Ewunetu, 2020).

Figure 4 - 17: Viscosity measurement of OB and ZnO NPs-DO

4.8. Investigating the effect of ZnO NPs on antimicrobial and light-absorbing characteristics of the biobased ointment

4.8.1. FTIR analysis of the ZnO NPs dispersed ointment

The FTIR spectrum of formulated ointment ZnO NPs-OB) in Figures 4-18 showed no significant shift in the position of the characteristic bands to ointment base (OB), i.e., FTIR spectra of the formulated ointment showed similar spectra as an ointment base. Carboxyl groups were observed with a slight shoulder-like peak at 1745, and 1649 cm^{-1} for OB was decreased in intensity ZnO NPs-OB. Slight shifting of absorption spectra and disappearance of peaks was also observed. This indicates that there was strong interaction occurred between bioconjugate and ZnO NPs dispersed into it. The peak around 3641-3081 cm^{-1} was responsible for N-H, and OH stretching appeared for OB, ZnO NPs, and formulated ZnO NPs-OB. Amide bands involved in peptide N-H groups might

be due to protein-containing molecules obtained from COL/ELS. Related works also confirm the presence of protein functional groups (Yoseph et al., 2020). A decrease in CH stretching was also observed for ZnO NPs-OB compared to OB.

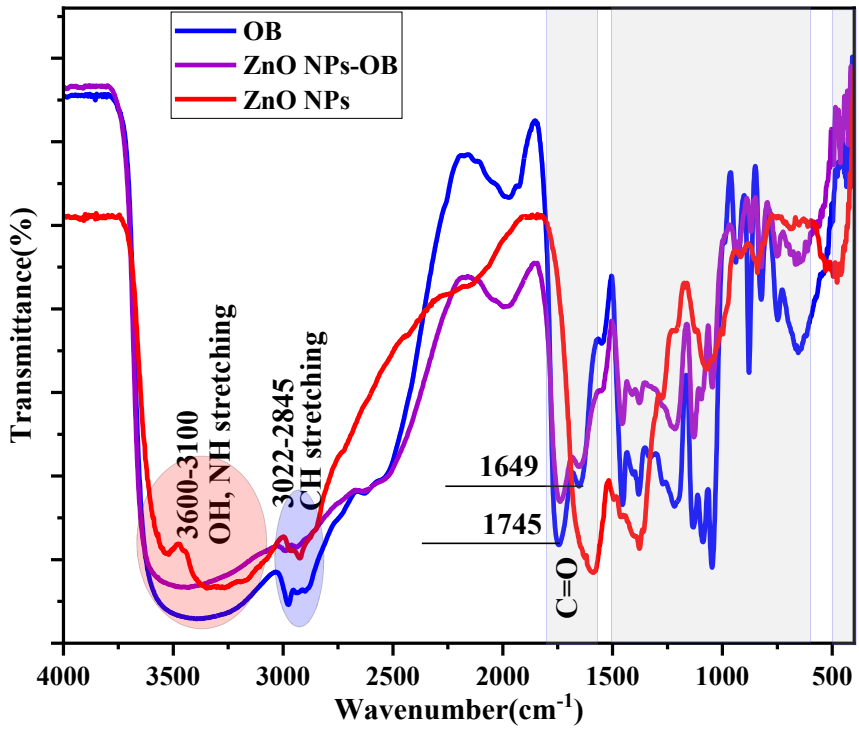

Figure 4 - 18: FTIR of the OB, ZnO NPs, and ZnO NPs-OB

Absorption peaks observed at 1745 and 1649 cm^{-1} indicate C=O and amide functional groups in ZnO NPs-OB. ZnO NPs in ZnO NPs-OB were also observed at a lower wavenumber of about 453 cm^{-1}. This result was also in line with the results of previous studies on the formation of ZnO NPs at lower energy regions in the range of 400-600 cm^{-1} (Elumalai & Velmurugan, 2015; Pal et al., 2018). Comparable studies conducted on biosynthesized nanoparticle ointment revealed that the FTIR spectrum showed no significant shift in the characteristic bands associated with the ointment base, which confirms no significant chemical interaction between the silver nanoparticle and ointment base (Adeleye et al., 2021a).

4.8.2. UV light absorbing characteristics of ZnO NPs-OB

The UV-Vis absorption spectra were obtained for ZnO NPs-OB to investigate its UV-vis radiation-absorbing capability. UV-visible absorption spectra of OB and ZnO NPs-OB were shown in

Figures 4-20. Based on the UV-Vis spectroscopy result obtained, no absorption peak was observed for bioconjugate (OB). Since OB hadn't shown any peak formed on UV-Vis spectroscopy, other peaks that appeared in ZnO NPs-OB were definitely due to the presence of ZnO NPs. The absorption peak of ZnO NPs-OB increase with increased ZnO NPs concentration from 0% to 5%.

The absorption peaks of ZnO NPs-OB were observed between 320 to 400 nm. Based on photon wavelength, UVA lies in the 315-400 nm (Amaro-ortiz et al., 2014). The minimum amount of energy required for ZnO NPs to excite an electron from the valance band to the conduction band was 3.30 eV, as stated in section 4.17. That means UV light of energy equal to or greater than 3.30 eV should be required to excite an electron from the valance band to the conduction band. During the excitation of electrons, enough UV light or photon energy is absorbed by ZnO NPs.

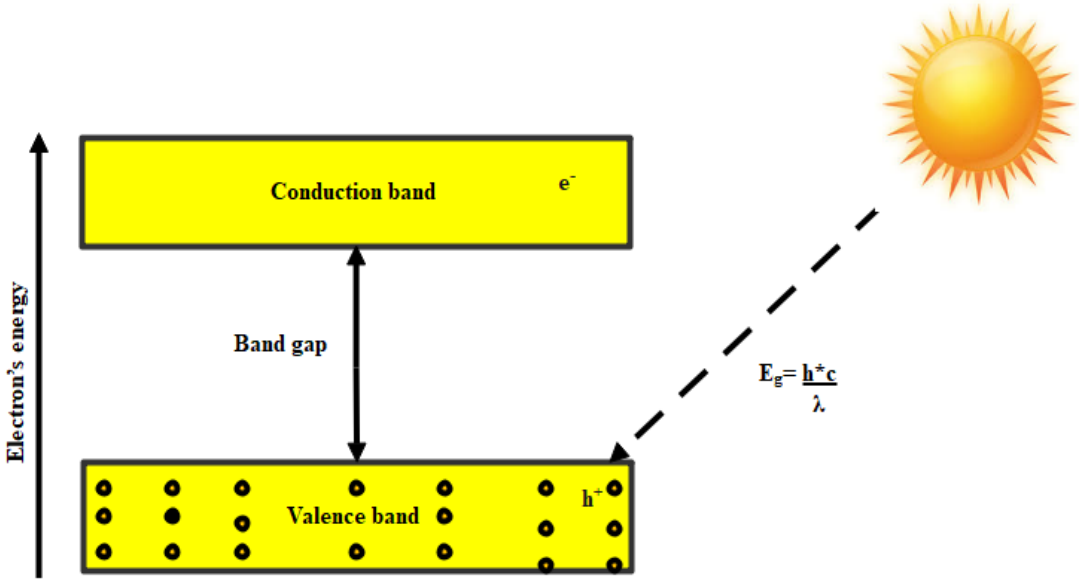

Figure 4 - 19:Graphical representation of the bandgap of ZnO NPs.

The valence band possesses many densely packed electron states that allow many absorption possibilities, as long as the energy absorption exceeds the bandgap width, as shown in Figures 4-19. That is partly why ZnO NPs crystals absorb more in UVA radiation. During absorption, UVA radiation was scattered and reflected back while permitting visible light that is important to our body, i.e., a good source of vitamin D. When the bandgap energy is met, the electron is excited into a free state, and can therefore participate in conduction. So, no UV radiation reaches our skin, and our skin is kept safe (Press, 2011).

Therefore, synthesized ZnO NPs-OB could absorb UVA and protect skin from harmful UVA radiation due to the unique property of ZnO NPs. The UV-Vis spectrum reveals a characteristic absorption peak of ZnO at the wavelength of around 343 nm, as shown in Figures 4-20. The good absorption of the ZnO-NPs in the UV region proves the applicability of this product in medical applications such as sunscreen protectors or antiseptic ointments. The increased absorption peak of ZnO NPs-OB was due to the increased concentration of ZnO NPs. It has been shown by this thesis work that ZnO NPs-OB can be used as a sunscreen ointment.

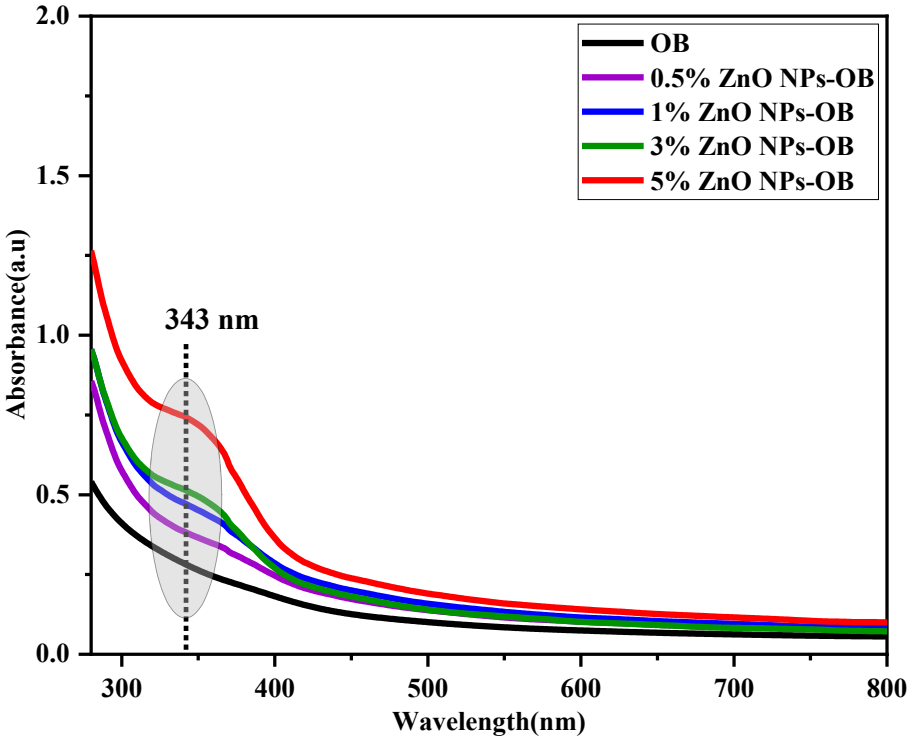

Figure 4 - 20: UV–Vis absorption spectra of ZnO NPs-OB.

4.8.3. Antimicrobial activity of ZnO NPs-OB

The disc diffusion method determined the in vitro antibacterial susceptibility test based on National Committee for Clinical Laboratory Standards (National Committee for Clinical Laboratory Standards, 2012). The OB and ZnO NPs-OB were tested for antibacterial susceptibility against E. coli and S. aureus. Results obtained from the antimicrobial study showed that ZnO NPs-OB has an excellent antimicrobial effect on both S. aureus and E. coli. Antimicrobial activities results were obtained in the zone of inhibition diameter (mm) as recorded in table 4-6.

As presented in tables 4-6, the antibacterial activity of ZnO NPs-OB increase as ZnO NP concentration increased. As the concentration of ZnO NPs increased from 0.5% to 5%, the inhibition zone of ZnO NPs-OB was increased. This result indicated the effect of ZnO NP on the antibacterial activity of ZnO NPs-OB. Formulation without biosynthesized ZnO NPs, i.e., ointment base (0% of ZnO NPs), had a smaller inhibition diameter compared against ZnO NPs-OB. Figure 4 - 21 clearly showed the inhibition zone of OB and ZnO NPs-OB for both S. aureus and E. coli.

Table 4 - 6: Antimicrobial activity of the OB and ZnO NPs-OB.

ZnO NPs-OB of Conc. 350 µg/mL	Bacteria Species and Zone of Inhibition in mm	
	E. coli ATCC25922	*S. aureus* ATCC25923
F_0	9	9
F_1	11	10
F_2	12.5	11.5
F_3	14	13
F_4	16.5	16
F_5	12.5	13
Ampicillin (Amp)	12	12.5

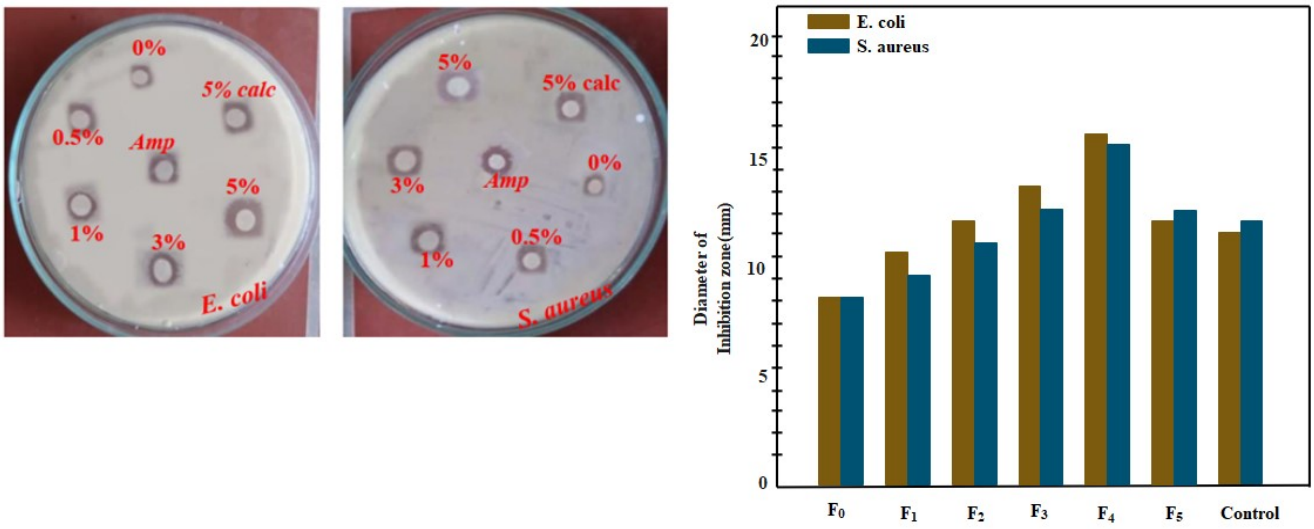

Figure 4 - 21: Antimicrobial activity of the ZnO NPs-OB.

ZnO NPs-OB was a kind of medicated ointment for skincare. Due to incorporating biosynthesized ZnO NPs, ZnO NPs-OB efficiency was increased against bacterial strain. It was observed that NPs were effective at small concentrations. This concept could also be related to minimizing drug dosage and developing effective drugs at low concentrations. The ZnO NPs-OB exhibited a different level of activities depending on the particular bacteria strains. The Maximum zone of about 16.5 mm inhibition was observed for ZnO NPs-OB against *E. coli,* and a minimum of 9 mm inhibition was observed for OB. Based on the above observed antimicrobial activity test, it was proven that the ZnO NPs-OB and OB have excellent antimicrobial activity toward the selected bacterial strains. The prepared ointments can be used for wound healing activity. Due to the COL/ELS matrix within the ointment base, ZnO NPs-OB could experience additional advantages such as regeneration or renewal of damaged skin cells. Since ZnO NPs-OB synthesizes from biobased materials, it was supposed to be biocompatible with human skin.

Antibacterial activity of ZnO NPs was either due to reactive oxygen species that affects and damages the bacterial cells or Zn ion that can interact with specific groups of bacterial enzymes and inhibit the functionality of the enzyme. In both cases, pathogenic organisms lose their ionic strength, and the cell functions, such as growth, metabolic activity, replication, etc., were inhibited and led to cell death (Jayabalan et al., 2019) (Meenatchi et al., 2020).

CHAPTER FIVE

5. CONCLUSION AND RECOMMENDATION

5.1. Conclusion

The biosynthesized ZnO NPs and ZnO NPs dispersed ointment have been successfully synthesized using green and renewable materials and characterized using different analytical instruments and techniques. This research focused on the green synthesis of ZnO NPs and the development of entirely biobased ointment from natural biomaterials such as COL/ELS and the advancement of its activity by incorporating ZnO NPs. The biobased ointment was proposed to overcome side effects associated with petroleum derivative ointment. Biosynthesis of ZnO NPs was also anticipated over conventional methods to overcome the side effects caused by traditional physical and chemical processes.

The effects of six main factors were studied to obtain the optimum condition for the biosynthesis of ZnO NPs. These were: types of solvents selected was methanol and distilled water of 50:50 mL (v/v), nucleation time of 3 hr, reaction temperature of 80 ℃, the ratio of moringa oleifera extract to precursor solution of 50:50 mL (v/v), precursor concentration of 0.025 M, and pH of 12. The effects were analyzed mainly through UV-Vis spectroscopy by comparing their UV light absorbance to the formation of ZnO NPs.

UV-Vis spectroscopy indicated the formation of ZnO NPs at 363 nm. From XRD analysis, the crystalline sizes obtained by the Scherrer equation were 12.85 nm and 9.1 nm for calcined and oven-dried ZnO NPs, respectively. FTIR peak appeared in the lower energy region at 497 cm^{-1} indicated the presence of ZnO NPs. Thermogravimetric studies revealed that ZnO NPs had three mass loss steps with a maximum mass loss temperature of about 65% at 390 ℃. ZnO NPs showed good antimicrobial activity with an inhibition zone of 16 mm against E. coli and 14 mm against S. aureus at 100 µg/mL. Moringa oleifera extracts improved the antimicrobial activities of ZnO NPs due to oil encircled nanoparticles. Biosynthesized ZnO NPs were used as active components in the formulation of bio-based ointment.

The biobased ointment was developed to overcome the negative impacts of petroleum derivatives ointments due to their chemical compositions. COL/ELS matrix and lactic acid were used to synthesize the ointment base by a polycondensation reaction. COL/ELS was completely soluble in lactic acid monomer. Lactic acid facilitated the delamination of α helix and β sheet of COL/ELS respectively through weakening secondary structure formed by NH and C=O. The broad shoulder-like peak at 1745 cm^{-1} indicated the COL/ELS matrix within an oligomer matrix of bioconjugate.

The ointment was formulated by dispersing 0.5%, 1%, 3%, and 5% of biosynthesized ZnO NPs on the ointment base. The ointment base and ZnO NPs-OB show emollient characteristics, suitable viscosity and spreadability, thick appearance, brown color, and homogenous with no signs of phase separation. ZnO NPs-OB showed UVA radiation-absorbing capability at the wavelength of 343 nm due to its bandgap energy. The bandgap energy of ZnO NPs was found to be 3.3 eV. The attachment of ZnO NPs to bioconjugate was observed from the FTIR result at 453 cm^{-1}. The formulated ZnO NPs-OB effectively inhibited the growth of E. coli and S. aureus at a low concentration of 350 µg/mL. The inhibition zone recorded were 16.5 mm and 16 mm for E. coli and S. aureus, respectively. ZnO NPs-OB was effective at lower concentrations, which could minimize the dosage required. Results obtained exhibited promising antimicrobial activity and UV light absorbing properties. Therefore, it could be considered a potential anti-microbial and sunscreen product and presumed to replace petroleum derivative ointment.

5.2. Recommendation

Biosynthesized ZnO NPs and ZnO NPs-OB had been studied qualitatively and quantitatively with different analytical instruments. Ointment developed had shown promising ointment properties. Based on the present study, the following tasks were recommended as future work.

- Optimization of the biosynthesis of the ZnO NPs should be done, and its yield should be determined.
- The stability of ZnO NPs and their distribution within the ointment base haven't been studied analytically. It should be done to develop ZnO NPs dispersed stable matrix.
- A skin penetration test, drug release, stability, rheological properties, and shelf life of ZnO NPs dispersed ointment should be studied.
- Even though COL/ELS has many applications in biomedical engineering, it was used to develop biocompatible ointment for skincare applications in this research. Further studies on its applications should be done on wound dressing, drug delivery, hydrogel synthesis, skin replacement, bone substitutes, etc.

REFERENCES

Abdulkhani, A., Hosseinzadeh, J., Ashori, A., Dadashi, S., & Takzare, Z. (2014). Preparation and characterization of modified cellulose nanofibers reinforced polylactic acid nanocomposite. *Polymer Testing*, *35*, 73–79. https://doi.org/10.1016/j.polymertesting.2014.03.002

Abdullah, F. H., Bakar, N. H. H. A., & Bakar, M. A. (2020). Optik Low temperature biosynthesis of crystalline zinc oxide nanoparticles from Musa acuminata peel extract for visible-light degradation of methylene blue. *Optik - International Journal for Light and Electron Optics*, *206*(October 2019), 164279. https://doi.org/10.1016/j.ijleo.2020.164279

Adeleye, O. A., Bakre, L. G., Bamiro, O. A., & Badru, A. O. (2021a). Formulation and Evaluation of Ehretia Cymosa Biosynthesized Silver Nanoparticle Anti-Inflammatory Ointment. *International Journal of Pharmaceutical Research*, *13*(02), 3662–3670.

Adeleye, O. A., Bakre, L. G., Bamiro, O. A., & Badru, A. O. (2021b). *Formulation and Evaluation of Ehretia Cymosa Biosynthesized Silver Nanoparticle Anti-Inflammatory Ointment*. *13*(2), 3662–3670.

Advance, A. N., On, R., Acid, S., For, O., & Acne, T. O. F. (2020). an Advance Review on Salicylic Acid Ointment for. *World Journal of Pharmaceutical Research*, *9*(5), 1940–1949.

Agarwal, H., & Shanmugam, V. K. (2020). A review on anti-inflammatory activity of green synthesized zinc oxide nanoparticle: Mechanism-based approach. *Bioorganic Chemistry*, *94*(October 2019), 103423. https://doi.org/10.1016/j.bioorg.2019.103423

Aguirre-Cruz, G., León-López, A., Cruz-Gómez, V., Jiménez-Alvarado, R., & Aguirre-Álvarez, G. (2020). Collagen hydrolysates for skin protection: Oral administration and topical formulation. *Antioxidants*, *9*(2). https://doi.org/10.3390/antiox9020181

Akbar, S., Tauseef, I., Subhan, F., Sultana, N., Khan, I., Ahmed, U., & Haleem, K. S. (2020). An overview of the plant-mediated synthesis of zinc oxide nanoparticles and their antimicrobial potential. *Inorganic and Nano-Metal Chemistry*, *0*(0), 1–15.

Ali, A., Akhtar, N., & Chowdhary, F. (2014). *Enhancement of human skin facial revitalization by moringa leaf extract cream*. 71–76. https://doi.org/10.5114/pdia.2014.40945

Alias, S. S., Ismail, A. B., & Mohamad, A. A. (2010). Effect of pH on ZnO nanoparticle properties synthesized by sol – gel centrifugation. *Journal of Alloys and Compounds*,

Altemimi, A., Lakhssassi, N., Baharlouei, A., & Watson, D. G. (2017). *and Identification of Bioactive Compounds from Plant Extracts*. https://doi.org/10.3390/plants6040042

Álvarez-chimal, R., García-pérez, V. I., & Álvarez-pérez, M. A. (2021). Materials Science & Engineering C Green synthesis of ZnO nanoparticles using a Dysphania ambrosioides extract . Structural characterization and antibacterial properties. *Materials Science & Engineering C*, *118*(August 2020), 111540. https://doi.org/10.1016/j.msec.2020.111540

Amaro-ortiz, A., Yan, B., & Orazio, J. A. D. (2014). *Ultraviolet Radiation, Aging and the Skin: Prevention of Damage by Topical cAMP Manipulation*. 6202–6219.

Anastas, P., & Eghbali, N. (2010). Green Chemistry: Principles and Practice. *Chemical Society Reviews*, *39*(1), 301–312. https://doi.org/10.1039/b918763b

Anwar, F., Latif, S., Ashraf, M., & Gilani, A. H. (2007). *Moringa oleifera : A Food Plant with Multiple Medicinal Uses*. *25*(September 2006), 17–25. https://doi.org/10.1002/ptr

Article, O. (2012). *Utilization of byproducts and waste materials from meat , poultry and fish processing industries : a review*. *49*(June), 278–293.

Athikomkulchai, S., Tunit, P., Tadtong, S., Jantrawut, P., Sommano, S. R., & Chittasupho, C. (2021). *Moringa oleifera Seed Oil Formulation Physical Stability and Chemical Constituents for Enhancing Skin Hydration and Antioxidant Activity*. 1–18.

Badnore, A. U., Sorde, K. I., Datir, K. A., Ananthanarayan, L., & Pratap, A. P. (2019). Preparation of antibacterial peel-off facial mask formulation incorporating biosynthesized silver nanoparticles. *Applied Nanoscience*, *9*(2), 279–287.

Bala, N., Saha, S., Chakraborty, M., Maiti, M., Das, S., Basu, R., & Nandy, P. (2014). RSC Advances Green synthesis of zinc oxide nanoparticles using Hibiscus subdari ff a leaf extract : e ff ect of. *RSC Advances*, *5*, 4993–5003. https://doi.org/10.1039/C4RA12784F

Bala, N., Saha, S., Chakraborty, M., Maiti, M., Das, S., Basu, R., & Nandy, P. (2015). *RSC Advances Green synthesis of zinc oxide nanoparticles using Hibiscus subdari ff a leaf extract : e ff ect of*. 4993–5003. https://doi.org/10.1039/c4ra12784f

Bandeira, M., Giovanela, M., Roesch-ely, M., Devine, D. M., & Crespo, S. (2020). Green synthesis of zinc oxide nanoparticles : A review of the synthesis methodology and mechanism of formation. *Sustainable Chemistry and Pharmacy*, *15*(January), 100223.

Bandeira, M., Possan, A. L., Pavin, S. S., Raota, C. S., Vebber, M. C., Giovanela, M., Roesch-

ely, M., & Devine, D. M. (2020). Nano-Structures & Nano-Objects Mechanism of formation , characterization and cytotoxicity of green synthesized zinc oxide nanoparticles obtained from Ilex paraguariensis leaves extract. *Nano-Structures & Nano-Objects*, *24*

Basnet, P., Chanu, T. I., Samanta, D., & Chatterjee, S. (2018). Journal of Photochemistry & Photobiology , B : Biology A review on bio-synthesized zinc oxide nanoparticles using plant extracts as reductants and stabilizing agents. *Journal of Photochemistry & Photobiology, B: Biology*, *183*(April), 201–221.

Beatriz, A., Cretella, M., Soley, S., Lúcia, P., Marquini, R., Riva, D., Ascari, J., Almeida, D., & Fleith, M. (2020). *Expanding the anti-in fl ammatory potential of Moringa oleifera : topical e ff ect of seed oil on skin in fl ammation and hyperproliferation*. *254*(March).

Bhaskar, R., Ola, M., Patil, P. H., & Nawandar, K. S. (2016). a Review on: Ointment and Ointment Bases. *Rajveer et Al. World Journal of Pharmaceutical Research*, *5*(9), 335.

Blinova, A. A., Blinov, A. V., Baklanova, O. A., Yasnaya, M. A., Baklanov, I. S., Siddiqui, A. A., Golik, A. B., Okolelova, A. I., Gvozdenko, A. A., Simonov, A. N., & Povetkin, S. N. (2021). Study of Wound-Healing Ointment Composition based on Highly Dispersed Zinc Oxide Modified with Nanoscale Silver. *International Journal Of Pharmaceutical And Phytopharmacological Research*, *11*(1), 134–142. https://doi.org/10.51847/cu6kx0jde3

Bose, S., & Bandyopadhyay, A. (2013). Introduction to Biomaterials. In *Characterization of Biomaterials*. Elsevier. https://doi.org/10.1016/B978-0-12-415800-9.00001-2

Charinpanitkul, T., Faungnawakij, K., & Tanthapanichakoon, W. (2008). Review of Recent Research on Nanoparticle Production in Thailand. *Advanced Powder Technology*, *19*(5)

Chattopadhyay, S., & Raines, R. T. (2014). Review collagen-based biomaterials for wound healing. *Biopolymers*, *101*(8), 821–833. https://doi.org/10.1002/bip.22486

Chekki, R., & Snoussi, A. (2016). *Chemical composition , antibacterial and antioxidant activities of Tunisian garlic (Allium sativum) essential oil and ethanol extract Chemical composition , antibacterial and antioxidant activities of Tunisian garlic (Allium sativum) essential oil and*. *January*. https://doi.org/10.13171/mjc.3.4.2014.09.07.11

Chen, Z. (2017). *Ultraviolet-B radiation effects on sweet potato growth and development*. Colorado State University.

Chin, C., Jalil, J., Ng, P. Y., & Ng, S. (2018). Development and formulation of Moringa oleifera

standardised leaf extract fi lm dressing for wound healing application. *Journal of Ethnopharmacology*, *212*(June 2017), 188–199. https://doi.org/10.1016/j.jep.2017.10.016

Chinnasamy, C., Tamilselvam, P., Karthick, B., Sidharth, B., & Senthilnathan, M. (2018). ScienceDirect Green Synthesis , Characterization and Optimization Studies of Zinc Oxide Nano Particles Using Costusigneus Leaf Extract. *Materials Today: Proceedings*, *5*(2),

Chitra, K., & Annadurai, G. (2014). *Antibacterial Activity of pH-Dependent Biosynthesized Silver Nanoparticles against Clinical Pathogen*. *2014*.

Cross, S. E., Innes, B., Roberts, M. S., Tsuzuki, T., Robertson, T. A., & McCormick, P. (2007). Human skin penetration of sunscreen nanoparticles: In-vitro assessment of a novel micronized zinc oxide formulation. *Skin Pharmacology and Physiology*, *20*(3), 148–154.

Darvishi, E., Kahrizi, D., & Arkan, E. (2019). Comparison of different properties of zinc oxide nanoparticles synthesized by the green (using Juglans regia L . leaf extract) and chemical methods. *Journal of Molecular Liquids*, *286*, 110831.

Dejen, K. D., Zereffa, E. A., Murthy, H. C. A., & Merga, A. (2020). Synthesis of ZnO and ZnO/PVA nanocomposite using aqueous Moringa Oleifeira leaf extract template: Antibacterial and electrochemical activities. *Reviews on Advanced Materials Science*, *59*(1)

Dhandapani, P., Siddarth, A. S., Kamalasekaran, S., Maruthamuthu, S., & Rajagopal, G. (2014). Bio-approach : Ureolytic bacteria mediated synthesis of ZnO nanocrystals on cotton fabric and evaluation of their antibacterial properties. *Carbohydrate Polymers*, *103*, 448–455.

Durán, N., Marcato, P. D., Alves, O. L., De Souza, G. I. H., & Esposito, E. (2005). Mechanistic aspects of biosynthesis of silver nanoparticles by several Fusarium oxysporum strains.

Education, P. (n.d.). *Band Gap*. http://www.pveducation.org/pvcdrom/pn-junction/band-gap

El-Gied, A. A. A., Abdelkareem, A. M., & Hamedelniel, E. I. (2015). Investigation of cream and ointment on antimicrobial activity of Mangifera indica extract. *Journal of Advanced Pharmaceutical Technology and Research*, *6*(2), 53–57.

Elumalai, K., & Velmurugan, S. (2015). Applied Surface Science Green synthesis , characterization and antimicrobial activities of zinc oxide nanoparticles from the leaf extract of Azadirachta indica (L .). *Applied Surface Science*, *345*, 329–336.

Elumalai, K., Velmurugan, S., Ravi, S., Kathiravan, V., & Ashokkumar, S. (2015). AC. *Spectrochimica Acta Part A: Molecular and Biomolecular Spectroscopy*, *143*, 158–164.

Fadhlan, M., Hermandy, S., Zaki, M., Yusoff, M., Yahya, M. S., & Awal, R. (2020). *The Green Synthesis of Nanoparticle Zinc Oxide (ZnO) Using Aloe Vera Leaf Extract : Structural and Optical Characterization Reviews*. *8*(10), 6896–6902.

Fazlzadeh, M., Khosravi, R., & Zarei, A. (2017). Green synthesis of zinc oxide nanoparticles using Peganum harmala seed extract , and loaded on Peganum harmala seed powdered activated carbon as new adsorbent for removal of Cr (VI) from aqueous solution. *Ecological Engineering*, *103*, 180–190. https://doi.org/10.1016/j.ecoleng.2017.02.052

Feldsine, P., Abeyta, C., & Andrews, W. H. (2002). AOAC International methods committee guidelines for validation of qualitative and quantitative food microbiological official methods of analysis. *Journal of AOAC International*, *85*(5), 1187–1200.

G, N. A., V, O. M., K, T. P., & Ahmed, H. (2019). *Chemical compositions of essential oils of some Kenyan Ocimum species*. *7*(3), 17–26.

Ghosh, D., Mondal, S., & Ramakrishna, K. (2019). A topical ointment formulation containing leaves extract of Aegialitis rotundifolia Roxb., accelerates excision, incision and burn wound healing in rats. *Wound Medicine*, *26*(1), 100168.

Golmohammadi, M., Honarmand, M., & Ghanbari, S. (2020). Spectrochimica Acta Part A : Molecular and Biomolecular Spectroscopy A green approach to synthesis of ZnO nanoparticles using jujube fruit extract and their application in photocatalytic degradation of organic dyes. *Spectrochimica Acta Part A: Molecular and Biomolecular Spectroscopy*, *229*

Gupta, K., & Chundawat, T. S. (2020). Biomass and Bioenergy Zinc oxide nanoparticles synthesized using Fusarium oxysporum to enhance bioethanol production from rice-straw. *Biomass and Bioenergy*, *143*(July), 105840.

Gupta, M., Tomar, R. S., Kaushik, S., Mishra, R. K., & Sharma, D. (2018). Effective antimicrobial activity of green ZnO nano particles of Catharanthus roseus. *Frontiers in Microbiology*, *9*(SEP), 1–13. https://doi.org/10.3389/fmicb.2018.02030

Gupta, V., Verma, P. K., Gupta, A., Kant, V., Kumar, P., & Sharma, M. (2020). Comparative evaluation for wound healing potentials of bulk and nano forms of zinc oxide ointment. *Nanosystems: Physics, Chemistry, Mathematics*, *11*(4), 453–461.

Heinlaan, M., Ivask, A., Blinova, I., Dubourguier, H. C., & Kahru, A. (2008). Toxicity of nanosized and bulk ZnO, CuO and TiO2 to bacteria Vibrio fischeri and crustaceans Daphnia

magna and Thamnocephalus platyurus. *Chemosphere*, *71*(7), 1308–1316.

Henry, R. D. and M. (2006). Lactic acid: recent advances in products, processes and technologies – a review. *Journal of Chemical Technology and Biotechnology*, 11.

Holmes, A. M., Song, Z., Moghimi, H. R., & Roberts, M. S. (2016). *Relative Penetration of Zinc Oxide and Zinc Ions into Human Skin after Application of Different Zinc Oxide Formulations* . https://doi.org/10.1021/acsnano.5b04148

Horch, R. E., & Stark, G. B. (1998). Comparison of the effect of a collagen dressing and a polyurethane dressing on the healing of split thickness skin graft (STSG) donor sites. *Scandinavian Journal of Plastic and Reconstructive Surgery and Hand Surgery*, *32*(4)

Jacob, E. Y. S. J. O., & Suleiman, J. O. T. M. A. T. (2021). A critical review of synthesis parameters affecting the properties of zinc oxide nanoparticle and its application in wastewater treatment. In *Applied Water Science*. Springer International Publishing.

Jamdagni, P., Khatri, P., & Rana, J. S. (2018). Green synthesis of zinc oxide nanoparticles using flower extract of Nyctanthes arbor-tristis and their antifungal activity. *Journal of King Saud University - Science*, *30*(2), 168–175. https://doi.org/10.1016/j.jksus.2016.10.002

Jarrar, M. (2015). *Anti-Aging EffectsofRetinol and Alpha Hydroxy Acid onElastin FibersofArtificially Photo-Aged Human Dermal Fibroblast Cell Lines*. *9*(4), 270–273.

Jayabalan, J., Mani, G., Krishnan, N., Pernabas, J., Milton, J., & Tae, H. (2019). Biocatalysis and Agricultural Biotechnology Green biogenic synthesis of zinc oxide nanoparticles using Pseudomonas putida culture and its In vitro antibacterial and anti-biofilm activity. *Biocatalysis and Agricultural Biotechnology*, *21*(August), 101327.

Jeyakumar, N., Narayanasamy, B., & Balasubramanian, D. (2020). Characterization and effect of Moringa Oleifera Lam . antioxidant additive on the storage stability of Jatropha biodiesel.

Jiang, J., Pi, J., & Cai, J. (2018). The Advancing of Zinc Oxide Nanoparticles for Biomedical Applications[1] J. Jiang, J. Pi, and J. Cai, "The Advancing of Zinc Oxide Nanoparticles for Biomedical Applications," vol. 2018, 2018. *Bioinorganic Chemistry and Applications*,

Jin, A., Wang, Y., Lin, K., & Jiang, L. (2020). *Bioactive Materials Nanoparticles modi fi ed by polydopamine : Working as " drug " carriers*. *5*(April), 522–541.

Khan, M. M., Saadah, N. H., & Khan, M. E. (2019). *Phytogenic Synthesis of Band Gap-Narrowed ZnO Nanoparticles Using the Bulb Extract of Costus woodsonii*. 334–344.

Kharissova, O. V., Dias, H. V. R., Kharisov, B. I., Pérez, B. O., & Pérez, V. M. J. (2013). The greener synthesis of nanoparticles. *Trends in Biotechnology*, *31*(4), 240–248.

Król, A., Pomastowski, P., Ra, K., & Buszewski, B. (2017). *Zinc oxide nanoparticles : Synthesis , antiseptic activity and toxicity mechanism*. *249*, 37–52.

Król, A., Railean-plugaru, V., Pomastowski, P., & Buszewski, B. (2019). Phytochemistry Letters Phytochemical investigation of Medicago sativa L . extract and its potential as a safe source for the synthesis of ZnO nanoparticles : The proposed mechanism of formation and antimicrobial activity. *Phytochemistry Letters*, *31*(December 2018), 170–180.

Kulinets, I. (2015). Biomaterials and their applications in medicine. In *Regulatory Affairs for Biomaterials and Medical Devices*. Woodhead Publishing Limited.

Kumar, M. R. A., Ravikumar, C. R., Nagaswarupa, H. P., Purshotam, B., Gonfa, B., Murthy, H. C. A., Kedir, F., & Tadesse, S. (2019). Journal of Environmental Chemical Engineering Evaluation of bi-functional applications of ZnO nanoparticles prepared by green and chemical methods. *Journal of Environmental Chemical Engineering*, *7*(6), 103468.

Kumar, S. (2017). *MEDICINAL IMPORTANCE OF Moringa oleifera : DRUMSTICK PLANT*

Kumar, V. B., Dolitzky, A., Michaeli, S., & Gedanken, A. (2018). Antiparasitic Ointment Based on a Biocompatibile Carbon Dot Nanocomposite. *ACS Applied Nano Materials*, *1*(4), 1784

Lakshmeesha, T. R., Sateesh, M. K., Prasad, B. D., Sharma, S. C., Kavyashree, D., Chandrasekhar, M., & Nagabhushana, H. (2014). Reactivity of crystalline ZnO superstructures against fungi and bacterial pathogens: Synthesized using nerium oleander leaf extract. *Crystal Growth and Design*, *14*(8), 4068–4079.

Letsholathebe, D., Thema, F. T., Mphale, K., Maabong, K., & Magdalane, C. M. (2021). Materials Today : Proceedings Green synthesis of ZnO doped Moringa oleifera leaf extract using Titon yellow dye for photocatalytic applications. *Materials Today: Proceedings*, *36*,

Lisnawati, N., Kumala, S., & Rahmat, D. (2018). *Formulation and evaluation of antibacterial activity of nanoparticles ointment preparation using Blimbi extract*. *4*(Atcc 25923), 32–39.

Lisnawati, N., Kumala, S., & Rahmat, D. (2019). Formulation and evaluation of antibacterial activity of nanoparticles ointment preparation using Blimbi extract. *Pharmaceutical and Biomedical Research*, *4*(Atcc 25923), 32–39. https://doi.org/10.18502/pbr.v4i3.542

Lu, J., Ali, H., Hurh, J., Han, Y., Batjikh, I., Jahan, E., Anandapadmanaban, G., & Kyu, J.

(2019). Optik The assessment of photocatalytic activity of zinc oxide nanoparticles from the roots of Codonopsis lanceolata synthesized by one-pot green synthesis method. *Optik - International Journal for Light and Electron Optics*, *184*(January), 82–89.

Lübeck, M., & Lübeck, P. S. (2019). Application of lactic acid bacteria in green biorefineries. *FEMS Microbiology Letters*, *366*, I60–I67. https://doi.org/10.1093/femsle/fnz024s

Ma, R. (2016). *extraction and characterization of acetic acid-soluble*.

Mabrouki, L., Rjeibi, I., Taleb, J., & Zourgui, L. (2020). *phytochemical screening by ft-ir analysis of methanolic extract leaves of moringa oleifera and in vitro evaluation of its anti-oxidant and anti-*. *9*(7), 341–351.

Madhumitha, G., Fowsiya, J., Gupta, N., Kumar, A., & Singh, M. (2019). Journal of Physics and Chemistry of Solids Green synthesis , characterization and antifungal and photocatalytic activity of Pithecellobium dulce peel – mediated ZnO nanoparticles. *Journal of Physical and Chemistry of Solids*, *127*(December 2018), 43–51.

Mahendran, S., & Abdul Rashid, N. (2016). Formulation, evaluation and antibacterial properties of herbal ointment containing methanolic extract of Clinacanthus nutans leaves. *International Journal of Pharmaceutical and Clinical Research*, *8*(8), 1170–1174.

Manzoor, U., Zahra, F. T., Rafique, S., Moin, M. T., & Mujahid, M. (2015). *Effect of Synthesis Temperature , Nucleation Time , and Postsynthesis Heat Treatment of ZnO Nanoparticles and Its Sensing Properties*. *2015*.

Marathe, G. K., Pandit, C., Lakshmikanth, C. L., Chaithra, V. H., Jacob, S. P., & D'Souza, C. J. M. (2014). To hydrolyze or not to hydrolyze: The dilemma of platelet-activating factor acetylhydrolase. *Journal of Lipid Research*, *55*(9), 1847–1854.

Mârza, S. M., Magyari, K., Bogdan, S., Moldovan, M., Peştean, C., Nagy, A., Tăbăran, F., Licarete, E., Suarasan, S., Dreanca, A., Baia, L., & Papuc, I. (2019). Skin wound regeneration with bioactive glass-gold nanoparticles ointment. *Biomedical Materials*

Matinise, N., Fuku, X. G., Kaviyarasu, K., Mayedwa, N., & Maaza, M. (2017). Applied Surface Science ZnO nanoparticles via Moringa oleifera green synthesis : Physical properties & mechanism of formation. *Applied Surface Science*, *406*, 339–347.

Mecham, R. P. (2008). Methods in elastic tissue biology: Elastin isolation and purification. *Methods*, *45*(1), 32–41. https://doi.org/10.1016/j.ymeth.2008.01.007

Meenatchi, T., Palanimurugan, A., Dhanalakshmi, A., Maheshkumar, V., & Natarajan, B. (2020). Green synthesis of Cynodon Dactylon capped concentrations on ZnO nanoparticles for antibacterial activity , ROS / ML-DNA treatment and compilation of best controlling microbes by mathematical comparisons. *Chemical Physics Letters*, *749*(March), 137429.

Meseret Ewunetu. (2020). *Development Elastin/Collagen - Lactic acid Bioconjugate Ointment Base: The effect of Osmium lamiifolium on its antimicrobial property*. [Unpublished MSc thesis]. Adama Science and Technology University.

Milkias, M. (2016). *Chicken Meat Production , Consumption and Constraints in*. 1–12.

Mirzaei, H., & Darroudi, M. (2017a). Zinc oxide nanoparticles_ Biological synthesis and biomedical applications. *Ceramics International*, *43*(1), 907–914.

Mirzaei, H., & Darroudi, M. (2017b). Zinc oxide nanoparticles: Biological synthesis and biomedical applications. *Ceramics International*, *43*(1), 907–914.

Moss, T. K. S. (2016). *The Effect of Increased Exposure of UVC Light on Human Skin Microbiota*.

Mulugeta, H., Kalid, B., & Amare, B. (2020). *Assessment of the production potential and constraints of chicken in some Chagni town , Awi - administrative zone , Amhara Region , Ethiopia*. *10*(2), 1–10.

Nadalian, M., Kamaruzaman, N., Yusop, M. S. M., Babji, A. S., & Yusop, S. M. (2019). Isolation, purification and characterization of antioxidative bioactive elastin peptides from poultry skin. *Food Science of Animal Resources*, *39*(6), 966–979.

Nadalian, M., Mohamad, S., Aida, W., Mustapha, W., & Azri, M. (2013). *Extraction and characterization of elastin from poultry skin Extraction and Characterization of Elastin from Poultry Skin*. *692*(December). https://doi.org/10.1063/1.4858735

Nagarajan, S., & Arumugam Kuppusamy, K. (2013). Extracellular synthesis of zinc oxide nanoparticle using seaweeds of gulf of Mannar, India. *Journal of Nanobiotechnology*, *11*(1),

National Committee for Clinical Laboratory Standards. (2012). *Performance Standards for Antimicrobial Disk Susceptibility Tests, Approved Standard, 7thed.* (Approved A). Clinical and Laboratory Standards Institute (CLSI).

Nations, U., Programme, E., Belkin, M., Hashomer, T., Rothschild, F., Diffey, B., Hospital, D., Radiological, N., Board, P., Hospital, R. A., Agency, E. P., & Urbach, F. (1994). *Protection*

Against Exposure to Ultraviolet Radiation.

Naveed, A., Haq, U., Nadhman, A., Ullah, I., Mustafa, G., Yasinzai, M., & Khan, I. (2017). *Synthesis Approaches of Zinc Oxide Nanoparticles : The Dilemma of Ecotoxicity*. *2017*(Table 1).

Ngom, I., Ngom, B. D., Sackey, J., & Khamlich, S. (2019). Biosynthesis of zinc oxide nanoparticles using extracts of Moringa Oleifera: Structural & optical properties. *Materials Today: Proceedings*, *36*, 526–533. https://doi.org/10.1016/j.matpr.2020.05.323

Ngom, I., Ngom, B. D., Sackey, J., & Khamlich, S. (2020). Materials Today : Proceedings Biosynthesis of zinc oxide nanoparticles using extracts of Moringa Oleifera : Structural & optical properties. *Materials Today: Proceedings*, *xxxx*.

Ngom, I., Ngom, B. D., Sackey, J., & Khamlich, S. (2021). Materials Today : Proceedings Biosynthesis of zinc oxide nanoparticles using extracts of Moringa Oleifera : Structural & optical properties. *Materials Today: Proceedings*, *36*, 526–533.

Orazio, J. D., Jarrett, S., Amaro-ortiz, A., & Scott, T. (2013). *UV Radiation and the Skin*. 12222

Pal, S., Mondal, S., Maity, J., & Mukherjee, R. (2018). *Synthesis and Characterization of ZnO Nanoparticles using Moringa Oleifera Leaf Extract : Investigation of Photocatalytic and Antibacterial Activity*. *14*(2), 111–119.

Parra, M. R., & Haque, F. Z. (2014). Aqueous chemical route synthesis and the effect of calcination temperature on the structural and optical properties of ZnO nanoparticles. *Integrative Medicine Research*, *3*(4), 363–369. https://doi.org/10.1016/j.jmrt.2014.07.001

Patel, N., & Gohil, P. (2012). A review on biomaterials: scope, applications & human anatomy significance. *International Journal of Emerging Technology and Advanced Engineering*, *2*(4), 91–101.

Paula, T. De, Pendiuk, J., Clara, A., Salom, S., Soley, S., Beatriz, A., Cretella, M., Fleith, M., & Almeida, D. (2021). *Phytomedicine Plus The oil from Moringa oleifera seeds accelerates chronic skin wound healing*. *1*, 1–11. https://doi.org/10.1016/j.phyplu.2021.100099

Pillai, A. M., Sivasankarapillai, V. S., Rahdar, A., Joseph, J., Sadeghfar, F., Anuf A, R., Rajesh, K., & Kyzas, G. Z. (2020). Green synthesis and characterization of zinc oxide nanoparticles with antibacterial and antifungal activity. *Journal of Molecular Structure*, *1211*, 128107.

Prasad, R. (2014). *Synthesis of Silver Nanoparticles in Photosynthetic Plants*. *2014*.

Prasad, V., & Dorle, A. K. (2006). Evaluation of ghee based formulation for wound healing activity. *Journal of Ethnopharmacology*, *107*(1), 38–47.

Press, D. (2011). *Titanium dioxide and zinc oxide nanoparticles in sunscreens : focus on their safety and effectiveness*. 95–112.

Rajarajeswari, P., Shaikh, R. S., & Ravangave, L. S. (2020). *Materials Today : Proceedings Effect of temperature reaction on chemically synthesized ZnO nanoparticles change in particle size*. *xxxx*. https://doi.org/10.1016/j.matpr.2020.09.126

Rana, A., Yadav, K., & Jagadevan, S. (2020). A comprehensive review on green synthesis of nature-inspired metal nanoparticles : Mechanism , application and toxicity. *Journal of Cleaner Production*, *272*, 122880. https://doi.org/10.1016/j.jclepro.2020.122880

Roselina, N. R. N., Azizan, A., Mei, K., Jumahat, A., & Bakar, M. A. A. (2013). Effect of pH on formation of Nickel Nanostructures through Chemical Reduction Method. *Procedia Engineering*, *68*, 43–48. https://doi.org/10.1016/j.proeng.2013.12.145

Ruszkiewicz, J. A., Pinkas, A., Ferrer, B., Peres, T. V., Tsatsakis, A., & Aschner, M. (2017). Neurotoxic effect of active ingredients in sunscreen products, a contemporary review. *Toxicology Reports*, *4*(March), 245–259. https://doi.org/10.1016/j.toxrep.2017.05.006

Saha, M., & Bandyopadhyay, P. K. (2017). Green Biosynthesis of Silver Nanoparticle Using Garlic , Allium sativum with Reference to Its Antimicrobial Activity Against the Pathogenic Strain of Bacillus sp . and Pseudomonas sp . Infecting Goldfish , Carassius auratus. *Proceedings of the Zoological Society*. https://doi.org/10.1007/s12595-017-0258-3

Sajid, M., & Płotka-Wasylka, J. (2020). Nanoparticles: Synthesis, characteristics, and applications in analytical and other sciences. *Microchemical Journal*, *154*(November 2019), 104623. https://doi.org/10.1016/j.microc.2020.104623

Salam, H. A., Rajiv, P., Kamaraj, M., Jagadeeswaran, P., Gunalan, S., & Sivaraj, R. (2012). *Plants : Green Route for Nanoparticle Synthesis*. *1*(5), 85–90.

Sangeetha, G., Rajeshwari, S., & Venckatesh, R. (2011). Green synthesis of zinc oxide nanoparticles by aloe barbadensis miller leaf extract : Structure and optical properties. *Materials Research Bulletin*, *46*(12), 2560–2566.

Sathishkumar, G., Rajkuberan, C., Manikandan, K., Prabukumar, S., Danieljohn, J., & Sivaramakrishnan, S. (2018). Corrigendum to ‘‘ Facile biosynthesis of antimicrobial zinc

oxide (ZnO) nanoflakes using leaf extract of Couroupita guianensis Aubl .” [Mater . Lett . *Materials Letters*, *188*, 2018. https://doi.org/10.1016/j.matlet.2018.03.170

Series, C. (2021). *Green synthesis of zinc oxide nanoparticles using Moringa oleifera l . water extract and its photocatalytic evaluation Green synthesis of zinc oxide nanoparticles using Moringa oleifera l . water extract and its photocatalytic evaluation*. 0–8.

Shabaani, M., Rahaiee, S., Zare, M., & Mahdi, S. (2020). Green synthesis of ZnO nanoparticles using loquat seed extract ; Biological functions and photocatalytic degradation properties. *LWT*, *134*(August), 110133. https://doi.org/10.1016/j.lwt.2020.110133

Shahriyari, S., Mohamadi, A., & Mohseni, S. (2019). Microbial Pathogenesis Biosynthesis , characterization and antimicrobial activities of zinc oxide nanoparticles from leaf extract of Mentha pulegium (L .). *Microbial Pthogenesis*, *131*(July 2018), 239–245.

Shin, H., Jo, S., & Mikos, A. G. (2003). Biomimetic materials for tissue engineering. *Biomaterials*, *24*(24), 4353–4364. https://doi.org/10.1016/S0142-9612(03)00339-9

Singh, A. K., Pal, P., Gupta, V., Yadav, T. P., Gupta, V., & Singh, S. P. (2017). Green synthesis, characterization and antimicrobial activity of zinc oxide quantum dots using *Eclipta alba*. *Materials Chemistry and Physics*. https://doi.org/10.1016/j.matchemphys.2017.09.049

Singh, K., Singh, J., & Rawat, M. (2019). Green synthesis of zinc oxide nanoparticles using Punica Granatum leaf extract and its application towards photocatalytic degradation of Coomassie brilliant blue R - 250 dye. *SN Applied Sciences*, *1*(6), 1–8.

Singh, T. A., Das, J., & Sil, P. C. (2020). Zinc oxide nanoparticles: A comprehensive review on its synthesis, anticancer and drug delivery applications as well as health risks. *Advances in Colloid and Interface Science*, *286*, 102317. https://doi.org/10.1016/j.cis.2020.102317

Soares, V. A., Xavier, M. J. S., Rodrigues, E. S., Oliveira, C. A. De, Farias, P. M. A., Stingl, A., Ferreira, N. S., & Silva, M. S. (2020). Green synthesis of ZnO nanoparticles using whey as an effective chelating agent. *Materials Letters*, *259*, 126853.

Sorbiun, M., Shayegan, E., & Ali, M. (2018). Green Synthesis of Zinc Oxide and Copper Oxide Nanoparticles Using Aqueous Extract of Oak Fruit Hull (Jaft) and Comparing Their Photocatalytic Degradation of Basic Violet 3. *International Journal of Environmental Research*, *12*(1), 29–37. https://doi.org/10.1007/s41742-018-0064-4

Stohs, S. J., & Hartman, M. J. (2015). *Review of the Safety and Efficacy of Moringa oleifera*.

804(February), 796–804.

Syedmoradi, L., Daneshpour, M., Alvandipour, M., Gomez, F. A., Hajghassem, H., & Omidfar, K. (2017). Point of care testing: The impact of nanotechnology. *Biosensors and Bioelectronics*, *87*, 373–387. https://doi.org/10.1016/j.bios.2016.08.084

Taylor, P. L., Ussher, A. L., & Burrell, R. E. (2005). Impact of heat on nanocrystalline silver dressings: Part I: Chemical and biological properties. *Biomaterials*, *26*(35), 7221–7229.

Thirumurugan, G., Satya Veni, V., Ramachandran, S., Seshagiri Rao, J. V. L. N., & Dhanaraju, M. D. (2011). Superior wound healing effect of topically delivered silver nanoparticle formulation using eco-friendly potato plant pathogenic fungus: Synthesis and characterization. *Journal of Biomedical Nanotechnology*, *7*(5), 659–666.

Tripathi, N., & Katiyar, V. (2018). Lactic acid oligomer (OLLA) grafted gum arabic based green adhesive for structural applications. *International Journal of Biological Macromolecules*,

Truong, D. H., Nguyen, D. H., Ta, N. T. A., Bui, A. V., Do, T. H., & Nguyen, H. C. (2019). Evaluation of the use of different solvents for phytochemical constituents, antioxidants, and in vitro anti-inflammatory activities of severinia buxifolia. *Journal of Food Quality*, *2019*.

Ul, Z., Khan, H., Masood, H., Samad, N., Ullah, A., Muhammad, N., Ul, S., Tahir, K., Zaman, S., Ullah, F., Imran, M., Ahmad, N., Ullah, F., Ahmad, A., Sayed, M., Shafique, M., Ahmad, S., Ali, M., & Zakir, A. (2019). Journal of Photochemistry & Photobiology , B : Biology Greener synthesis of zinc oxide nanoparticles using Trianthema portulacastrum extract and evaluation of its photocatalytic and biological applications. *Journal of Photochemistry & Photobiology, B: Biology*, *192*(December 2018), 147–157.

Uma, K., & Xin, H. (2016). *Antifungal Effect of Plant Extract and Essential Oil*. *13*, 1–7.

Usha, S. Y., & Ashish, M. A. (2015). Review on: an Ointment. *Human*, *4*(2), 170–192. www.ijppr.humanjournals.comwww.ijppr.humanjournals.com

Venkatachalam, A., & Jesuraj, J. P. (2021). *Moringa oleifera Leaf Extract-Mediated Green Synthesis of Nanostructured Alkaline Earth Oxide (MgO) and Its Physicochemical Properties*. *2021*.

Vidhya, E., Vijayakumar, S., Prathipkumar, S., & Praseetha, P. K. (2020). Gene Reports Green way biosynthesis : Characterization , antimicrobial and anticancer activity of ZnO nanoparticles. *Gene Reports*, *20*(April), 100688.

Vongsak, B., Sithisarn, P., Mangmool, S., Thongpraditchote, S., Wongkrajang, Y., & Gritsanapan, W. (2013). Maximizing total phenolics, total flavonoids contents and antioxidant activity of Moringa oleifera leaf extract by the appropriate extraction method.

Wilson, R. T. (2010). *Poultry production and performance in the Federal Democratic Republic of Ethiopia*. *66*(September), 441–454. https://doi.org/10.1017/S0043933910000528

Yeo, G. C., Aghaei-Ghareh-Bolagh, B., Brackenreg, E. P., Hiob, M. A., Lee, P., & Weiss, A. S. (2018). Correction to: Fabricated Elastin (Advanced Healthcare Materials, (2015), 4, 16, (2530-2556), 10.1002/adhm.201400781). *Advanced Healthcare Materials*, *7*(23), 3–5.

Yoon, J., & Oh, S. (2021). Journal of Industrial and Engineering Chemistry Synthesis of amine modi fi ed ZnO nanoparticles and their photocatalytic activities in micellar solutions under UV irradiation. *Journal of Industrial and Engineering Chemistry*, *xxxx*, 1–7.

Yoseph, Z., Gladstone, J., Assefa, B., Selvi, A. T., Sreeram, K. J., & Rao, J. R. (2020). Extraction of elastin from tannery wastes : A cleaner technology for tannery waste management. *Journal of Cleaner Production*, *243*, 118471.

Yu, J., Kim, H., Go, M., Bae, S., & Choi, S. (2017). *ZnO Interactions with Biomatrices : Effect of Particle Size on ZnO-Protein Corona*. https://doi.org/10.3390/nano7110377

Zaheer, T., Imran, M., Pal, K., Sohail, M., Zahid, R., Islam, A., Asif, M., Rauf, S., Kasib, M., & Sindhu, D. (2021). Synthesis , characterization and acaricidal activity of green-me diate d ZnO nanoparticles against Hyalomma ticks. *Journal of Molecular Structure*, *1227*, 129652.

Zak, A. K. et al. “. (2011). *Synthesis and characterization of a narrow size distribution of zinc oxide nanoparticles.* ” International journal of nanomedicine vol. 6 (20.

Zarubica, A. R. (2020). *different types of biomaterials : structure and application :*

Zhang, S., & Duan, E. (2018). Fighting against Skin Aging: The Way from Bench to Bedside. *Cell Transplantation*, *27*(5), 729–738. https://doi.org/10.1177/0963689717725755

Zhang, W., Wang, Y., Lee, B. T. K., Liu, C., Wei, G., & Lu, W. (2014). A novel nanoscale-dispersed eye ointment for the treatment of dry eye disease. *Nanotechnology*, *25*(12).

Zhang, Z., Zhu, H., Zheng, Y., Zhang, L., Wang, X., Luo, Z., Tang, J., Lin, L., Du, Z., & Dong, C. (2020). The effects and mechanism of collagen peptide and elastin peptide on skin aging induced by D-galactose combined with ultraviolet radiation.

Zou, Y., Zhang, Y., Hu, Y., & Gu, H. (2018). *Ultraviolet Detectors Based on Wide Bandgap*.